UNIVERSITÄT FÜR BODENKULTUR WIEN
University of Natural Resources
and Life Sciences, Vienna

Doctoral Dissertation

Millifluidic devices to accelerate process development with the main focus on protein precipitation and filtration

submitted by

Maria del Carme Pons Royo, MSc

in partial fulfilment of the requirements for the academic degree

Doktorin der Bodenkultur (Dr.nat.techn.)

Vienna, September 2022

Supervisor:
Ao.Univ.Prof. Dipl.-Ing. Dr.nat.techn. Alois Jungbauer
Institut für Bioverfahrenstechnik
Department für Biotechnologie

Affidavit

I hereby declare that I have authored this dissertation independently and that I have not used any assistance other than that which is permitted. The work contained herein is my own except where explicitly stated otherwise. All ideas taken in wording or in basic content from unpublished sources or from published literature are duly identified and cited, and the precise references included. Any contribution from colleagues is explicitly stated in the authorship statement of the published papers.

I further declare that this dissertation has not been submitted, in whole or in part, in the same or a similar form, to any other educational institution as part of the requirements for an academic degree.

I hereby confirm that I am familiar with the standards of Scientific Integrity and with the guidelines of Good Scientific Practice, and that this work fully complies with these standards and guidelines.

Vienna, September 2022 Maria del Carme Pons Royo *(manu propria)*

Aquesta tesi està dedicada a la meva família

Si todo sale mal es porque estás en el buen camino.

Dr. Cristian Cardenas, Nancy, 2019

Supervisor team and reviewers

Supervisory team

[1,2] Univ.Prof. Dipl.-Ing. Dr. nat. techn. Alois Jungbauer

[1,2] Dipl.-Ing. Peter Satzer, Ph.D.

Reviewers

[1,2] Priv.-Doz. Dipl.-Ing. Dr. Astrid Dürauer

[3] Prof. Anurag Singh Rathore

Affiliations

[1]Institute of Bioprocess Science and Engineering (IBSE), Department of Biotechnology, University of Natural Resources and Life Sciences, Vienna, Austria

[2]Austrian Centre of Industrial Biotechnology (ACIB), Vienna, Austria

[3]Indian Institute of Technology Delhi, Delhi, India

Preface

This dissertation was funded by the European Union's Horizon 2020 research and innovation program under the Marie Skłodowska-Curie grant agreement No 812909 CODOBIO, within the Marie Skłodowska-Curie International Training Networks framework.

Acknowledgments

Després de molts entrebancs i dificultats, aquest viatge va arribant al seu final. Encara recordo els moments on aquest dia semblava que no arribaria mai, però finalment és aquí. Encara i la llàstima que m'afligeix, sempre em quedaran tots els bons records i experiències viscudes, recordant-me que més que un final és un nou principi i noves metes.

Firstly, I would like to thank my supervisors, Alois Jungbauer and Peter Satzer, for all the support and freedom given during these years. Such project would have not been possible without you.

També, vull agrair tot el suport a la meva família, als meus pares i al meu germà per tot el suport donat els darrers anys (també hauríem d'agrair-li al Llumí que es el que més hores s'ha passat assegut al meu costat mentre escrivia aquesta tesis).

Por supuesto, también debo agradecer todo el apoyo de mis amigos de Nancy que me proporcionaban un soplo de aire fresco para desconectar de mi día a día durante la tesis. a Daniela con sus historias locas, Giovanny y Adam por todos los buenos momentos vividos y los que nos quedan por vivir. A Cristian y Juan Carlos por todo su apoyo en los momentos complicados durante la tesis y en las mudanzas. A Pat y todo el grupo de Nancy. Aussi pour Joris et tous mes amis de Slovakia avec j'ai vécu de si belles et folles expériences (comme presque été mangé par les ours). Also, Ziad, Kamil and all the Lebanese crew.

Finally, I also would like to thank all my colleagues from BOKU with which I shared such amazing experiences throughout this journey. All the coffee pauses, parties, conferences and trips. Without them, such an experience would not have been the same.

Merci Novasep qui m'a offert l'opportunité de faire cette thèse de doctorat, merci tout particulièrement à Laurent qui a consacré beaucoup de temps à ma formation au début

Table of content

List of publications

Publication I

Mode and dosage time in polyethylene glycol precipitation process influences protein precipitate size and filterability

Pons Royo, M. d. C., Beulay, J.-L., Valery, E., Jungbauer, A., & Satzer, P. (2022). Mode and dosage time in polyethylene glycol precipitation process influences protein precipitate size and filterability. Process Biochemistry.

https://doi.org/10.1016/j.procbio.2022.01.017

In this work, I investigated the effect of the mode and dosage time of polyethylene glycol on antibody precipitation on product attributes and the resulting filterability of the precipitates. Results proved that sequential and continuous addition of PEG had several advantages over the conventional batch PEG addition approach and improved further purification steps.

Publication II

Milliscale reactors for integration of continuous precipitation and filtration

Pons Royo, M.d.C., Montes-Serrano, I., Valery, E., Jungbauer, A. and Satzer, P. (2022), Milliscale reactors for integration of continuous precipitation and filtration. J Chem Technol Biotechnol.

https://doi.org/10.1002/jctb.7187

In this work, I developed and designed millidevices to screen the necessary parameters for process setup in the smallest form factor possible. I used computational fluid dynamics (CFD) models to evaluate the millifluidic designs and scale-down parameters. I used such devices to determine the most appropriate precipitation conditions such as the dosage time of the precipitating agent and the resulting filterability of the precipitates in tangential flow filtration and depth filtration.

Publication III

Design of millidevices to expedite apparent solubility measurements

Pons Royo, M. d. C., Beulay, J.-L., Valery, E., Jungbauer, A., & Satzer, P. (2022). Design of millidevices to expedite apparent solubility measurements. Reaction Chemistry & Engineering. https://doi.org/10.1039/D2RE00022A

In this work, I developed and designed millidevices to determine solubility curves. The reactors had multiple injection points for precipitant that allowed a controlled and precise addition of the precipitating agent at different concentrations. The simple and flexible design allowed the reduction of the number of pumps required to only one for each solution and the distribution of the precipitating agent at different concentrations without valves. I demonstrated its applicability by determining the solubility curve using 2 industrially relevant precipitating agents, PEG6000 and $ZnCl_2$ of 4 antibodies and $CaCl_2$ to measure apparent solubility curves for dsDNA.

Publication IV – Submitted

Continuous precipitation of antibodies by feeding of solid polyethylene glycol

Maria del Carme Pons Royo, Tommaso de Santis, Daniel Komuzcki, Alois Jungbauer, Peter Satzer

In this work, I continuously performed protein precipitation by adding directly PEG6000 in solid form. I obtained yields and purity comparable to the conventional addition of 40 % PEG stock solution. With such a new approach, I showed a remarkably reduction in buffer consumption and equipment size. Production costs and footprint were also significantly reduced compared to conventional capture steps.

Additional contributions

Patents

WO2022083901 – Apparatus and method for the purification of biomolecules.

Pons Royo, Maria del Carme; Valery, Eric.

Abstract

Protein precipitation may be an alternative to conventional affinity capture of antibodies. Typically, protein precipitation is performed by direct addition of the precipitating agent in a single dose. Such approach does not consider co-precipitation of impurities and neglects the dynamics of precipitate formation and inclusion of unwanted impurities. To overcome such drawbacks, a gradual dosage of polyethylene glycol was proposed which impacted the final purity and yield. In addition, dosage time resulted in different filterability of precipitates. For continuous PEG addition, precipitation conditions need to be adjusted to improve product quality and inform about the design of further purification steps. To obtain all required data for scaling-up precipitation processes, devices for continuous protein precipitation were developed. Such a device has a size of 1–5ml in form of a tubular reactor with multiple injection points for controlled and precise addition of precipitating agent. Millidevices were used to study and determine the most appropriate precipitation conditions such as the dosage time of the precipitating agent, resulting filterability and the apparent solubility curves of antibodies and impurities. However, the main unsolved impediment to consider protein precipitation as an option at a large scale was the elevated buffer consumption. Therefore, a powder feeding device to directly add PEG in solid form combined with millidevices was used for continuous protein precipitation. Such an alternative process was economically and environmentally evaluated and compared to current state-of-art processes for the capture step. Total costs of goods and environmental footprint were significantly reduced. Findings presented in this work will help to expedite the development of fully end-to-end platforms for continuous bioprocesses. The economic and environmental assessment will help to guide the developers to more efficient and environmentally friendly processes.

Kurzfassung

Die Proteinpräzipitation kann ein alternative Technologie zum herkömmlich verwendeten ersten Aufreinigungsschritt für monoklonale Antikörper: Typischerweise wird die Proteinpräzipitation durch direkte Zugabe des Fällungsmittels in einer einzigen Dosis durchgeführt. Ein solcher Ansatz berücksichtigt nicht die Mitfällung von Verunreinigungen und vernachlässigt die Dynamik der Präzipitation und damit den Einschluss unerwünschter Verunreinigungen. Um solche Nachteile zu überwinden, wurde eine graduelle Zudosierung von Polyethylenglykol implementiert, mit der die endgültige Reinheit und Ausbeute verbessert werden konnte. Außerdem führte die Zugabe in Abhängigkeit zur Zudosierungsgeschwindigkeit zu unterschiedlicher Filtrierbarkeit der Präzipitate. Um alle erforderlichen Daten für das Scale-up von Präzipitationsprozessen zu erhalten, wurden Hochdurchsatz-Instrumente zur kontinuierlichen Proteinfällung entwickelt. Solche miniaturisierten Systeme wurden verwendet, um die am besten geeigneten Fällungsbedingungen wie die Dosierungszeit des Fällungsmittels, die resultierende Filtrierbarkeit und die Löslichkeitskurven von Antikörpern und Verunreinigungen zu untersuchen und zu bestimmen. Das größte ungelöste Hindernis, Proteinpräzipitation als Option in großem Maßstab zu implementieren, ist traditionell der große Puffer- und Wasserverbrauch, da das Fällungsmittel in Wasser vorgelöst werden muss. Daher wurde zur kontinuierlichen Proteinfällung ein Pulverzuführgerät zur direkten Zugabe von PEG in fester Form in Kombination mit den miniaturisierten Rohrreaktoren verwendet. Ein solches alternatives Verfahren wurde wirtschaftlich und ökologisch bewertet und mit aktuellen Verfahren nach dem Stand der Technik für den ersten Aufreinigungsschritt verglichen. Die CoGs und der ökologische Fußabdruck wurden dadurch deutlich reduziert. Die in dieser Arbeit vorgestellten Ergebnisse werden dazu beitragen, die Entwicklung vollständig kontinuierliche Bioprozesse zu beschleunigen.

Introductory overview

Protein precipitation become an interesting alternative to the costly protein A column for the capture step of monoclonal antibodies (mAbs). Herein, advances on precipitation as a purifying technology for mAbs will be presented. For further development and optimization of precipitation processes, novel devices will be described. Such devices mimic protein precipitation and further steps. In addition, the impact of implementing emerging technologies in the current process will be underlined. For a wider context of the applicability of precipitation, the current state of continuous process of biopharmaceuticals will be reviewed, with related topics such as regulatory aspects and economic and environmental impact.

Current status of continuous antibody production processing

Current mAbs production is based on hybrid processing which combines continuous and batch-wise unit operations. Such a process is more economically favourable compared to batch processes since it involves benefits from both mode operations, such as lowest consumables and medium costs (Figure 1) [2,3]. The production process of antibodies starts with the seed train to generate an adequate cell density to start the fermentation. The preferred production hosts for antibodies are mammalian cells, in particular Chinese Hamster Ovary (CHO) which are able to perform post-translational modifications [4]. However, antibodies have been successfully produced in a huge variety of production systems such as bacteria [5] and yeast [6]. Current mammalian cell lines present a doubling time of 20 – 30 hours and seed expansion require around 20-30 days to obtain enough cell density to inoculate a production reactor. Such slow doubling time results in an inefficient and inflexible process. Traditionally, cells were passed through increasingly larger cultivation systems until a certain cell density. However, such an approach was tedious and labour intensive which increased the risk of contamination. Thus, generating sufficient biomass to inoculate the production bioreactor was a critical part of the bioprocess. Currently, such seed train is intensified by retaining the cells into perfusion devices to accelerate the expansion and generation of high cell densities. When sufficient cells are available, the production bioreactor is inoculated at higher cell concentrations.

Different configurations can be used in upstream processing for cell cultures, batch, fed-batch, chemostat and perfusion. However, only the last two are operated in continuous and their use depends on the production host [7]. For example, continuous fermentations like a chemostat can be typically used for organisms with a fast replication rate, such as bacteria. In this design, fresh media is continuously added and cells are continuously removed. But this configuration

is not suitable for mammalian cell fermentation with a much lower replication rate and are susceptible to waste metabolites and media composition. In earlier stages, fermentations with mammalian cells represented the major bottleneck of the antibodies production. The main reasons were low yields and cell densities obtained, medium complexity, serum requirements and shear sensitivity [8]. In the past decades, upstream process has been significantly optimized with the improvements in culture media and cell line engineering. Such improvements allowed mAb titers to rise up to 10 g/L [9-12]. Furthermore, recent advances in cell retention enabled continuous fermentation with CHO cells by perfusion mode reactors. Perfusion systems consist of a reactor where cells are retained using different mechanisms such as continuous centrifugation [13], tangential flow filtration (TFF) or alternating flow filtration (ATF) [14-16]. Fresh media is continuously added while depleted media and waste metabolites are continuously removed [17]. Such a design allows cell densities over 200 million cells/mL and titers above 5 mg/mL [18]. Furthermore, such a system reduces the bioreactor size, increases the volumetric productivity and results in higher product quality consistency than in fed-batch reactors. Nevertheless, some drawbacks need to be also taken into consideration while operating perfusion reactors with mammalian cells. Due to the slow growth rate of mammalian cells, long-term fermentations, up to 90 days, are necessary to achieve sufficient cell concentration and high volumetric productivities. Long fermentation will increase cell debris and impurities such as host cell proteins (HCPs) and after certain aging mammalian cells undergo and productivity will change over time. Then, such fluctuations in impurities and product concentration will need to be assessed by the downstream process (DSP). Perfusion systems can be already found implemented in several industrial processes [19, 20].

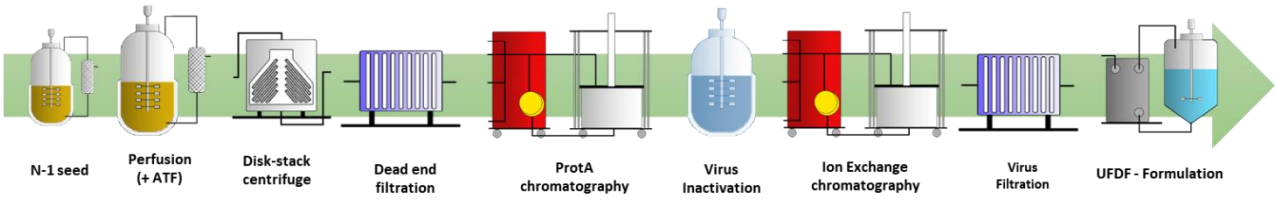

Figure 1. Flow scheme of a conventional antibody production process.

Continuous upstream processing is reasonably well established, but further development is still required to achieve continuous downstream processes [19]. The first step in a purification strategy is the primary recovery. In perfusion fermentations where the production system is coupled to a TFF or ATF for cell retention, no further primary separation is needed. Such retention systems will function as an effective cell removal step. However, for other configurations like chemostat or fed-batch such a step will be required. Typically, primary separation is performed by centrifugation or filtration. Centrifugation can be performed continuously in comparison to filtration, which is inherently a batch-wise operation. Filtration can be operated continuously by implementing different filters in parallel. While one filter is

used, a second filter is exchanged. However, such exchange operations can lead to sterility problems. Additionally, due to the improvements in fermentation technologies, larger and more complex burden are being placed on conventional clarification operations. To facilitate the clarification process, several pre-treatments can be used. For instance, the addition of flocculants such as Poly(diallyldimethylammonium chloride) (pDADMAC) to increase particle size and enhance their separation by filtration or centrifugation [21]. In addition, other impurities like dsDNA and HCPs will be also flocculated and removed during this step.

The next purification operation is the capture step by affinity chromatography which is typically the bottleneck in biomanufacturing and a significant contributor to the manufacturing costs of goods. DSP for antibodies is currently based on a series of chromatography columns set-ups which are primarily differentiated by the number of columns used and the loading sequence [22]. Some examples are the periodic counter-current chromatography (PCC) with 3 or 4 columns, multi-column counter-current solvent gradient purification (MCSGP) presented with 2 columns, simulated moving bed chromatography (SMB) with 8 columns and other parallelization or simplified technologies, which are operated in semi-continuous mode. Such technologies rely on optimizing column loading by overloading a column over the breakthrough point and loading the loss material in the subsequent column [22]. All columns follow the same operations and the cycle is continuously repeated. By increasing the number of columns and reducing the changing times, the process will be closer to a fully continuous operation mode. However, the system costs will increase since more expensive and complex equipment will be required and which will also increase the points of potential failure [23]. As well as resin stability and lifetime will need to be continuously validated. In the case of PCC, the elution phase can be continuous but for others in which the discharge is discontinuous, it is necessary to add a tank after the chromatography step to be able to provide a continuous flow to the subsequent unit operations. Even the high recovery and specificity, chromatography systems present several limitations such as low capacity, limited stability under operation conditions or scale-related problems. The latest improvements in the upstream process, with titers above 5 g/L [18], reduces significantly the performance of chromatography columns. Thus, more columns need to be added to cope with current titers. But this comes at expenses of much higher costs since the volume of resin and necessary instrumentation and equipment are also higher. Because of the price pressure over the biotechnological products is high enough, in the past years, non-chromatographic and titer-independent alternatives become more attractive to overcome such drawbacks. In the past years, other systems such as monoliths or membrane absorbers gained interest. These technologies remove limitations of particle diffusion of the chromatography beats since particles move by convection, resulting in faster volumetric throughput rates [24, 25].

At the end of the process, there are the polishing operations where two orthogonal viral removal operations are required. In batch mode, the product is concentrated in a hold tank and incubated for 30-60 minutes at low pH to inactivate viruses and then filtrated. Lately, both separations steps have been integrated in a single unit operation and adapted to be operated continuously by eliminating the intermediate hold tanks, using tubular reactors or using continuous flow through operations [26, 27]. The final operation is the formulation where the active drug is mixed with excipients to obtain the final product ensuring its stability. Formulation is typically done by ultra/diafiltration process. Since such operation do not requires intermediate hold tanks, this step has been already designed to operate continuously by using a cascade of membranes or a single-pass tangential flow filtration (SPTFF) [28].

Continuous manufacturing for biopharmaceuticals – current limitations

Since biopharmaceutical companies were obtaining sufficient revenues over the past twenty years, companies did not pay attention to costs and efficiency of manufacturing processes [29, 30], and innovation was mainly taking place in small companies or start-ups [19]. However, the biopharmaceutical market is, now, facing new challenges and uncertainties [2, 22, 31, 32]. Companies started considering more flexible and cost-effective manufacturing strategies such as bioprocess intensification (BI) and integrated continuous biomanufacturing (ICB). Such approach consist of an end-to-end continuous process enabling the continuous mass flow from the production bioreactor to the final downstream process (DSP) unit operation [33]. Regardless if it is process intensification or continuous manufacturing such improvements can meet the requirement for the market pressures [2, 3, 29, 34-39]. Many industries such a chemical or food industries have already switched from batch to continuous production to maximize process flexibility and minimize production costs [40-42]. In continuous processes, the production flow is operated uninterrupted from the supply of raw materials to the final product. Apart from costs reduction and flexibility, other benefits that bring such transition are the increase in productivity, more consistent product quality, more amenable to scale-up, automate and flexible to be adopted across different drugs and higher reliability and safety due to the continuous control and monitoring of the process and reduction of the environmental impact [9, 43-45]. Integrated continuous manufacturing has gained attention from the biopharmaceutical industry, but its implementation did not get impulse yet. One of the main reasons is the higher regulators and safety standards for pharmaceutical products [19]. Furthermore, there are still unsolved concerns regarding regulatory aspects, proper definitions of processes, process control and monitoring strategies. Besides the regulatory aspects, also the increasing interest in continuous manufacturing also highlighted the current limitations of its implementation.

Such limitations include the lack of authentic continuous unit operations, lack of process understanding or better performance in batch-wise operations in comparison to continuous. In response to the increasing interest in ICB, the US Food and Drug Administration (FDA) industry guidance already in 2019 included continuous manufacturing for biopharmaceuticals. These guidelines particularly outlined the implementation of real-time monitoring to address process and control [46] in line with quality-by-design (QbD) [47]. To be able to implement such technologies combining real-time measurements and model-based predictions such as process analytical technology (PAT), better process understanding and risk assessment is necessary.

A main technical concern is that a definition of "continuous manufacturing" does not exist. As well as other terms such as continuous, fully continuous, etc are not well-defined and are typically used for operations where the inflow or outflow, are not continuous. Some operations that are operated in semi-continuous or periodically are defined as continuous. In general, every unit operation in batch can be adapted to work continuously by adding hold tanks in between unit operations. But, in a real continuous process, unit operations should be integrated between units and hold volumes minimized. In addition, differences in residence time distribution (RTD) between units need to be considered to integrate all unit operations in a fully continuous process without the need of intermediate tanks to provide a steady state flow [48].

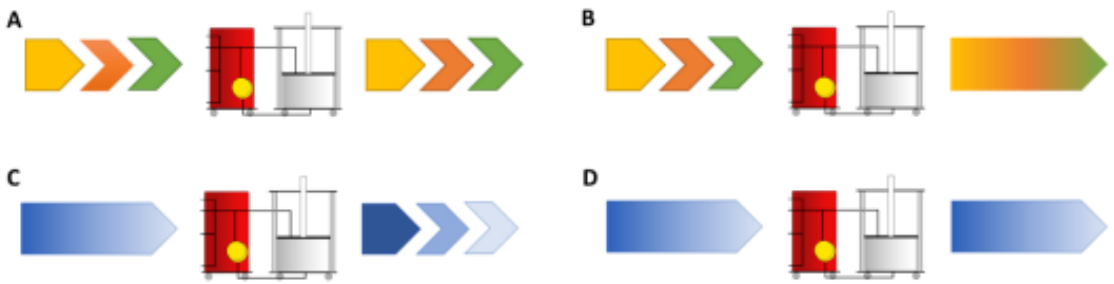

Figure 2. Graphical representation of the different operation modes. A) fully batch process B) semi-continuous process with a discontinuous inflow but continuous outflow C) semi-continuous process with continuous inflow but discontinuous outflow and D) fully continuous process where inflow and outflow are continuous. Published with permission of the author (Satzer [49], CC BY-NC).

Another technical concern is the interconnection between unit operations to have an operational end-to-end manufacturing process. Not only the different RTDs are a problem, but also the fluctuations in product and impurities concentrations. This can lead to major problems in downstream, since a common process using chromatography systems is designed to deal with constant product concentration. Such fluctuations can lead to a reduction in yield and purity. To investigate further limitations and to determine the suitability of a process, new scale-down models need to be developed and implemented [2]. Efforts from industries and universities are being made to solve all these

above-mentioned issues, an example is the EU project CODOBIO a research program focused on continuous downstream processing combining process control strategies, new process design and miniaturization of current technologies.

Another crucial element to consider during process development is the ecological impact. Since such an aspect gained more attention in the past years, Process mass intensity (PMI) a metric comparing the total resource consumption in mass per mass of a determined product, was developed. Such a parameter can be used to compare the environmental impact of different process scenarios bioprocesses. In the biopharmaceutical industry the main contributor to PMI is water consumption. Therefore, water must be reduced to improve not only process economics but also the environmental footprint. [50]

Non-chromatographic technologies

In the past years, several non-chromatographic alternatives have been investigated to replace protein A affinity chromatography. Crystallization [51], aqueous two-phase extraction [52, 53], membrane filtration [54] and precipitation [55-60] are some examples. Such technologies are widely used in the purification of small molecules and low-value products, and currently have been adapted for more complex products such as antibodies. One of the main advantages is that contrary to affinity columns, these alternatives increase selectivity and productivity with higher titers [28]. However, adapting such technologies entail additional challenges. For instance, the use of solvents for protein precipitation and extraction may produce changes in protein conformation or denaturation. Therefore, recent studies performed have been focused on finding suitable working conditions to preserve the native structure of the proteins during the process. Due to its simplicity and effectiveness, protein precipitation became one of the most attractive alternative technologies.

Protein precipitation

Precipitation is a unit operation widely used in upstream processing for the recovery of proteins from culture broths or cell homogenates. It is also applied in the downstream process for the recovery of low-value products and to remove impurities or subproducts from fermentations. Precipitation is an interesting unit operation at the beginning of the downstream process to reduce the volume to be processed and minimize the size and cost of the equipment for the subsequent processing steps. Precipitation can be used to remove the impurities or the target protein. Removing the impurities from the main target by precipitation is an easy operation since the main molecule should not be affected by the change of solubility and should remain in the solution preserving the native structure and functionality. When precipitation is employed

to precipitate the main product, the operation becomes slightly more complicated, since the protein structure and functionality can be affected and further resolubilization steps are necessary.

Protein precipitation is based on reducing the solubility of a protein below its solubility limits on which protein precipitates. The behavior of a protein under certain solution conditions is represented in a phase diagram (Figure 3). These diagrams are divided into 2 main zones: undersaturation, where protein is below the saturation limit and precipitation will not occur; and supersaturation where protein is at the maximum concentration that can be dissolved under certain solution conditions and precipitation will occur instantaneously. This last one is divided into 3 subregions: metastable zone, nucleation zone, and precipitation zone. In the metastable zone, aggregates growth will be promoted but not the formation of new nucleis. In the nucleation zone, nucleis will be spontaneously formed. The last region is the precipitation zone, at this point the protein reached the maximum concentration and it will precipitate in an uncontrolled manner forming amorphous aggregates.

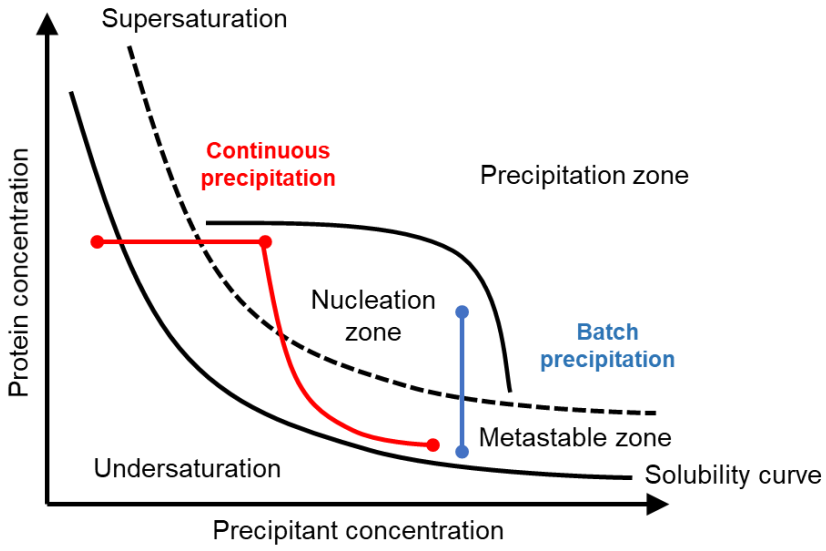

Figure 3. Phase diagram of protein precipitation/crystallization. Hypothetical pathways in continuous precipitation and batch are represented in red and blue lines (Adapted from [61, 93]).

Several methodologies are used to reduce the solubility of the desired product, such addition of salts, solvents, polymers, changes in pH, temperature or ionic strength. However, it also depends on the nature and concentration of the protein. Typically, solubility data that can be found in literature referrers to pure solutes and solvents. Since other factors such as concentration of impurities, precipitating agent, temperature, pH and ionic strength have a significant impact on solubility, solubility curves need to be determined experimentally. The solubility of the antibodies is lowered with the increase of precipitating agent concentration by

following a semi-logarithmic behavior without direct interaction with the antibodies [62]. Such behavior is given by equation (1).

$$logS = logS_0 - \beta c \quad (1)$$

Where S is the solubility of the protein, S_0 is the solubility of the protein in absence of a precipitating agent, β represents the slope of the curve and c is the concentration of the precipitating agent. This formula can be used to calculate the concentration of precipitating agent necessary to precipitate a protein under certain conditions. Furthermore, it can be also applied for impurities that typically show more flat curves. The differences in solubility at a certain concentration of precipitating agent can be exploited to obtain a product with higher purity [63, 64].

Methods for protein precipitation

In the biopharma industry, the most notable process where protein purification is applied is in plasma fractionation [57]. Protein precipitation is a well-established process for process purification, which was the first time described by Cohn and is still being used [65, 66]. The Cohn process is a series of purification steps based on adjusting pH, ethanol concentration, temperature and conductivity to precipitate each fraction based on the differences in solubility of the blood components. Due to the high specificity and recovery yields, the process was adapted to purify monoclonal antibodies [67]. Several organic solvents can be used for protein precipitation including ethers, acetone and alcohols [68]. The mechanism of ethanol precipitation seems to be due to a decrease of dielectric point, which results in dehydration of proteins [69]. This increases van der Waals forces between dehydrated proteins and as a consequence, proteins precipitate. Nevertheless, because the addition of solvents can lead to changes in the protein conformation, denaturation and loss of its biological activity, further alternatives were necessary to be evaluated. In addition, since ethanol is an inflammable compound that requires approved fire-proof facilities and extra operational measures, companies are reticent to use it [70].

Another precipitating agent with a long safety record in the pharmaceutical industry is polyethylene glycol (PEG) [57]. Already in the 60s, studies were made to investigate protein precipitation using non-ionic polymers like PEG. Nowadays, the use of such polymers has been widely extended for protein crystallization, precipitation and formulation studies. For example, PEG precipitation is already a well-established purification method for purifying IgG from human plasma, virus-like particles (VPL) and viral vaccines [71-74]. Recently, PEG precipitation has been also adapted for mAbs purification [56, 58, 75]. Besides PEG as a purification method, it is also combined with conjugated molecules to increase their time

circulation in the blood stream altering the pharmacokinetic profile. In addition, it can be widely found in a variety of consumer products such as cosmetics, food and pharmaceutical products [76]. PEG is a synthetic biocompatible polymer, which can be synthesized with a broad range of geometries, molecular weight and distributions. Depending on the molecular weight, PEG can be found in liquid form (< 1000 Dalton) or solid form (> 1000 Dalton). They are well miscible in water up to high concentrations due to their non-ionic and polar character, but resulting in highly viscous solutions which hinder their mixing and removal. The viscosity of PEG solutions is highly dependent on temperature. Since PEG solutions behave as Newtonian liquids, viscosity is also independent of shear rate. Another benefit of such a non-ionic polymer is that protein precipitation can be performed under mild conditions and without interacting directly with the protein, avoiding protein denaturation or activity loss.

PEG-induced precipitation is described by volume exclusion effect. PEG molecules exclude water from the water shell surrounding the protein surface. In consequence, proteins are concentrated in the remaining water molecules available and interactions between proteins increase, resulting in their precipitation. Studies have found that PEGs ranging from 3350 to 6000 g/mol are the most suitable for protein precipitation due to the resulting lower intrinsic viscosity and the minimal denaturation produced at room temperature. If the molecular weight of the polymer is increased, the protein solubility and the required amount of polymer for precipitation will decrease [3] but at the expense of higher viscosity. However, the hydrodynamic radius of PEG plays an even more important role in the efficiency of PEG precipitation, rather than molecular mass [64, 77]. Despite several studies have been performed, the mechanism behind protein precipitation is still not understood [74]. Apart from the excluded volume, several models such as steric exclusion have been proposed to predict the precipitation behaviour of the desired protein into a crude mixture. According to the theory of attractive depletion, PEG is sterically excluded from the surface of the protein, where PEG concentration is lower around the protein in comparison to the bulk. When two depletion zones overlap, a concentration gradient is formed resulting in attraction between proteins and their precipitation. Modelling and simulations can be used to reduce the number of experiments required and to gain a deeper process understanding [78]. However, even with the approximations obtained with such models, none of these models can reliably predict protein precipitation. Thus, precipitation process development and optimization rely mainly on experimental approaches.

In comparison to chromatography systems, precipitation has relatively lower selectivity within complex mixtures. Even precipitation can achieve high concentration factors, resulting precipitates may contain impurities that should be removed. To improve selectivity, differential or fractional precipitation has been developed by combining different precipitation

methodologies. PEG precipitation is strictly related to differences in size. If two proteins to be separated do not differ in size at least by a factor of two, other precipitation methods should be applied to increase the selectivity. Another method for protein precipitation is by using salts. The mechanism of using salts for protein precipitation like ammonium sulfate or $CaCl_2$ is known as salting-out. When salts and ions are added to a solution, the hydration layer between molecules is disrupted and the surrounding water moves to expose the hydrophobic zones of the proteins which leads to protein-protein interactions, causing precipitation and aggregation. For example, calcium chloride is combined with phosphate to form insoluble precipitates which co-precipitates large and negative molecules such as dsDNA, high molecular weight impurities (HMWI) and HCPs. In addition, precipitation with zinc chloride has been also reported [33] [18, 75, 79]. A suggested way of how might work is that $ZnCl_2$ form reversible bridges between proteins reducing their solubility, resulting in the precipitation of the antibodies. However, $ZnCl_2$ precipitation is highly influenced and affected by the media composition. Therefore, it cannot be always applied [80].

Differences in isoelectric points (pI) can be also exploited as a methodology for precipitation. Each protein presents a characteristic charge under determined pH conditions. Proteins can be positively or negatively charged depending on the amino acids that are composed of. At the pH which a protein has net charge of zero is known as the isoelectric point. Below that pH, protein will be positively charged and above this pH negatively charged. Because of the reduction in electrostatic repulsions, proteins exhibit their lowest solubility at pH near their pI. Hence, proteins of the same size can be separated if they present different charges at a determined pH. An example of this method is acid precipitation. Such precipitation method has been used to precipitate the remaining HCPs or cell culture broth clarification [21, 81, 82]. Mammalian cells are mostly positively charged while antibodies have a more neutral – basic pH around 7.8 – 10 [83]. Then, HCPs can be selectively precipitated from antibodies by adding acid and adjusting the pH to the pI of the HCPs. Another example is precipitations with caprylic acid (CA) [55, 84] [85]. CA was employed for the purification of antivenom from equine plasma and more recently in antibody purification [86]. The mechanism of CA precipitation is still not fully understood. Some studies found that CA interacts directly with the protein. The change in pH induces partial unfolding of the protein which exposes additional binding sites to which CA can directly bind. Then, when more CA molecules are incorporated in form of mixed micelles. Then, the interfacial surface of the protein becomes highly hydrophobic and induces protein-protein interaction with causes the precipitation of the formed complexes [87]. Combination of different precipitating methodologies allowed precipitation to achieve similar yield and purity to protein A chromatography.

Other protein precipitation methodologies

Charged polymers have been widely employed to optimize precipitation and clarification of cell culture broths. Some commonly used polymers are polyethyleneimine (PEI) [88], pDADMAC [21,89-90], chitosan and stimulus-responsive polymers, such as modified polyallylamine (mPAA) [91]. However, additional purification steps and analysis are necessary to verify their removal, since PEI, for example, is toxic. In addition, charged polymers could strongly bind to ion exchange columns, which interferes with other purification steps [92].

Another methodology for precipitation is by employing heat. This methodology takes advantage of differences in the melting point between impurities and the target protein [93]. By increasing the temperature, proteins will lose their structure, unfold, aggregate and precipitate. Such methodology can easily apply for the removal of impurities since protein structure will be irreversibly denaturized. This methodology has the drawback that the process must be able to deal with high temperatures without interfering with the target protein or other compounds in the broth.

Practical aspects of precipitation processes

As mentioned, precipitation is influenced by the nature and concentration of the protein, pH, temperature, etc. Such factors significantly influence the effectiveness and quality of the resulting precipitates, which will also impact their recovery. Particle characteristics such as particle size and size distribution (PSD), density, and mechanical strength [94-97] need to be considered during precipitation operation. From an ideal recovery point of view, stronger particles and narrower PSD are easy to filtrate than gelatinous or less strong particles with wider PSD. Precipitation consists mainly of two processes, nucleation and growth. During the nucleation phase, sub-micron particles are formed and during the growth, particles mature into bigger particles by colliding and aggregating with other particles [98]. Nucleation is the initial step during precipitation, where nucleais are formed. This process occurs within seconds and requires good mixing to obtain uniform distribution of the precipitating agent to avoid inhomogeneous distribution and formation of concentration gradients. Afterwards, nucleis will collide between particles forming bigger particles. This step can be promoted by mixing. After the agglomerates are formed those can still grow, and become stronger and denser particles. This can be due to chemical composition adjustments. However, at this step mixing should be less intense, since particles can break resulting in wider particle size distribution, which hinders further solid-liquid separation steps. As mentioned above, solid-liquid separations are more effective when particles are large and incompressible.

Batch versus continuous processing

The current focus of the bioprocessing industry is to achieve a successful shift from batch to continuous processing. Such a concern is reflected in the increased and renewed interest towards non-chromatographic alternatives such as protein precipitation. Precipitation is independent of the feed concentration [99] and it can be simply scaled-up just by increasing proportionally the amount of precipitating agent to a determined volume. Therefore, a single reactor can be used for different concentrations. Basic designs for protein precipitation are stirred tank reactor (STR) and tubular or plug-flow reactor for continuous operation. In STRs, the first obstacle during reactor design is to establish a proper mixing to start the nucleation without interfering with the optimal conditions for particle growth. All mixing vessels have an inhomogeneous power input and shear forces throughout the reactor. This changes the precipitate structure and will lead to further inconsistencies between small- and large-scale mixing vessels. Furthermore, traditional precipitation processes are based on the direct addition of precipitant in a single dose, which aggravates the mixing issues. Additionally, such precipitation mode has limited control on the co-precipitation of impurities with the main product and not considering batch-to-batch variations (Figure 3). Additionally, an excess of the precipitating agent in certain regions of the bioreactor will provoke difficulties during the resolubilization of the precipitates.

Several reactor designs have been proposed to overcome such drawbacks. Since precipitation consists of mixing a protein solution with a precipitating agent up to a certain concentration, an interesting reactor design for protein precipitation is a tubular reactor. Such operation can be easily adapted to work in a fully continuous mode without interrupting the mass flow for the product by using a tubular reactor [59, 75, 100]. Such a reactor can be simply modified to achieve a determined residence time by changing the tube dimensions or the flow velocity through the reactor. Another design is the coiled inverted reactor [101, 102], which promotes a secondary flow pattern that enhances radial mixing, simulating a plug-flow. Since nucleation and aggregates growth are governed by different mechanisms, several studies proposed a two-reactor process for each step. However, such reactors are still designed for a single addition of precipitating agent, which will cause the above-mentioned issues. To overcome the above-mentioned drawbacks, new precipitation strategies and reactor designs need to be tested to limit the co-precipitation of impurities and improve particle characteristics. For example, multiple additions of precipitating agent [58, 102]

Economic analysis – Limitations in precipitation-based processes

Several economic analyses comparing different alternatives for the capture step have been performed. Such studies showed that precipitation-based processes can economically compete with conventional downstream processes based on chromatographic systems [99]. However, even with the economic and performance benefits, protein precipitation is not widespread in the biopharmaceutical industry. Economic analysis revealed that the main contribution to CoGs (Cost of goods) is dominated by materials, more specifically the large amounts of stock solution of the precipitating agents [99]. During precipitation, protein solution is constantly diluted with a stock solution of precipitating agent up to a concentration where precipitation conditions are reached. Because of the constant addition of the precipitating agent, the initial product is constantly diluted and the final volume to be processed increases, as well as, the size of the equipment, facilities and costs. Additionally, such large volumes significantly impact on the costs and footprint associated to HVAC (Heating – Ventilation – Air Conditioning) energy consumption and water processing by cleanrooms and storage areas. To reduce such dilution effect during precipitation, stock solutions need to be near to the maximal solubility. But in the case of a precipitant such as PEG, it requires long mixing times and the viscosity increases significantly. Therefore, process design needs to be adapted to be able to handle such highly viscous conditions during pumping and mixing [97]. Despite the benefits that precipitation can add to reduce downstream process costs, volume reduction is a requisite to attract further industries to implement precipitation.

Solid-liquid separation

After precipitation, precipitates should be recovered or removed from the main solution. Two main options are currently available for liquid-solid separation, centrifugation and filtration. Separation by centrifugation is based on differences in density of the components. Centrifuges are available to work fully in continuous in comparison with filtration, for example, disc-stack centrifugation [103], tubular bowl [104] and multi-chamber bowl centrifuges [105]. Centrifugation of biological solids can be difficult due to particles tending to be small and the suspension fluid relatively viscous. Thus, the difference between densities is considerably small and centrifugation performance is significantly reduced. Additionally, the use of centrifuges to recover protein precipitates, may compact the resulting aggregates and difficult further resolubilization. Therefore, resolubilization will require long and vigorous mixing, leading to aggregates or denaturation of the proteins. Furthermore, during the centrifugation process, shear forces may break the larger particles into smaller particles, complicating further separation steps. Filtration is therefore more attractive for solid-liquid separation since avoids the compaction of precipitates. Nevertheless, further drawbacks need to be assessed such as

the increase of viscosity, which reduces the mass flow through the membrane [75], and reduction in filter capacity due to wider particle size distribution of the aggregates. Furthermore, the resulting characteristics of the aggregates such as density or compactness will have a significant impact on filter performance.

Filtration

Filtration is a versatile unit operation that can be used in different stages during the downstream of a molecule. It is used to separate components such as cell and cell debris from a broth, concentrate a target protein, remove viruses, exchange buffers or desalting, etc. Compared to other solid-liquid separations, filtration presents several benefits such as low energy requirements or no need to use solvents or harsh chemicals. Filtration is based on differences in particle size between components. A fluid is passed through a filter, particles with bigger particle sizes than the pore size of the filter will be retained while smaller particles will flow through. There are two modes to perform filtration, dead-end filtration, where the feed flows orthogonally to the filter layer and tangential flow filtration, where the feed flows parallel to the filter membrane. Dead-end filters are not recommended for processes where the main product is precipitated, since the target product will be retained in the filter and in most cases retained particles cannot be flushed away. In addition, such filters are not suitable for working in continuous mode, since the filter will be filled with precipitates and the flux will decline over time. However, this operation can be adapted to be fully continuous by implementing a series of filters in parallel. During, dead-end filtration the filtration rate is greatest at the beginning since there are no deposited solids and filter resistance is 0. Filter resistances increase with the cake thickness depending on the structure of the particles and how are deposited. For example, incompressible particles in a low viscous solution are easy to filtrate. Some precipitating agents such as PEG or ammonium sulfate produce aggregates with similar densities to the surrounding liquid, which complicates further processing. Many protein precipitates are also colloidal or gelatinous, which creates extra equipment and handling difficulties.

In TFF, precipitates can be easily recovered and resolubilized. Precipitates remain circulating in parallel while impurities are flushed away. Furthermore, the material that is accumulated in the membrane is flushed, which prevents the decay of permeate flux through the filter membrane. TFF can be operated in a two steps set-up consisting in a concentration step, where the buffer is removed and the targeted product is concentrated and a second step where precipitates are washed out of impurities [75, 106]. However, filtration can only be fully operated in continuous mode when using single-pass tangential flow filtration or a series of multiple filtration units in a cascade. Even TFF prevents the formation of filter cake, a thick

layer near the membrane, known as the concentration polarisation layer, can be formed and reduce the flux during filtration. In a TFF operation, a pump is used to generate a feed flow across the membrane surface. The generated pressure creates a pressure gradient that forces solutes to pass through the membrane by convective flow. However, when larger particles attempt to flow towards the membrane, those are rejected and remain near the surface of the membrane creating the polarisation layer. Therefore, at the start of the operation when the pressure is low, flux is pressure dependent but when the pressure starts increasing due to the accumulation of materials, flux becomes mass-transfer controlled. At that stage, mass transfer is controlled by the rate at which the material retained in the membrane is transported back to the fluid [97].

Several strategies can be used to improve mass transfer and filterability without the need for increased operational pressure. Such as:

- Increasing the filter area or the porosity to reduce cake resistance.
- Increase the average size or keep particle size distribution with minimum variations.
- Improve particle characteristics such as density or compactness
- Increase the flow velocity across the membrane to enhance mass transfer.
- Change the properties of the fluids such as viscosity or density by reducing the

Nevertheless, since the characteristics of the particles significantly influence the filtration performance and excessive or insufficient mixing results in particle breakage or broad particle size distribution, improving filterability starts on the precipitation step.

Scale-up and scale-down for precipitation processes and filtration

During process development, it is essential to acquire all relevant data. Process scale-down offers the opportunity to investigate and evaluate several process parameters by minimizing the development costs and time [107]. During scaling-down, is essential to be able to mimic the operation conditions to bring them to different scales, ensuring identical operation conditions [108]. When scaling-up and -down precipitation-based processes, two main operations need to be considered, the process of precipitation by itself and the recovery of the precipitates by filtration. Filtration processes are typically scaled up linearly. Basic process parameters such as the transmembrane pressure, fluid velocity, etc, can be easily determined on lab scale and applied at large or smaller scales. If filter characteristics such as filter material, pore size or geometry are kept the same between scales, filtration performance should be also the same. For example, for depth filtration, the filtration area is simply increased and other filters can be parallelized to achieve continuous processing. For TFF, instead of increasing the size of the membranes, it is typically scaled-up by increasing or decreasing the number of membranes.

This is because if membranes are excessively large, the pressure drop between the inlet and the outlet can be a limiting factor during the operation [97]. The pressure-build-up during filtration indicates the maximum possible load on a specific filter size and therefore determines the necessary scalable filtration area for a given process.

Because of the simplicity of scalability of filtration and operations, flocculation becomes the key operation during precipitation and for further solid-liquid separation. It is a complex process where several mechanisms and variables are involved, such as the initial concentration of impurities, flocculation time, flocculent dosage, temperature, reactor and impeller design, etc. [109]. Flocculation processes have been typically scaled up by using the Camp number (N_{Ca}), which considers that flocculation performance at any vessel can be achieved by mixing at the same average velocity gradient during a determined time. But flocculation is affected by several variables and consists of many mechanisms. Thus, it is necessary to apply a multidimensional approach, instead of a simple Camp number approach. For example, by increasing the mixing intensity particle collision is promoted and accelerated the formation and growth of the precipitates. But if agitation is excessively intense, turbulent shear forces will break the flocs into smaller particles, which also will difficult the recovery of the precipitates. Breakage of the flocs occurs mainly in the impeller region, where the greatest energy dissipation rate is. Then, it is essential to consider the number of flocs passing though the impeller region [109]. Hence, the same flocculation time should be kept similar between two flocculation processes to provide the same passages of the floc on the impeller region. Mixing intensity also needs to be considered since floc growth and breakage are also affected. The acting forces are proportional to the local energy dissipation, which can be approximated to the power input of a specific impeller. Therefore, constant power input should be kept similar between two flocculation processes. Furthermore, the chemical environment has also a significant impact on flocculation and it is typically characterized by the flocculent dosage. Thus, another scale-up correlation is keeping a similar dosage time between two flocculation processes. By fulfilling these criteria, the same flocculation results should be obtained at different scales [109, 110]. For flocculation screenings the scale-down is limited. Therefore, new scale-down models need to be developed to ensure the critical process parameters for fast and efficient process development.

Miniaturization and microdevices

Miniaturization dates back to the early 60s in the industry of microelectronics, but it was not until the 90s when the first microfluidic device was manufactured. Such a device consisted of a gas chromatographer with a 1.5 m microchannel engraved in silicon [111]. Since then, the field of microfluidic devices has grown dramatically. The main reason for such an increasing interest is the need to attain reliable and robust autonomous systems to obtain all required information of a process or system, reducing time and costs. In the biopharma sector, a considerable part of the company budget is spent on R&D. Due to current pressure over the market, companies require fast and low-cost methodologies to obtain novel products as soon as possible to remain competitive [29]. Over the last 20 years, high-throughput screening (HTS) technologies have been used for process development, which already reduced the cost and time of research and development. However, further cost reduction is still needed [112]. Additionally, not all unit operations can be properly scaled-down or two unit operations cannot be integrated for further optimization [113, 114]. The possibility to integrate several units, control and automation systems into microdevices, triggered the attention of researchers from different fields such as bioprocesses, synthetic chemistry and biology. The exponential growth of this field resulted in considerable advances in fields such as medicine, chemistry and biology [115].

Microdevices for scale-down precipitation processes

The transformation towards continuous and integrated manufacturing goes through a better process understanding. To swift from batch to continuous process, it is essential to perform continuous experiments, because not all the engineering and scalability parameters can be estimated form batch experiments. Furthermore, such a process can be even more challenging when the outcome of one unit operation highly influences the subsequent unit operation. Continuous experiments require long experimental times which translates to larger amounts of materials compared to batch. Hence, miniaturized systems become a crucial technology to perform such experiments. Processes can be studied under real working conditions, obtaining all the relevant data during the early-stage development. Downscale devices present several advantages over macroscopic systems, such as the reduction of material required and development time [116-119], automation in lab operations which minimizes human experimental errors and increases throughput analysis of experimental conditions. As mentioned above, precipitation and flocculation are affected by several parameters that need to be considered to implement protein precipitation at larger scales. However, the amount of material to perform a single experiment is around 600 mL [75] (Figure 4), which is inconceivable during early-stage development.

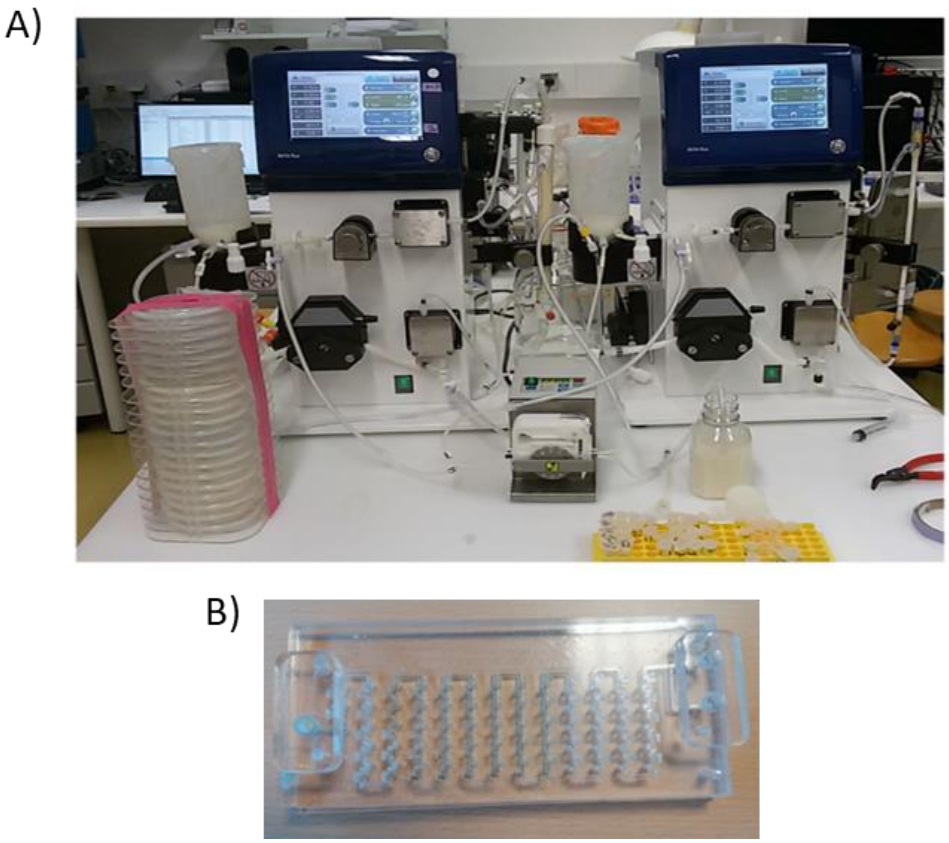

Figure 4. A) Set-up of continuous precipitation connected to a filtration set-up. B) Miniaturized system of the continuous precipitation set-up. Image A is extracted from [75].

Therefore, microfluidic devices are an interesting technology to overcome these drawbacks. However, microdevices are still a novel technology and all its benefits are not fully optimized. Scaling down processes to the limit has other disadvantages such as changes in flow patterns, adsorption in the microchannels, evaporation and complexity increase and the integration of multiple devices instead of only individual components. Because of the rigidity of several materials and the limited performance of miniaturized equipment, valves, pumps or connections cannot be easily integrated and must be combined with more flexible materials such as Polydimethylsiloxane (PDMS) [120]. The addition of microvalves or micropumps will increase manufacturing costs and the complexity of the design of the device [121]. Another key limitation factor in microfluidics fabrication is the lack of clean rooms and specialized training, which limits the accessibility for many scientists. Therefore, new scale-down models need to be developed to ensure mimicking the critical process parameters for fast and efficient process development, keeping the design simple and low-cost.

Microdevices – Theoretical aspects

Microfluidic can be defined as the study of fluid behaviour such as flow or mixing at miniaturized scale. Because physical properties in microdevices differ from those occurring at the macroscopic scale, while designing microdevices fluid properties need to be considered.

- **Flow regime:** In microdevices only laminar flows occur, contrary to flows observed at larger scales [122]. Flow behaviour can be described by the Reynolds number (Re), which considers fluid features such as density, viscosity, velocity, etc. For Re > 2000 is considered laminar flow. But in the case of microfluidics, Re is well below. Working at such low numbers in microdevices implies difficulties during mixing processes. To overcome such drawbacks, turbulences and dean vortexes are induced by complex geometries, such as 3D serpentines [123, 124].
- **Diffusivity:** Because of the low Reynold numbers in microfluidics, mixing is mainly driven by diffusion. But since the channel size is much smaller, the diffusion time will be reduced in comparison to traditional laboratory methods such as microplates [117].
- **Surface-to-volume ratio:** The ratio between the surface to the volume of a substance that passes through at a determined time is much higher than at larger scales. It has a significant impact because flow patterns differ and mass transfer enhances as the dimension of the device is reduced, which accelerates diffusion processes. Therefore, it needs to be considered while scaling-up[125].
- **Pressure-driven flows:** Several strategies are used to move the fluids through the channels such as capillarity, gravity-drive, electrokinetic flow, etc. But the most commonly used and easy to operate are pressure-driven flows. The flow is characterized by a parabolic profile with the highest velocity in the center of the channel and the velocity at the walls is considered zero [129]. However, pressure-driven flows present certain inconvenient such as the hydrodynamic fluidic resistance, hydrodynamic dispersion of the samples [126-128], etc.

Microfabrication – Materials and Technologies

The increasing interest over the past decades in miniaturizing chemical and biological processes pushed the development of new and emerging materials and technologies for manufacturing microfluidic devices, also known as Lab on a Chip (LOC). Although the wide range of materials and technologies available is an advantage, the selection of the most suitable material for each particular application should be carefully evaluated [129, 130]. The selected material must be compatible with the used chemicals, process temperatures,

biochemical and biophysical methods and further functional elements involved. Not only the features of each material but as well, the manufacturing costs must be considered, since typically microdevices are used as disposables, such devices should be inexpensive and able to be mass-produced. Some of the typical materials used are glass, PDMS, silicon or thermoplastics such as Poly(methyl methacrylate) (PMMA), Polystyrene (PS), Polycarbonate (PC), etc. In addition, new methodologies still need to be developed regarding microfabrication such as sealing, interconnections, integration of pumps, detection, etc [131, 132].

Some of the first substrates used for microfabrication were glass and silicon. Technologies for both materials are already well-established since both were applied for a long time in the microelectronic industry. The manufacturing process consists of photolithography or etching of a wafer coated with a photoresist which is irradiated with UV to transfer a micropattern to a photoresist mask. Another substrate extensively used in the fabrication of microfluidics is PDMS due to its ease and low cost of microfabrication. PDMS is an elastomer consisting of a cross-linked polymer chain. It is characterized by its gas permeability, elasticity and versatility, which makes this material suitable for a wide range of applications including biologic systems. Microdevices can be produced by several techniques such as negative molding, cutting, or simply bonded to others via plasma activation to other PDMS or other materials like glass or silicon. PDMS can be also found in liquid form which can be cured at mild temperatures and cast with nanometer resolution by using photoresist templates. However, PDMS presents several limitations, for instance, the integration of sensors, water evaporation, sensitivity to certain chemicals, absorption of small hydrophobic molecules, etc. Due to the limitations of PDMS and its high costs, thermoplastics become a popular substrate for mass-production of microfluidic devices. Thermoplastics can be easily designed and cut by laser cutting systems which provide precise and reproducible results, micromilling or hot embossing. Thermoplastics can be mouldable when reaching the glass transition temperature (T_g) and recuperate their characteristics when cooled down [133]. Because of these properties, thermoplastics can be easily bound by applying constant and controlled heat and pressure. Several thermoplastics can be found in the market depending on specific requirements. The most common thermoplastics are PMMA, PS, PC and Cyclic Olefin (Co-) Polymers (COP/COC) [134, 135]. However, such materials are not suitable for operations where aeration is required due to the low gas transfer, such as cell cultures. Another substrate that was originally developed for electronic devices is Low-Temperature Cofired Ceramics (LTCC). LTCC are ceramics constituted by glass and Al_2O_3 and sintered at lower temperatures compared to conventional ceramics. Such material eases the integration of fluidic and electronics by creating multilayers.

To even further reduce manufacturing costs, in the past years new materials have been released in the market. For example, paper-based devices [136], which gained interest due to

the noteworthy low cost and operation requirements, or hydrogels [137]. Paper-based microdevices are characterized by having high porosity which enhances liquid thread. In contrast to other materials, paper-based material channels are not closed. The surface is modified hydrophobically and the aqueous solution is precisely conducted through the hydrophilic areas. However, detection methods in such devices are relatively limited compared to other materials. Typically, colorimetry is the most used detection method.

As mentioned, hydrogels are also a promising alternative for developing microdevices mimicking biological systems. They consist of a 3D extracellular matrix made of hydrophilic polymer chains. Such matrixes are highly porous, which allows the diffusion of small molecules through the membrane [132]. Such materials are mainly used mainly in 3D cell culture for tissue-engineering.

Other prototyping tools

A part from microfluidic devices, in recent years, other emerging open-source technologies and prototyping tools have been developed [138]. Tools such as laser cutters and 3D printers become essential in many laboratories. Such technologies increase the scientific capacity and empower researches to design and customize devices depending on their needs. Before these technologies, designing and prototyping devices would have been dependent on third parties and probably at high costs, which limited the applicability of trial-and-error approach to optimize and design devices.

There are three types of laser cutting, but the most commonly used is the CO_2 laser [139]. It is suitable to cut, engrave and boring. The laser beam is produced inside a crystal tube filled with gas, which reacts and increases the energy creating heat. The light is reflected along the tube to increase its intensity. When the light becomes powerful enough, the light is redirected outside by several mirrors and through a focus lens to the working material. The mirror system is combined with a control unit which allows the laser head to move in a different direction, creating different patterns and shapes.

Figure 5. CO_2 laser cutter from Trotec Q500 for rapid prototyping (Picture extracted from www.happylab.at).

3D printing or additive manufacturing is a technology that allows the construction of objects in three dimensions from computer-aided design (CAD) models. A huge variety of materials that can be used and processes in the way of layers are created [140]. The most-commonly used techniques are fusion deposition modelling (FDM), stereolithography (SLA) and digital light processing (DLP) [112]. In FDM, the material is in form of a filament that is melted o softened and extruded to create different layers that solidify immediately. In SLA, photopolymers, epoxies, etc are photopolymerized using a laser which hardens the liquid material forming a solid part. Contrary that DLP, the polymer needs to be cured with UV light after it is jetted.

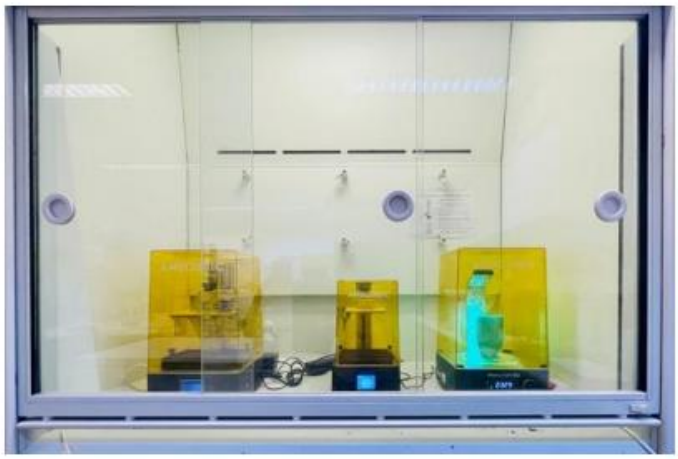

Figure 6. SLA 3D printers (left and middle) and curing station (right). (Published with permission of the author Komuczki).

Such technologies can be combined with previously mentioned miniaturization techniques and open-source microcontrollers to build up more complex devices [141]. The availability of biopolymers allowed to transfer of such techniques to biotechnological applications such as the development of microbioreactors for cell culture [142] or 3D printed columns for chromatography processes [143]. Undoubtedly, further challenges in bioprocesses will be assessed by novel and disruptive technologies.

Objectives

The overall objective of this work was to debottleneck current restrictions in development and optimization of continuous precipitation process for purification of antibodies by developing and optimizing laboratory devices. Such devices at millilitre scale should be able to rapidly and cost-effectively screen precipitation and filtration conditions. Therefore, it was aimed to develop and fabricate devices using innovation prototyping tools such as laser cutting tool or 3D printing and employed for purification of antibodies.

The following objectives were defined:

- Investigate and identify the key parameters with high impact on precipitation and filtration. Propose engineering approaches and reactor geometries to improve the purification process.
- Develop and demonstrate a continuous protein precipitation and compare on quality properties of the products compared to batch-wise process. Determine if continuous manufacturing led to more consistent product quality.
- Develop and characterize milliscale fluidic devices capable of mimicking critical process parameters for fast and efficient process development.
- Evaluate economical and environmentally a continuous precipitation process and compare it to current state-of-art methodologies used for antibodies capture step. Identify the process limitations and propose and demonstrate alternative processes for protein precipitation by using rapid prototyping tools.

Contributions

Findings of this work are presented in this doctoral thesis and four publications. The first article was published in Process Biochemistry with the title “Mode and dosage time in polyethylene glycol precipitation process influences protein precipitate size and filterability”. A sequential addition of PEG was proposed to circumvent the limitations of single addition of precipitating agent. Furthermore, its effect on further separation steps such as filtration was investigated. The second article was published in Journal of Chemical Technology & Biotechnology, entitled “Milliscale reactors for integration of continuous precipitation and filtration”. Millidevices were designed and developed as screening tools to obtain all relevant process data in the smallest volume possible. Such devices were used to determine the optimal dosage time for higher purification factors and resulting filterability. Its applicability was extended to other uses such as determination of solubility curves for antibodies and impurities. Results were published in a third article in Reaction Chemistry & Engineering with the title “Design of millidevices to expedite apparent solubility measurements”. The last article was submitted in Separation and purification technology with the title “Continuous precipitation of antibodies by feeding of solid polyethylene glycol”. In this article limitations of precipitation-based processes were assessed. The analysis concluded that the amount of buffer preparation, storage and clean rooms were the major economic and environmental limitations. Prototyping tools were used to overcome such limitations by proposing a new PEG precipitation process using PEG in a solid form, reducing buffer consumption, manufacturing costs and environmental impact.

Paper I - Effect of dosage mode on protein precipitation

Traditional precipitation processes are based on direct addition of precipitant in a single dose, with limited control on co-precipitation of impurities and not considering batch-to-batch variations. In previous studies, continuous addition of PEG6000 presented several advantages to the convention batch addition of PEG6000 [58]. However, the impact of resulting precipitates on subsequent purification steps was also omitted. In this first publication (Publication I), the effect of mode and dosage time of PEG6000 on particle size distribution, fractal dimension and its effect on process parameters such as yield and purity was evaluated. Furthermore, the 3D structure of the precipitates was studied by fractal dimension analysis to determine the precipitate properties such as strength and compactness and its influence on further solid-liquid separation by TFF and depth filtration.

Protein precipitation was performed by adding 40 % PEG stock solution in a single, gradual or stepwise addition for 5 and 15 minutes (Figure 7).

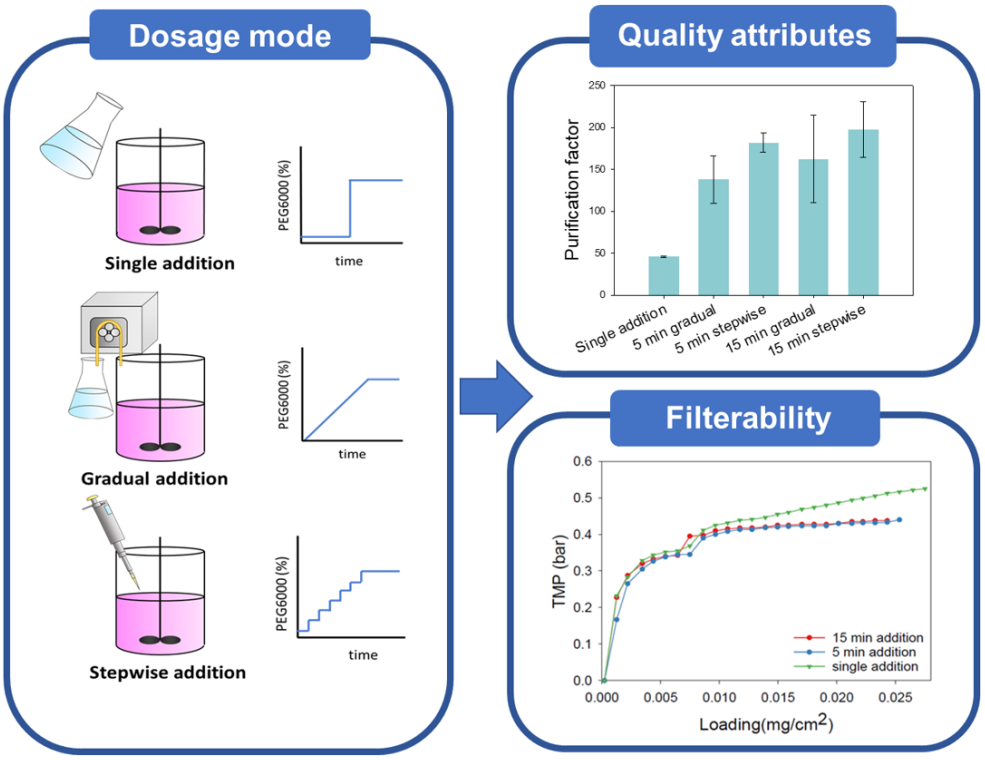

Figure 7. Experimental setup of the single addition, gradual and stepwise PEG6000 addition. Extracted from Pons Royo et al.[144]

The particle size and particle size distribution were evaluated using an FBRM sensor which monitored the mean particle size for 4 different antibody solutions. FBRM results showed that short additions of PEG resulted in higher median PSD, whereas longer additions showed the opposite result. There were no differences in the PSD when PEG addition was performed in gradual or sequential mode. However, when PEG was added in a single addition, the median chord length increased significantly by a factor of 1.8 at the expenses of wider PSD. The resulting precipitates were evaluated by size exclusion and protein A chromatography to determine the purification factor. Higher purification factors were obtained when precipitation was performed in gradual and sequential mode for 5 and 15 minutes compared to conventional single addition. To get an insight into the homogeneity of the fractal characteristics of particles and characteristics such as compactness and density were assessed. Furthermore, to evaluate the filterability of the precipitated solutions in terms of maximum possible load and built-up pressure depending on the precipitation mode, precipitated solutions were filtrated through a depth filter. Since for recovery of antibodies, TFF is a more suitable option, the built-up pressure method was also assessed through a TFF. For both filtration modes, gradual addition of precipitating agent reduced pressure on the filter and increased the loading capacity on the filters. Therefore, larger volumes can be processed, reducing operational costs. Precipitation methodology can be adjusted to improve the product quality attributes and improve further purification steps. Such a study highlighted the importance of connecting unit

operations during the design of continuous precipitation processes, as it was clearly observed the mode of precipitation had a remarkable influence on the next filtration steps. It also highlighted the importance of implementing methodologies capable of generating size distributions, density distributions and fractal dimension distributions to assess precipitation behavior. Such methodologies could be used to adjust the precipitation methodology to improve the product quality attributes and inform about the design of further purification steps.

Paper II - Millidevices for dosage determination

After demonstrating that the mode and addition time of precipitating agent affect the final purity and further purification unit operations, the second publication (Publication II) was focused on designing and developing millidevices for screening precipitation conditions. Such millidevices were able to determine the optimal dosage time for higher purification factors and improved filterability. Millidevices were designed fulfilling certain requirements such as low total volume, 1-5 mL and residence time between 1 - 5 min. Due to the limitations in-house, devices were manufactured from PMMA layers by laser cutting. Proper bonding is indispensable for layered devices to avoid leakages, which has a big impact on their performance and reliability. PMMA layers were adhered to each other by heat binding and applying slight pressure (Figure 8).

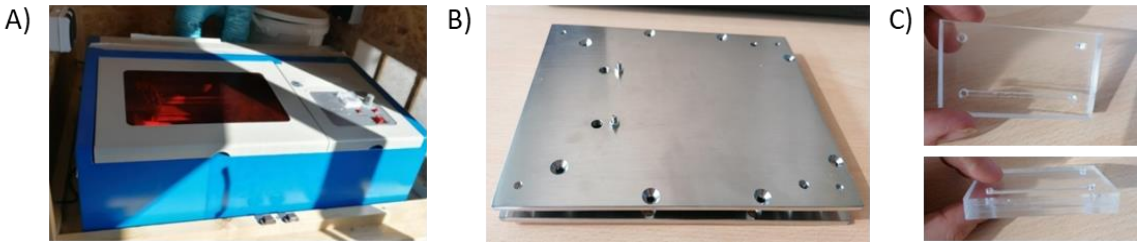

Figure 8. Millidevices were designed using CorelDRAW 2020 (Corel Co., Canada) and laser cut (Laser Trotec Speedy 100, Trotec GmbH, Austria). The microchannels were 1 mm wide and 3 mm deep. The main mixing channels and injection microchannels were cut in 3 mm and inlets and outlets in 4 mm poly(methyl methacrylate) (PMMA) sheets (Acrylstudio GmbHW, Austria). The PMMA sheets were heated to 165 ◦C for at least 45 min and cooled down at room temperature. Prior to the bonding process, PMMA sheets were cleaned by rinsing with 70 % ethanol.

Since antibody precipitation is performed by 40% PEG solution which is characterized by its high viscosity, vigorous mixing was required. Mixing in microscale devices is highly limited due to the low Reynold numbers and absence of turbulences. To overcome such limitations, instead of microdevices, devices were designed in a slightly bigger size. To determine the most appropriate mixing design for the devices, different geometries were designed in AutoDesk inventor. Each geometry was studied by CFD calculations in terms of mixing performance, power input, pressure drop, shear stress and Camp number. Detailed information regarding the CFD simulations can be found in Publication II. CFD allowed for predicting parameters such as the mixing behavior of the fluid flows and other hydrodynamic phenomena, essential for further scaling-up. Such studies enhance the development of devices in the early stages without the need for a trial-and-error approach. In addition, to ease its useability, devices were designed to minimize the number the pumps required and without valves. Furthermore, the devices integrated a standardized female Luer lock system which allowed to be directly connected to typical laboratory equipment, without the need for flexible materials such as polydimethylsiloxane.

Devices consisted in the main mixing channel where the precipitating agent and protein solution are mixed and which was modified depending on the experimental time required (1, 2, 3 or 5 min) and a main channel for the precipitating agent. Both channels were coupled by a dispensing system consisting of multiple additions points grouped along the surface of the mixing channel. This dispenser allows a continuous and controlled addition of the precipitating agent along the device without valves and avoiding oversaturation of the precipitating agent (Figure 10). Devices were designed to add the precipitating agent smoothly, addition points were divided in 5 regions corresponding to 1/5 of the total time of the plate.

A) B)

Figure 9. Design of the multiple precipitation devices. A) Mixing channel for the addition of solution to be purified, b) the main channel for the precipitating agent, c) example of addition channels distributed along the surface of the mixing channel connecting the mixing channel with the main channel for the precipitating agent. Figure retrieved from Pons Royo et al. [145]

A) B)

Figure 10. Multilayer milidevices with multiple additions at different layers showing a) main channel to introduce the precipitant agent continuously injected at different points along the mixing channel and b) addition channels grouped in addition zones along the surface of the mixing channel. Figure retrieved from Pons Royo et al. [145]

Millidevices were used to evaluate the effect of time addition of PEG on the final purity with two antibody supernatants. Protein precipitation was performed by single addition or gradual addition of 40 % PEG at different times (Figure 11). Findings showed an increase in the purification factor of 3-fold and 5-fold higher purification factor for both antibody solutions when PEG was added during 3 and 5 minutes compared to other dosage times. Such results corroborated findings on Publication I. Furthermore, results showed that the designed milidevices can be used to determine the most appropriate dosage time to reduce co-precipitation of impurities during precipitation.

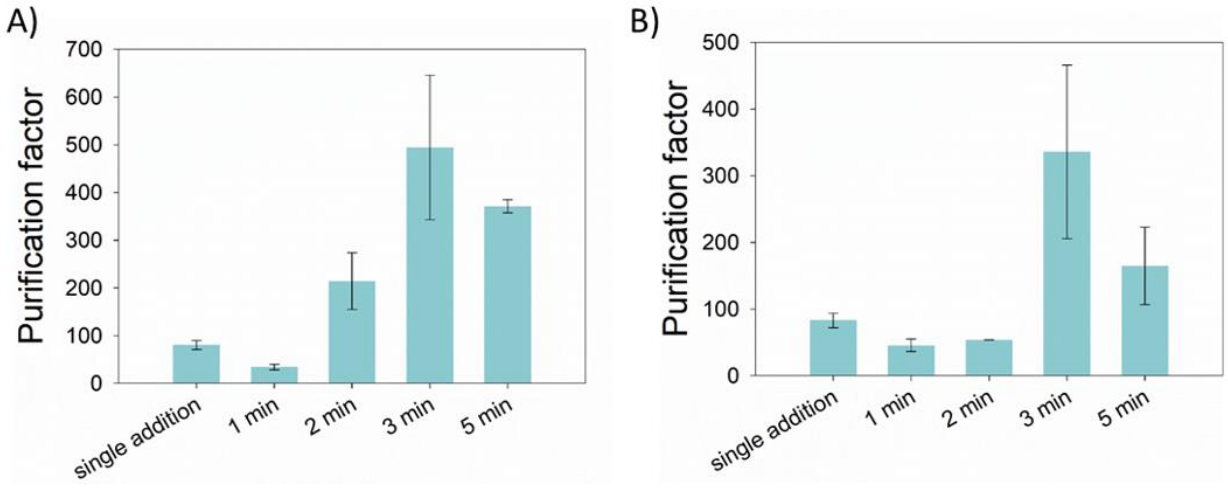

Figure 11. Purification factors achieved using milidevices for a) MAb1 and b) mAb2. Precipitates were recovered by centrifugation, washed with 20 % PEG6000 and resolubilized with 1 x PBS pH 3.5. Data are given as mean ± standard deviation in the case of triplicate analysis. Figure extracted from Pons Royo et al. [145]

To mimic flocculation conditions in the millidevices as performed in a stirred tank reactor, scale-down parameters were evaluated. Results showed that to be able to mimic such a condition, channel size of the millidevices should satisfy P/V=const as in a stirred tank reactor. For filtration studies, millidevices were adapted to a 3 mm channel size. Afterwards, the impact of the multiple additions of precipitating agent on depth filtration and tangential flow filtration were evaluated. Antibody solutions were precipitated using the millidevices with and without multiple additions for 5 min and in a stirred tank reactor. Solutions were filtered using a TFF system at constant flow and transmembrane pressure (TMP) was recorded during the experiment (Figure 12). Results obtained with a depth filter can be found in Publication II.

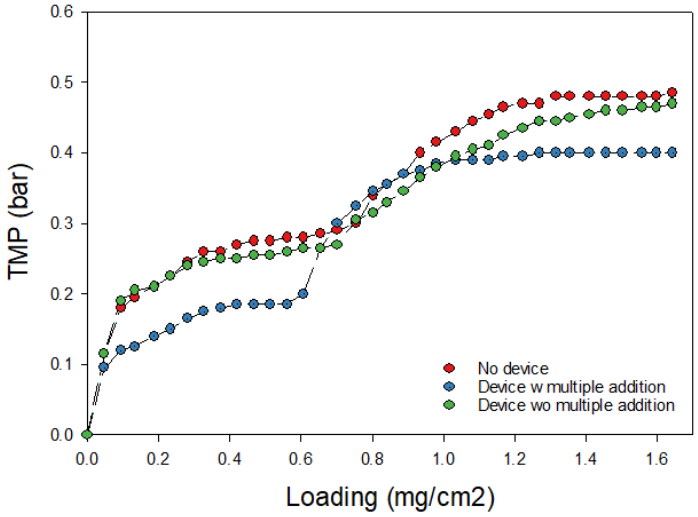

Figure 12. Impact of addition time of PEG for precipitation on the performance of depth filtration for mAb2. Figure retrieved from Pons Royo et al. [145]

Results show significant differences in the filterability of protein precipitates for samples precipitated using multiple additions and without. Such results corroborated findings in Publication I. Gradual addition of PEG using multiple additions improved particle characteristics and subsequent solid-liquid separation on TFF (Figure 12) and depth filtration (Publication II). Findings show that the millidevices were able to simulate precipitation conditions carried out in a stirred tank reactor. The use of such tools could cut down development costs and time drastically if used for predicting the process performance of subsequent solid-liquid separations.

Paper III - Millidevices for solubility curve determination

After the successful results with the millidevices, the third publication (Publication III) was focused on extending the designed millidevices to further analysis such as the determination of solubility curves. Protein solubility is a critical attribute to consider during process development, which typically is determined manually. It provides essential information on protein behaviour under certain solution conditions.

Devices were composed of a first channel for the protein solution and a second channel for the precipitating agent. Both channels were coupled to 4 mixing channels by a valve-free dispenser with different injection points. The dispenser coupled to the precipitating agent channel was composed of several outlets depending on the final concentration to be reached. Each mixing channel was coupled at 1, 2, 3 or 4 addition points, which at 1 ml/min flow of 40% PEG6000 stock solution, 1 hole correspond to 3.6 ± 0.4 % PEG6000 in 1 mL antibody solution, 2 holes 6.6 ± 0.5 %, 3 holes 9.2 ± 0.5 % and 4 holes 11.4 % ± 0.5 %. The same mechanism was used to distribute equally the main antibody solution in 4 different mixing channels by keeping constant the number of holes. With such a design, antibodies can be continuously harvested under different conditions. As in previous studies (Publication II), the design was kept as simple as possible to be able to be used in an Äkta system to reduce the number of required pumps and valves-free.

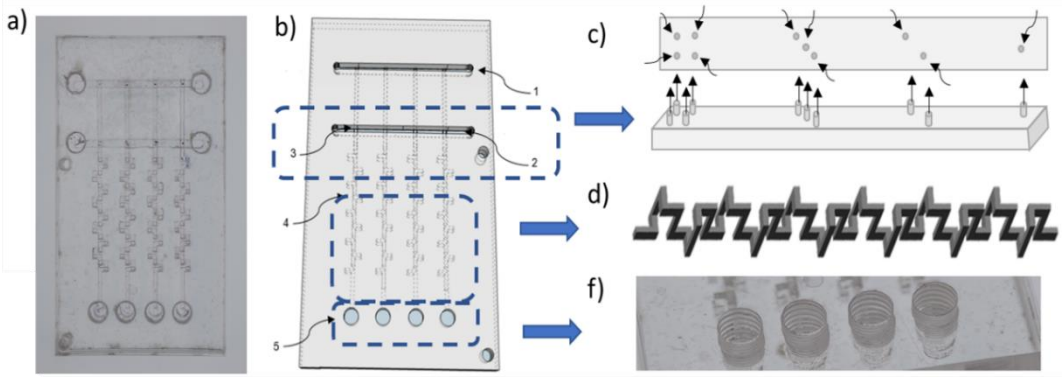

Figure 13. a) Final results of the apparent solubility curve prototype and b) 3D design of the developed device for apparent solubility curve determination: 1) cell culture supernatant addition channel, 2) precipitating agent addition channel, 3) injection points, 4) mixing/maturation area and 5) outlet for each studied condition. c) Schematic representation of the injection channel. The injection channels are grouped in different injections zones to introduce the precipitant agent continuously and at different concentrations. d) Geometrical design of the mixing channel for liquids with distinct viscosities. f) Female luer lock fitting integrated in the inlets and outlets of the device. Extracted from Pons Royo et al. [1]

Furthermore, each inlet and outlet integrated a standardized female Luer lock system which allows being directly connected to commonly used lab equipment such as peristaltic pumps or more complex equipment such as an Äkta system, without the need for flexible materials such as PDMS.

The applicability of such a device was evaluated by determining solubility curves of 4 different antibody solutions with 2 process-relevant precipitating agents, PEG6000 and $ZnCl_2$ and $CaCl_2$ for dsDNA as impurity. Results were compared to solubility curves determined manually. For the determination of the solubility curve using PEG6000, millidevice was connected directly to an Äkta system and the flow rate was set to the desired conditions. The precipitating agent was distributed over a range of 3.6 % to 11.4 % PEG6000. Samples were taken directly from the devices and analysed using a protein A column. Further results can be found in Publication III.

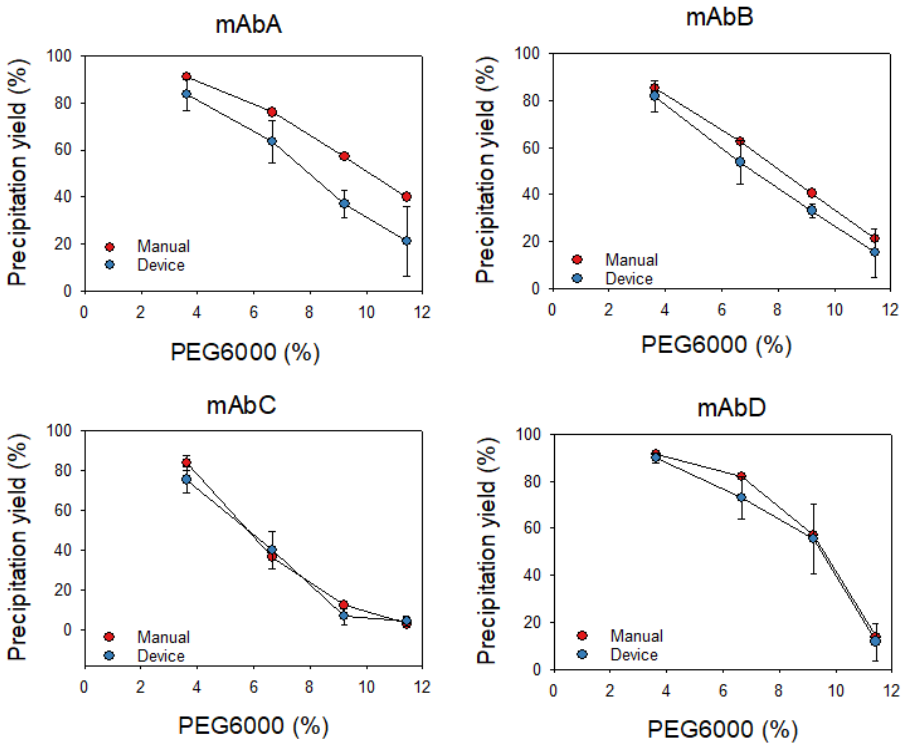

Figure 14. Comparison of solubility curves obtained with 40 % PEG6000 over a range of 3.65 % -11.43 % for mAbA, mAbB, mAbC and mAbD manually and using the milidevices. (Figure extracted from Pons Royo et al. [1]).

Results showed accurate measurements of apparent solubility curves, resulting in comparable shapes as measurements performed manually. Furthermore, the flow distribution was very accurate and precise. In comparison to other methodologies, the experimental time, reagents and sample manipulation were clearly reduced. Furthermore, several solution conditions can be tested simultaneously with only a single solution, without extra sample handling steps required. In addition, the automation of the experiments will allow the screening of larger experimental conditions in less time and reducing the operator effects. Such devices can be easily modified and customized depending on the experimental for any precipitation protocol or precipitation strategies, such as degradation or stability studies. Findings show that millidevices should be used and implemented to ease the screening conditions for the design and scaling down of processes.

Paper IV - Solid polyethylene glycol precipitation

Latest economic studies concluded that precipitation-based processes reduce manufacturing costs in comparison to protein A chromatography processes. Such studies also highlighted materials as the main contribution to CoGs, more precisely, the large amounts of concentrated stock solutions. Protein precipitation is performed by adding a precipitating agent into the protein solution to reach precipitation conditions. This step increases the volume of protein solution to be processed and subsequent unit operations, facilities such as storage areas and clean rooms and costs associated with these facilities such as energy consumption and water treatment. Therefore, reducing the amount of buffer required for such a process is essential to make more attractive precipitation-based processes for the pharmaceutical industry. For such a reason, the fourth article was focused on developing a new precipitation process by adding PEG6000 continuously in a solid form without dilutions to overcome such impediments (Publication IV).

For continuous protein precipitation with solid PEG6000, in-house-made prototypes such as the millidevices and the Dissolvr feeding unit were used. The antibody supernatant was combined continuously with PEG6000 in solid form in a vessel tank. The protein solution then was conducted through a mixing millidevice where precipitation occurred (Figure 15). Protein precipitation was continuously performed for 4h. Results showed comparable recovery yields, 80 % to 85 % and purities of 100 % and 98 % were achieved independent of the PEG form.

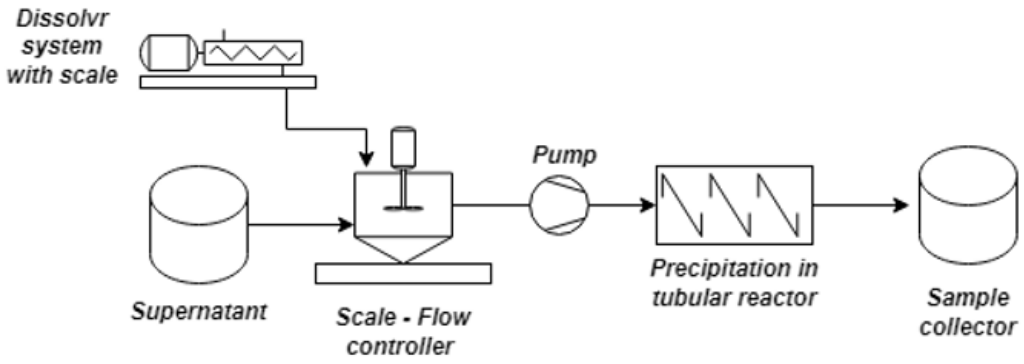

Figure 15. Experimental set-up for continuous protein precipitation using PEG6000 added in solid form. The feeding device feeds solid PEG into a mixing vessel and transported through a tubular reactor (Figure retrieved from Publication IV – Submitted).

Afterwards, an economic and environmental evaluation of solid PEG precipitation was performed and compared to conventional PEG precipitation and other standard purification process based on affinity chromatography. We evaluated and compared 4 different scenarios for the capture step of monoclonal antibodies. The first scenario corresponded to a typical batch protein A step. The second scenario was a state-of-the-art method such as PCC protein A. The third scenario corresponds to a conventional PEG precipitation in a liquid form, and the

fourth scenario is protein precipitation by the direct addition of PEG in solid form. More detailed information regarding the simulations can be found in Publication IV – Submitted.

The outcome of the economical evaluation showed that solid PEG was the most inexpensive method to purify mAbs among the four scenarios considered (Figure 16). The solid PEG method was 47 % cheaper compared to the liquid PEG and 60 % cheaper than Protein A - PCC. For precipitation-based, the major cost comes from facility-dependent costs or depreciated capital costs which represent approximately 76 % of the COGs followed by raw materials and labor. Cost reduction between precipitation-based scenarios was almost entirely to the reduction in equipment costs since two mixing tanks are replaced by the Dissolvr system. Besides the equipment-related costs, facility-dependent costs and utilities derived from HVAC and WFI (water for injection) were also reduced, which at these scales are the dominating factor in such a process.

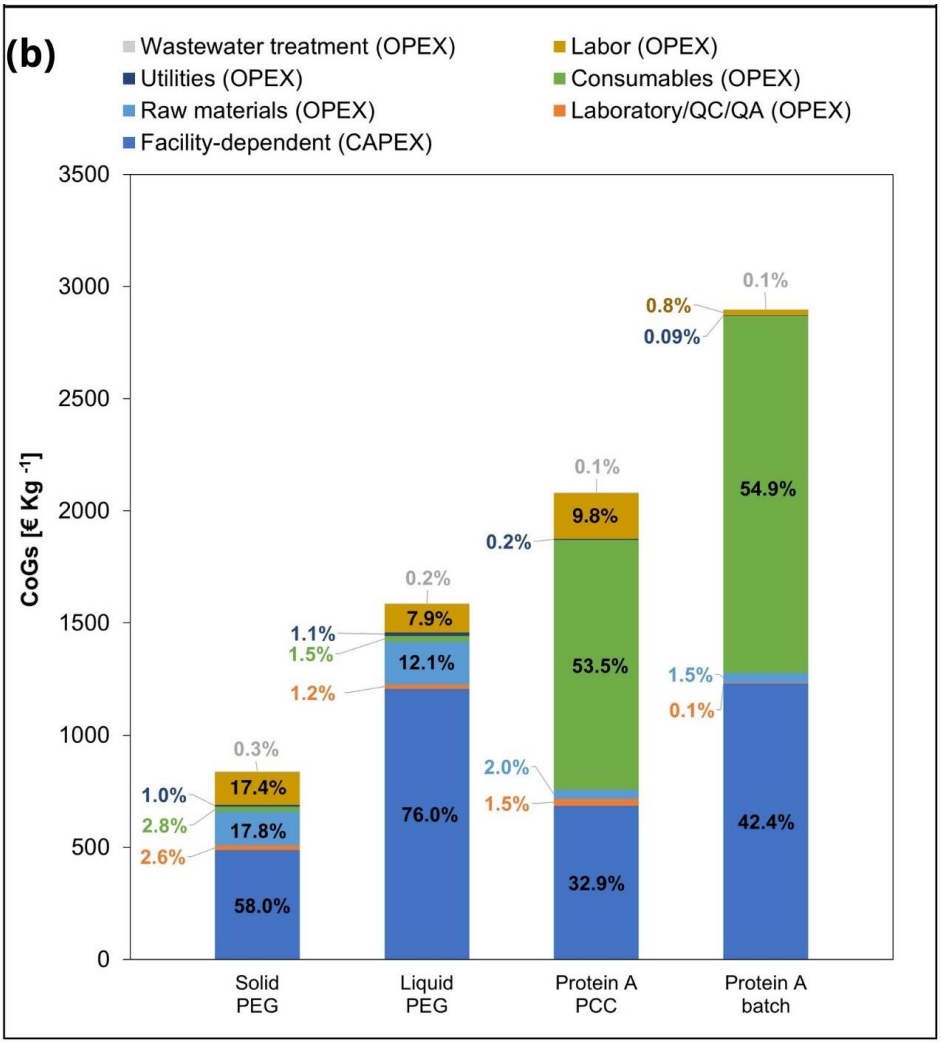

Figure 16. Comparison of COGs for the four different scenarios (Figure retrieved from Publication IV – Submitted).

For chromatography-based processes, facility-dependent costs account only for 33 % and 42 % for PCC and batch protein A, respectively, while consumables account for 55 % of the total costs. The higher cost of the Protein A methods is instead explained by the very high selling price of the resin and equipment. Since chromatographic units in PCC mode require less resin than in batch mode, PCC model allows for saving significantly consumable costs. Furthermore, the economic analysis highlighted that a key parameter in protein A processes is the replacement frequency of the resin.

Looking at the environmental impact, water and steam are responsible for almost the entire process mass intensity (PMI) in the four scenarios. HVAC also contributes significantly to the emissions of the precipitations processes but it is negligible for protein A capturing given the small cleanroom area occupied by the chromatographic units. Liquid PEG is the scenario with the highest impact. Such impact was reduced by 55 % similar to chromatography-based scenarios with the solid PEG precipitation. Such results showed that the precipitation-based approach can compete with the current purification processes, in economic and environmental terms.

Summary and Conclusions

Conclusions

The main objective of this thesis was to develop and optimize devices at milliliter scale to rapidly and cost-effectively screen precipitation and filtration conditions. Such devices allow for debottlenecking of current restrictions in development and optimization of continuous precipitation process for purification of antibodies.

Protein precipitation was performed on a laboratory scale using mAbs as a model system in 3 different modes of PEG addition, single, stepwise and gradual. Critical quality attributes of the products, such as purity, yield, PSD, 3D structure, compactness and density of the resulting precipitates were compared with the different addition modes. Additionally, filtration studies were performed to investigate the influence of the resulting precipitates on further purification steps. The continuous addition of precipitating agent was better compared to the conventional single addition of PEG precipitation approach in terms of purity and yield. It can be concluded that the dosage and mode of addition influence the precipitate properties, which also affect the subsequent separation step, the harvest of the precipitate by microfiltration. Multiple and continuous additions improved the filtration flux. Therefore, precipitation studies must be coupled with filtration studies and batch precipitation methodology should be rendered continuous to improve subsequent unit operations.

Millidevices were designed and developed to screen optimal conditions for precipitation such as dosage time and resulting filterability. The use of such tools cut down development costs and time drastically if used for predicting the process performance of subsequent solid-liquid separations. The use of such millidevices was extended to determine process parameters such as apparent solubility. The implementation of such devices and automation enhances and eliminates human-prone errors.

Then precipitation was further improved by using addition of solid PEG instead of a concentrated PEG stock solution. Similar yields and purities compared to conventional precipitation processes could be obtained but the process economics and environmental footprint were substantially improved. Techno-economic analysis highlight that capital expenditures are the main cost drivers for the continuous precipitation processes. Therefore, scaling down the equipment would be beneficial from the economic and environmental perspective, as well to reduce the carbon footprint associated with HVAC energy consumption in clean rooms.

To conclude, the objectives of this doctoral thesis were achieved:

- The key parameters with higher impact in protein precipitation and filtration were identified. Results were used to determine the most suitable reactor geometry and engineering approaches to improve protein precipitation and filtration.
- The quality properties of the products were compared with the different dosage addition modes. Results highlighted that continuous addition of precipitating agents led to more consistent product quality.
- Milliscale fluidic devices capable of mimicking critical process parameters for fast and efficient process development were developed.
- Process limitations of precipitation-based processes were identified and an alternative process was proposed and demonstrated using rapid prototyping tools. The conventional and alternative continuous precipitation processes were compared to other current state-of-art methodologies used for antibodies capture step, in terms of economics and environmental footprint.

References

1. Pons Royo, M.d.C., Beulay, J.-L., Valery, E., Jungbauer, A. & Satzer, P. Design of millidevices to expedite apparent solubility measurements. *Reaction Chemistry & Engineering* (2022).
2. Khanal, O. & Lenhoff, A.M. Developments and opportunities in continuous biopharmaceutical manufacturing. *mAbs* **13**, 1903664 (2021).
3. Klutz, S., Holtmann, L., Lobedann, M. & Schembecker, G. Cost evaluation of antibody production processes in different operation modes. *Chemical Engineering Science* **141**, 63-74 (2016).
4. Chon, J.H. & Zarbis-Papastoitsis, G. Advances in the production and downstream processing of antibodies. *New Biotechnology* **28**, 458-463 (2011).
5. Robinson, M.P. et al. Efficient expression of full-length antibodies in the cytoplasm of engineered bacteria. *Nat Commun* **6**, 8072 (2015).
6. Li, H. et al. Optimization of humanized IgGs in glycoengineered Pichia pastoris. *Nat Biotechnol* **24**, 210-215 (2006).
7. Yang, O., Qadan, M. & Ierapetritou, M. Economic Analysis of Batch and Continuous Biopharmaceutical Antibody Production: A Review. *J Pharm Innov* **14**, 1-19 (2019).
8. Li, F., Vijayasankaran, N., Shen, A.Y., Kiss, R. & Amanullah, A. Cell culture processes for monoclonal antibody production. *MAbs* **2**, 466-479 (2010).
9. Somasundaram, B., Pleitt, K., Shave, E., Baker, K. & Lua, L.H.L. Progression of continuous downstream processing of monoclonal antibodies: Current trends and challenges. *Biotechnol Bioeng* **115**, 2893-2907 (2018).
10. Shukla, A.A., Wolfe, L.S., Mostafa, S.S. & Norman, C. Evolving trends in mAb production processes. *Bioengineering & Translational Medicine* **2**, 58-69 (2017).
11. Huang, Y.M. et al. Maximizing productivity of CHO cell-based fed-batch culture using chemically defined media conditions and typical manufacturing equipment. *Biotechnol Prog* **26**, 1400-1410 (2010).
12. Kim, J.Y., Kim, Y.G. & Lee, G.M. CHO cells in biotechnology for production of recombinant proteins: current state and further potential. *Appl Microbiol Biotechnol* **93**, 917-930 (2012).
13. Takamatsu, H., Hamamoto, K., Ishimaru, K., Yokoyama, S. & Tokashiki, M. Large-scale perfusion culture process for suspended mammalian cells that uses a centrifuge with multiple settling zones. *Appl Microbiol Biotechnol* **45**, 454-457 (1996).
14. Clincke, M.F. et al. Very high density of CHO cells in perfusion by ATF or TFF in WAVE bioreactor™. Part I. Effect of the cell density on the process. *Biotechnol Prog* **29**, 754-767 (2013).
15. Clincke, M.F. et al. Very high density of Chinese hamster ovary cells in perfusion by alternating tangential flow or tangential flow filtration in WAVE Bioreactor™-part II: Applications for antibody production and cryopreservation. *Biotechnol Prog* **29**, 768-777 (2013).
16. Clincke, M.F. et al. Study of a recombinant CHO cell line producing a monoclonal antibody by ATF or TFF external filter perfusion in a WAVE Bioreactor™. *BMC Proc* **5 Suppl 8**, P105 (2011).
17. Bielser, J.M., Wolf, M., Souquet, J., Broly, H. & Morbidelli, M. Perfusion mammalian cell culture for recombinant protein manufacturing - A critical review. *Biotechnol Adv* **36**, 1328-1340 (2018).
18. Li, Z., Gu, Q., Coffman, J.L., Przybycien, T. & Zydney, A.L. Continuous precipitation for monoclonal antibody capture using countercurrent washing by microfiltration. *Biotechnol Prog* **35**, e2886 (2019).
19. Fisher, A.C. et al. The Current Scientific and Regulatory Landscape in Advancing Integrated Continuous Biopharmaceutical Manufacturing. *Trends Biotechnol* **37**, 253-267 (2019).

20. www.biophorum.com (2022). Monoclonal Antibodies (MAbs) Global Market Report 2022.
21. Burgstaller, D. et al. Continuous cell flocculation for recombinant antibody harvesting. *Journal of Chemical Technology & Biotechnology* **93**, 1881-1890 (2018).
22. Kavara, A., Sokolowski, D., Collins, M. & Schofield, M. in Approaches to the Purification, Analysis and Characterization of Antibody-Based Therapeutics. (ed. A. Matte) 81-103 (Elsevier, 2020).
23. Satzer, P. et al. Impact of failure rates, lot definitions and scheduling of upstream processes on the productivity of continuous integrated bioprocesses. *Journal of Chemical Technology & Biotechnology* **n/a**.
24. Weaver, J., Husson, S.M., Murphy, L. & Wickramasinghe, S.R. Anion exchange membrane adsorbers for flow-through polishing steps: Part II. Virus, host cell protein, DNA clearance, and antibody recovery. *Biotechnology and Bioengineering* **110**, 500-510 (2013).
25. Etzel, M.R. & Riordan, W.T. Viral clearance using monoliths. *Journal of Chromatography A* **1216**, 2621-2624 (2009).
26. Kateja, N., Nitika, N., Fadnis, R.S. & Rathore, A.S. A novel reactor configuration for continuous virus inactivation. *Biochemical Engineering Journal* **167** (2021).
27. Martins, D.L. et al. Truly continuous low pH viral inactivation for biopharmaceutical process integration. *Biotechnology and bioengineering* **117**, 1406-1417 (2020).
28. Zydney, A.L. Continuous downstream processing for high value biological products: A Review. *Biotechnol Bioeng* **113**, 465-475 (2016).
29. Walther, J. et al. The business impact of an integrated continuous biomanufacturing platform for recombinant protein production. *J Biotechnol* **213**, 3-12 (2015).
30. Farid, S.S., Baron, M., Stamatis, C., Nie, W. & Coffman, J. Benchmarking biopharmaceutical process development and manufacturing cost contributions to R&D. *MAbs* **12**, 1754999 (2020).
31. Gerstweiler, L., Bi, J. & Middelberg, A.P.J. Continuous downstream bioprocessing for intensified manufacture of biopharmaceuticals and antibodies. *Chemical Engineering Science* **231**, 116272 (2021).
32. Badr, S. et al. Integrated design of biopharmaceutical manufacturing processes: Operation modes and process configurations for monoclonal antibody production. *Computers & Chemical Engineering* **153**, 107422 (2021).
33. Coffman, J. et al. A common framework for integrated and continuous biomanufacturing. *Biotechnology and Bioengineering* **118**, 1735-1749 (2021).
34. Croughan, M.S., Konstantinov, K.B. & Cooney, C. The future of industrial bioprocessing: batch or continuous? *Biotechnol Bioeng* **112**, 648-651 (2015).
35. Godawat, R., Konstantinov, K., Rohani, M. & Warikoo, V. End-to-end integrated fully continuous production of recombinant monoclonal antibodies. *J Biotechnol* **213**, 13-19 (2015).
36. Konstantinov, K.B. & Cooney, C.L. White paper on continuous bioprocessing. May 20-21, 2014 Continuous Manufacturing Symposium. *J Pharm Sci* **104**, 813-820 (2015).
37. Schmidt, A., Richter, M., Rudolph, F. & Strube, J. Integration of Aqueous Two-Phase Extraction as Cell Harvest and Capture Operation in the Manufacturing Process of Monoclonal Antibodies. *Antibodies* **6**, 21 (2017).
38. Zhou, H., Fang, M., Zheng, X. & Zhou, W. Improving an intensified and integrated continuous bioprocess platform for biologics manufacturing. *Biotechnology and Bioengineering* **118**, 3618-3623 (2021).
39. Zobel, S., Ditz, R. & Strube, J. Continuous Biomanufacturing – Platform Alternatives for scFv and mAb. *Chemie-Ingenieur-Technik* **88**, 1214 (2016).
40. Badman, C. et al. Why We Need Continuous Pharmaceutical Manufacturing and How to Make It Happen. *Journal of Pharmaceutical Sciences* **108**, 3521-3523 (2019).
41. Rathore, A.S. & Shereef, F. The influence of domestic manufacturing capabilities on biologic pricing in emerging economies. *Nature Biotechnology* **37**, 498-501 (2019).

42. Rathore, A.S., Agarwal, H., Sharma, A.K., Pathak, M. & Muthukumar, S. Continuous Processing for Production of Biopharmaceuticals. *Preparative Biochemistry & Biotechnology* **45**, 836-849 (2015).
43. Rathore, A.S., Agarwal, H., Sharma, A.K., Pathak, M. & Muthukumar, S. Continuous processing for production of biopharmaceuticals. *Prep Biochem Biotechnol* **45**, 836-849 (2015).
44. Mascia, S. et al. End-to-end continuous manufacturing of pharmaceuticals: integrated synthesis, purification, and final dosage formation. *Angew Chem Int Ed Engl* **52**, 12359-12363 (2013).
45. Shukla, A.A., Wolfe, L.S., Mostafa, S.S. & Norman, C. Evolving trends in mAb production processes. *Bioeng Transl Med* **2**, 58-69 (2017).
46. Rathore, A., Saxena, N., Thakur, G. & Deore, N. Challenges in process control for continuous processing for production of monoclonal antibody products. *Current Opinion in Chemical Engineering* **31**, 100671 (2021).
47. Grangeia, H.B., Silva, C., Simões, S.P. & Reis, M.S. Quality by design in pharmaceutical manufacturing: A systematic review of current status, challenges and future perspectives. *Eur J Pharm Biopharm* **147**, 19-37 (2020).
48. Sencar, J., Hammerschmidt, N. & Jungbauer, A. Modeling the Residence Time Distribution of Integrated Continuous Bioprocesses. *Biotechnol J* **15**, e2000008 (2020).
49. Satzer, P. (2021). Continuous Purification Technologies.
50. Cataldo, A.L., Burgstaller, D., Hribar, G., Jungbauer, A. & Satzer, P. Economics and ecology: Modelling of continuous primary recovery and capture scenarios for recombinant antibody production. *J Biotechnol* **308**, 87-95 (2020).
51. Siyu, P. & Kunn, H. Continuous crystallization as a downstream processing step of pharmaceutical proteins : a review. *Chemical Engineering Research and Design* **160**, 89-104 (2020).
52. Rosa, P.A., Azevedo, A.M., Sommerfeld, S., Bäcker, W. & Aires-Barros, M.R. Aqueous two-phase extraction as a platform in the biomanufacturing industry: economical and environmental sustainability. *Biotechnol Adv* **29**, 559-567 (2011).
53. Rosa, P.A., Azevedo, A.M., Sommerfeld, S., Bäcker, W. & Aires-Barros, M.R. Continuous aqueous two-phase extraction of human antibodies using a packed column. *J Chromatogr B Analyt Technol Biomed Life Sci* **880**, 148-156 (2012).
54. Yamada, T., Yamamoto, K., Ishihara, T. & Ohta, S. Purification of monoclonal antibodies entirely in flow-through mode. *Journal of Chromatography B* **1061-1062** (2017).
55. Sommer, R. et al. Capture and intermediate purification of recombinant antibodies with combined precipitation methods. *Biochemical Engineering Journal* **93**, 200-211 (2015).
56. Sommer, R. et al. Combined polyethylene glycol and CaCl2 precipitation for the capture and purification of recombinant antibodies. *Process Biochemistry* **49**, 2001-2009 (2014).
57. Martinez, M., Spitali, M., Norrant, E.L. & Bracewell, D.G. Precipitation as an Enabling Technology for the Intensification of Biopharmaceutical Manufacture. *Trends in Biotechnology* **37**, 237-241 (2019).
58. Hammerschmidt, N., Hobiger, S. & Jungbauer, A. Continuous polyethylene glycol precipitation of recombinant antibodies: Sequential precipitation and resolubilization. *Process Biochemistry* **51**, 325-332 (2016).
59. Hammerschmidt, N., Hintersteiner, B., Lingg, N. & Jungbauer, A. Continuous precipitation of IgG from CHO cell culture supernatant in a tubular reactor. *Biotechnology Journal* **10**, 1196-1205 (2015).
60. Dutra, G., Komuczki, D., Jungbauer, A. & Satzer, P. Continuous capture of recombinant antibodies by ZnCl 2 precipitation without polyethylene glycol. *Eng Life Sci* **20**, 265-274 (2020).
61. Chayen, N.E. & Saridakis, E. Protein crystallization: from purified protein to diffraction-quality crystal. *Nature Methods* **5**, 147-153 (2008).

62. Juckes, I.R. Fractionation of proteins and viruses with polyethylene glycol. *Biochim Biophys Acta* **229**, 535-546 (1971).
63. Atha, D.H. & Ingham, K.C. Mechanism of precipitation of proteins by polyethylene glycols. Analysis in terms of excluded volume. *Journal of Biological Chemistry* **256**, 12108-12117 (1981).
64. Sim, S.L. et al. Protein precipitation by polyethylene glycol: a generalized model based on hydrodynamic radius. *J Biotechnol* **157**, 315-319 (2012).
65. Cohn, E.J. et al. Preparation and Properties of Serum and Plasma Proteins. IV. A System for the Separation into Fractions of the Protein and Lipoprotein Components of Biological Tissues and Fluids1a,b,c,d. *Journal of the American Chemical Society* **68**, 459-475 (1946).
66. Cohn, E.J. et al. A System for the Separation of the Components of Human Blood: Quantitative Procedures for the Separation of the Protein Components of Human Plasma1a,b,c. *Journal of the American Chemical Society* **72**, 465-474 (1950).
67. Tscheliessnig, A. et al. Ethanol precipitation for purification of recombinant antibodies. *Journal of Biotechnology* **188**, 17-28 (2014).
68. Fine, J.M. In: J.M. Curling, Editor, Methods of plasma protein fractionation, Academic Press (1980). *Revue française de transfusion et immuno-hématologie* **25**, 355-356 (1982).
69. van Oss, C.J. On the mechanism of the cold ethanol precipitation method of plasma protein fractionation. *Journal of Protein Chemistry* **8**, 661-668 (1989).
70. Lain, B., Cacciuttolo, M. & Zarbis-Papastoitsis, G. Development of a High-Capacity MAb Capture Step Based on Cation-Exchange Chromatography. *BioProcess International* **7** (2009).
71. Buchacher, A. & Iberer, G. Purification of intravenous immunoglobulin G from human plasma--aspects of yield and virus safety. *Biotechnol J* **1**, 148-163 (2006).
72. Tsoka, S., Ciniawskyj, O.C., Thomas, O.R., Titchener-Hooker, N.J. & Hoare, M. Selective flocculation and precipitation for the improvement of virus-like particle recovery from yeast homogenate. *Biotechnol Prog* **16**, 661-667 (2000).
73. Zeltins, A. Construction and characterization of virus-like particles: a review. *Mol Biotechnol* **53**, 92-107 (2013).
74. Großhans, S., Wang, G. & Hubbuch, J. Water on hydrophobic surfaces: mechanistic modeling of polyethylene glycol-induced protein precipitation. *Bioprocess and Biosystems Engineering* **42**, 513-520 (2019).
75. Burgstaller, D., Jungbauer, A. & Satzer, P. Continuous integrated antibody precipitation with two-stage tangential flow microfiltration enables constant mass flow. *Biotechnology and Bioengineering* **116**, 1053-1065 (2019).
76. Padín-González, E. et al. Understanding the Role and Impact of Poly (Ethylene Glycol) (PEG) on Nanoparticle Formulation: Implications for COVID-19 Vaccines. *Frontiers in Bioengineering and Biotechnology* **10** (2022).
77. Sim, S.L. et al. Branched polyethylene glycol for protein precipitation. *Biotechnol Bioeng* **109**, 736-746 (2012).
78. Baumann, P. & Hubbuch, J. Downstream process development strategies for effective bioprocesses: Trends, progress, and combinatorial approaches. *Engineering in Life Sciences* **17**, 1142-1158 (2017).
79. Dutra, G., Komuczki, D., Jungbauer, A. & Satzer, P. Continuous capture of recombinant antibodies by ZnCl2 precipitation without polyethylene glycol. *Engineering in Life Sciences* **20**, 265-274 (2020).
80. Satzer, P., Tscheließnigg, A., Sommer, R. & Jungbauer, A. Separation of recombinant antibodies from DNA using divalent cations. *Engineering in Life Sciences* **14**, 477-484 (2014).
81. Lydersen, B.K., Brehm-Gibson, T. & Murel, A. Acid precipitation of mammalian cell fermentation broth. *Ann N Y Acad Sci* **745**, 222-231 (1994).
82. Westoby, M., Chrostowski, J., de Vilmorin, P., Smelko, J.P. & Romero, J.K. Effects of solution environment on mammalian cell fermentation broth properties: Enhanced

impurity removal and clarification performance. *Biotechnology and Bioengineering* **108**, 50-58 (2011).
83. Lingg, N., Tan, E., Hintersteiner, B., Bardor, M. & Jungbauer, A. Highly linear pH gradients for analyzing monoclonal antibody charge heterogeneity in the alkaline range. *J Chromatogr A* **1319**, 65-71 (2013).
84. Brodsky, Y., Zhang, C., Yigzaw, Y. & Vedantham, G. Caprylic acid precipitation method for impurity reduction: an alternative to conventional chromatography for monoclonal antibody purification. *Biotechnol Bioeng* **109**, 2589-2598 (2012).
85. Perosa, F., Carbone, R., Ferrone, S. & Dammacco, F. Purification of human immunoglobulins by sequential precipitation with caprylic acid and ammonium sulphate. *J Immunol Methods* **128**, 9-16 (1990).
86. Raweerith, R. & Ratanabanangkoon, K. Fractionation of equine antivenom using caprylic acid precipitation in combination with cationic ion-exchange chromatography. *Journal of immunological methods* **282**, 63-72 (2003).
87. Morais, V. & Massaldi, H. A model mechanism for protein precipitation by caprylic acid: application to plasma purification. *Biotechnol Appl Biochem* **59**, 50-54 (2012).
88. Salt, D.E., Hay, S., Thomas, O.R.T., Hoare, M. & Dunnill, P. Selective flocculation of cellular contaminants from soluble proteins using polyethyleneimine: A study of several organisms and polymer molecular weights. *Enzyme and Microbial Technology* **17**, 107-113 (1995).
89. McNerney, T. et al. PDADMAC flocculation of Chinese hamster ovary cells: enabling a centrifuge-less harvest process for monoclonal antibodies. *MAbs* **7**, 413-428 (2015).
90. Tomic, S. et al. Complete clarification solution for processing high density cell culture harvests. *Separation and Purification Technology* **141**, 269-275 (2015).
91. Kang, Y.K. et al. Development of a novel and efficient cell culture flocculation process using a stimulus responsive polymer to streamline antibody purification processes. *Biotechnol Bioeng* **110**, 2928-2937 (2013).
92. Gregory, J. & Barany, S. Adsorption and flocculation by polymers and polymer mixtures. *Advances in Colloid and Interface Science* **169**, 1-12 (2011).
93. Buyel, J.F., Gruchow, H.M., Boes, A. & Fischer, R. Rational design of a host cell protein heat precipitation step simplifies the subsequent purification of recombinant proteins from tobacco. *Biochemical Engineering Journal* **88**, 162-170 (2014).
94. Guan, J., Amal, R. & Waite, T.D. Effect of aggregate size and structure on specific resistance of biosolids filter cakes. *Water Science and Technology* **44**, 215-220 (2001).
95. Lee, J.-D. et al. Effect of Coagulation Conditions on Membrane Filtration Characteristics in Coagulation−Microfiltration Process for Water Treatment. *Environmental Science & Technology* **34**, 3780-3788 (2000).
96. Lee, S.A., Fane, A.G., Amal, R. & Waite, T.D. The effect of floc size and structure on specific cake resistance and compressibility in dead-end microfiltration. *Separation Science and Technology* **38**, 869-887 (2003).
97. Doran, P.M. Bioprocess engineering principles: Second edition. (2012).
98. McGinty, J., Yazdanpanah, N., Price, C., ter Horst, J.H. & Sefcik, J. in The Handbook of Continuous Crystallization 1-50 (The Royal Society of Chemistry, 2020).
99. Hammerschmidt, N., Tscheliessnig, A., Sommer, R., Helk, B. & Jungbauer, A. Economics of recombinant antibody production processes at various scales: Industry-standard compared to continuous precipitation. *Biotechnol J* **9**, 766-775 (2014).
100. Gu, Q., Li, Z., Coffman, J.L., Przybycien, T.M. & Zydney, A.L. High throughput solubility and redissolution screening for antibody purification via combined PEG and zinc chloride precipitation. *Biotechnology Progress* **36**, e3041 (2020).
101. Kateja, N., Agarwal, H., Saraswat, A., Bhat, M. & Rathore, A.S. Continuous precipitation of process related impurities from clarified cell culture supernatant using a novel coiled flow inversion reactor (CFIR). *Biotechnology Journal* **11**, 1320-1331 (2016).

102. Kateja, N., Kumar, D., Sethi, S. & Rathore, A.S. Non-protein A purification platform for continuous processing of monoclonal antibody therapeutics. *Journal of Chromatography A* **1579**, 60-72 (2018).
103. Martinez, M., Mannall, G., Spitali, M., Norrant, E.L. & Bracewell, D.G. Reactor design for continuous monoclonal antibody precipitation based upon micro-mixing. *Journal of Chemical Technology & Biotechnology* (2020).
104. Hoare, M., Dunnill, P. & Bell, D.J. Reactor design for protein precipitation and its effect on centrifugal separation. *Ann N Y Acad Sci* **413**, 254-269 (1983).
105. Boychyn, M., Doyle, W., Bulmer, M., More, J. & Hoare, M. Laboratory scaledown of protein purification processes involving fractional precipitation and centrifugal recovery. *Biotechnology and Bioengineering* **69**, 1-10 (2000).
106. Jungbauer, A. Continuous downstream processing of biopharmaceuticals. *Trends Biotechnol* **31**, 479-492 (2013).
107. Müller, D. et al. Process intensification in the biopharma industry: Improving efficiency of protein manufacturing processes from development to production scale using synergistic approaches. *Chemical Engineering and Processing - Process Intensification* **171**, 108727 (2022).
108. Boychyn, M., Doyle, W., Bulmer, M., More, J. & Hoare, M. Laboratory scaledown of protein purification processes involving fractional precipitation and centrifugal recovery. *Biotechnol Bioeng* **69**, 1-10 (2000).
109. Šulc, R. & Ditl, P. Scale-up rules for flocculation. *International Journal of Mineral Processing* **167**, 79-85 (2017).
110. Espuny Garcia del Real, G., Davies, J. & Bracewell, D.G. Scale-down characterization of post-centrifuge flocculation processes for high-throughput process development. *Biotechnology and Bioengineering* **111**, 2486-2498 (2014).
111. Terry, S.C., Jerman, J.H. & Angell, J.B. A gas chromatographic air analyzer fabricated on a silicon wafer. *IEEE Transactions on Electron Devices* **26**, 1880-1886 (1979).
112. Silva, T.C., Eppink, M. & Ottens, M. Automation and miniaturization: enabling tools for fast, high-throughput process development in integrated continuous biomanufacturing. *Journal of Chemical Technology & Biotechnology* **n/a**.
113. Montes-Serrano, I., Satzer, P., Jungbauer, A. & Dürauer, A. Characterization of hydrodynamics and volumetric power input in microtiter plates for the scale-up of downstream operations. *Biotechnology and Bioengineering* **119**, 523-534 (2022).
114. Yassouridis, C. et al. Strategy to equivalence testing for development and scale up of biopharmaceutical downstream processes. *Chemical Engineering Science* **235** (2021).
115. Azizipour, N., Avazpour, R., Rosenzweig, D., Sawan, M. & Ajji, A. Evolution of Biochip Technology: A Review from Lab-on-a-Chip to Organ-on-a-Chip. *Micromachines* **11**, 599 (2020).
116. Marques, M.P.C. & Fernandes, P. Microfluidic Devices: Useful Tools for Bioprocess Intensification. *Molecules* **16**, 8368-8401 (2011).
117. Whitesides, G.M. The origins and the future of microfluidics. *Nature* **442**, 368-373 (2006).
118. Niculescu, A.-G., Chircov, C., Bîrcă, A.C. & Grumezescu, A.M. Fabrication and Applications of Microfluidic Devices: A Review. *International Journal of Molecular Sciences* **22**, 2011 (2021).
119. Wellsandt, T., Stanisch, B. & Strube, J. Characterization Method for Separation Devices Based on Micro Technology. *Chemie Ingenieur Technik* **87**, 150-158 (2015).
120. Shakeri, A., Khan, S. & Didar, T.F. Conventional and emerging strategies for the fabrication and functionalization of PDMS-based microfluidic devices. *Lab on a Chip* **21**, 3053-3075 (2021).
121. Thorsen, T., Maerkl, S.J. & Quake, S.R. Microfluidic large-scale integration. *Science* **298**, 580-584 (2002).
122. Folch, A. (2012). Introduction to BioMEMS (1st ed.). CRC Press.

123. Solehati, N., Bae, J. & Sasmito, A.P. Optimization of Wavy-Channel Micromixer Geometry Using Taguchi Method. *Micromachines* **9**, 70 (2018).
124. Clark, J., Kaufman, M. & Fodor, P. Mixing Enhancement in Serpentine Micromixers with a Non-Rectangular Cross-Section. *Micromachines* **9** (2018).
125. Stone, H. 5-30 (2007).
126. Reyes, D.R., Iossifidis, D., Auroux, P.-A. & Manz, A. Micro Total Analysis Systems. 1. Introduction, Theory, and Technology. *Analytical Chemistry* **74**, 2623-2636 (2002).
127. Batchelor, G.K. An Introduction to Fluid Dynamics. (Cambridge University Press, Cambridge; 2000).
128. Stone, H.A. in CMOS Biotechnology. (eds. H. Lee, R.M. Westervelt & D. Ham) 5-30 (Springer US, Boston, MA; 2007).
129. Ren, K., Zhou, J. & Wu, H. Materials for microfluidic chip fabrication. *Acc Chem Res* **46**, 2396-2406 (2013).
130. Hou, X. et al. Interplay between materials and microfluidics. *Nature Reviews Materials* **2**, 17016 (2017).
131. Thorsen, T., Maerkl, S.J. & Quake, S.R. Microfluidic Large-Scale Integration. *Science* **298**, 580-584 (2002).
132. Ren, K., Zhou, J. & Wu, H. Materials for Microfluidic Chip Fabrication. *Accounts of Chemical Research* **46**, 2396-2406 (2013).
133. Becker, H. & Gärtner, C. Polymer microfabrication technologies for microfluidic systems. *Analytical and Bioanalytical Chemistry* **390**, 89-111 (2008).
134. Nunes, P.S., Ohlsson, P.D., Ordeig, O. & Kutter, J.P. Cyclic olefin polymers: emerging materials for lab-on-a-chip applications. *Microfluidics and Nanofluidics* **9**, 145-161 (2010).
135. Giri, K. & Tsao, C.-W. Recent Advances in Thermoplastic Microfluidic Bonding. *Micromachines* **13**, 486 (2022).
136. Nishat, S., Jafry, A.T., Martinez, A.W. & Awan, F.R. Paper-based microfluidics: Simplified fabrication and assay methods. *Sensors and Actuators B: Chemical* **336**, 129681 (2021).
137. Goy, C.B., Chaile, R.E. & Madrid, R.E. Microfluidics and hydrogel: A powerful combination. *Reactive and Functional Polymers* **145**, 104314 (2019).
138. Davis, J.J., Foster, S.W. & Grinias, J.P. Low-cost and open-source strategies for chemical separations. *J Chromatogr A* **1638**, 461820 (2021).
139. Kreutz, E.W., Backes, G., Gasser, A. & Wissenbach, K. Rapid prototyping with CO2 laser radiation. *Applied Surface Science* **86**, 310-316 (1995).
140. Krujatz, F. et al. Additive Biotech—Chances, challenges, and recent applications of additive manufacturing technologies in biotechnology. *New Biotechnology* **39**, 222-231 (2017).
141. Au, A.K., Huynh, W., Horowitz, L.F. & Folch, A. 3D-Printed Microfluidics. *Angew Chem Int Ed Engl* **55**, 3862-3881 (2016).
142. Heuer, C., Preuß, J.-A., Habib, T., Enders, A. & Bahnemann, J. 3D printing in biotechnology—An insight into miniaturized and microfluidic systems for applications from cell culture to bioanalytics. *Engineering in Life Sciences* **n/a**.
143. Simon, U. & Dimartino, S. Direct 3D printing of monolithic ion exchange adsorbers. *J Chromatogr A* **1587**, 119-128 (2019).
144. Pons Royo, M.d.C., Beulay, J.-L., Valery, E., Jungbauer, A. & Satzer, P. Mode and dosage time in polyethylene glycol precipitation process influences protein precipitate size and filterability. *Process Biochemistry* **114**, 77-85 (2022).
145. Pons Royo, M.d.C., Montes-Serrano, I., Valery, E., Jungbauer, A. & Satzer, P. Milliscale reactors for integration of continuous precipitation and filtration. *Journal of Chemical Technology & Biotechnology* **n/a**.

Paper I

Maria del Carme Pons Royo, Jean-Luc Beulay, Eric Valery, Alois Jungbauer, Peter Satzer,

Mode and dosage time in polyethylene glycol precipitation process influences protein precipitate size and filterability,

Process Biochemistry,

Volume 114, 2022

https://doi.org/10.1016/j.procbio.2022.01.017.

Keywords: Precipitation; Gradual; mAbs; Filtration; PEG

Process Biochemistry 114 (2022) 77–85

Contents lists available at ScienceDirect

Process Biochemistry

journal homepage: www.elsevier.com/locate/procbio

Mode and dosage time in polyethylene glycol precipitation process influences protein precipitate size and filterability

Maria del Carme Pons Royo [a,b], Jean-Luc Beulay [a], Eric Valery [a], Alois Jungbauer [b,c,*], Peter Satzer [c]

[a] Department of Innovation, Novasep, 81 Boulevard de la Moselle, 54340, Pompey, France
[b] Department of Biotechnology, University of Natural Resources and Life Sciences, 1190, Vienna, Austria
[c] Austrian Centre of Industrial Biotechnology (ACIB), Muthgasse 18, 1190, Vienna, Austria

ARTICLE INFO

Keywords:
Precipitation
Gradual
mAbs
Filtration
PEG

ABSTRACT

Precipitation has gained interest as alternative to the costly protein A chromatography for monoclonal antibody purification. Traditional precipitation processes are based on direct addition of precipitant in a single dose, with limited control on co-precipitation of impurities and not considering batch-to-batch variations. We propose a gradual dosage of polyethylene glycol to prevent co-precipitation and control resulting floc size. We used focused beam reflectance measurement to demonstrate that the PEG6000 dosage time and the final concentration significantly changes the particle size distribution (PSD). We demonstrated that gradual and stepwise precipitant addition was superior to conventional batch PEG precipitation, improving product yield and purity by a factor of 4 for HCP removal, for samples pre-treated with $CaCl_2$ and caprylic acid. We studied the 3D structure of the precipitates by fractal dimension and showed that precipitates exhibited different compactness and density depending on the dosage time, resulting in different filterability in tangential flow filtration and depth filtration. To switch from batch to continuous PEG addition, the 3D structure of precipitates needs to be considered due to its high impact on the resulting process performance. Focused beam reflectance measurement (FBRM) and fractal dimension can be used to adjust the precipitation methodology to improve the product quality attributes and inform about the design of further purification steps.

1. Introduction

In recent years, precipitation has become an alternative for the capture of recombinant antibodies from cell culture broth. Although protein A chromatography is the preferred purification step in the biopharmaceutical industry, because of its high recovery, yield and specificity [1] alternative technologies are necessary to bring manufacturing costs down for monoclonal antibodies. Precipitation has gained interest as an alternative due to the limitations and cost of affinity chromatography during downstream processing. Precipitation, widely used in low-value products, is a versatile and cheap unit operation that can be operated fully continuously and does not require expensive equipment or materials. Previous studies have shown that the combination of polyethylene glycol (PEG), caprylic acid (CA) and $CaCl_2$ purification steps enable a fully continuous and non-chromatographic process with a similar purity and yield that is highly competitive to affinity chromatography [2]. This renewed interest in precipitation is also observed in the growth of the number of publications concerning antibody precipitation procedures [1], and the amount of precipitating agents that have been investigated in the past years, such as ethanol [3], PEG [2,4–8] or $ZnCl_2$ [9] in combination with tangential flow filtration (TFF), continuous centrifugation [10,11] or aqueous two-phases systems [12] to switch from batch to a continuous process. However, a better understanding of the precipitation mechanisms and the impact of precipitation on further purification steps is required. In addition, the majority of research on antibody precipitation is focused on single addition precipitation approaches, where there is limited control on the coprecipitation and do not consider variations in impurities such as the host cell

Abbreviations: CA, caprylic acid; CHO, Chinese hamster ovary; FBRM, focused beam reflectance measurement; Df, fractal dimension; HCP, host cell proteins; HMWI, high molecular weight impurities; MWT, polymer molecular weight distribution; PEG, polyethylene glycol; PSD, particle size distribution; TFF, tangential flow filtration; TMP, transmembrane pressure.

* Corresponding author.
E-mail addresses: Carme.pons-royo@boku.ac.at (M.C. Pons Royo), alois.jungbauer@boku.ac.at (A. Jungbauer).

https://doi.org/10.1016/j.procbio.2022.01.017
Received 22 November 2021; Received in revised form 17 January 2022; Accepted 18 January 2022
Available online 21 January 2022

protein (HCP) or high molecular weight impurities (HMWI) from batch to batch. To circumvent this problem, multiple precipitation strategies have been already proposed [2,3,6,13]. Hammerschmidt and co-workers [6] demonstrated that sequential addition of precipitating agent is advantageous to classic PEG techniques in terms of purity and yield.

Furthermore, successful implementation of a precipitation step by the industry requires to consider the recovery of the precipitated protein of interest. Several technologies have been used and implemented for the purification of the antibodies and removal of impurities and other recombinants [14]. Some of the preferred methodologies are centrifugation, including disc-stack centrifugation [11], tubular bowl [15] and multi-chamber bowl centrifuges [16] and filtration systems such as tangential flow filtration (TFF) [4,9], single pass TFF [17] and counter-current TFF [18–20]. However, when it comes to solid-liquid separation for precipitation processes several problems remain unsolved, particularly when the desired product is in the solid fraction. The use of centrifuges for protein recovery, compacts the PEG precipitates and increase the density of the particles, which will require vigorous stirring to redissolve the precipitate and leading to prolonged process time and denaturation and aggregation of the antibodies. Besides, the shear disruption during the process lead to the breakage of the larger particles into smaller particles, complicating further separation steps. Tangential flow filtration is a gentler methodology that avoids compaction of the precipitates and re-solubilization problems. Nevertheless, the addition of PEG6000 increases the viscosity of the solution significantly hindering filtration performance. The increase of viscosity increases the transmembrane pressure and limits the maximum flux achievable, consequently reducing the mass flow through the membrane [4]. Approaches for stepwise addition of precipitation agents or slow gradual addition can be used to control the resulting particle size distribution and aging parameters related to the Camp number such as particle density [21], has high potential for improving the filterability during TFF and the performance of the combined precipitation and precipitate harvest. Precipitation in the case of single addition precipitation consists mainly of two processes, nucleation and growth, while due to the addition of precipitant in a single dose, both will happen at the same time. During nucleation sub-micron particles, called nuclei, are formed that mature into bigger particles through aggregation and collision leading to increasing particle size. To acquire a larger particle size with a narrow particle size distribution (PSD), it is essential to limit the nucleation rate and the creation of new nuclei during the process, while promoting the particle growth to form larger aggregates [21]. However, targeting the exact band for particle growth with virtually no nucleation can be difficult, and is protein dependent. Thus, the continuous addition of precipitant agent is key to control growth and limit the nucleation during particle growth for a desired size and size distribution enhancing solid-liquid separation [10,11], which will minimize difficulties during filtration as the pore size of the filtration membrane can be better optimized for narrow particle size distributions and for a better filtration rate.

In addition to particle size distribution, other parameters play an important role during filtration such as the aging process, the compactness and density of the precipitates [22]. Determination of compactness and density can be done by different methodologies, one powerful method to characterize the shape of complex structures like precipitates is the fractal dimension. Various methods exist to determine fractal dimensions, one based on light scatter yielding an average fractal dimension of the mixture, and recently a microscopy-based 3D reconstruction of precipitate structures was presented by our working group. Microscopy based reconstruction is a powerful tool to compare and to better understand structures of different particles and particle populations. A 3D aggregate is considered to be fractal if its density decreases with radial distance from the core [23]. Therefore, smaller fractal numbers are correlated to larger precipitates formed by looser external layers, less compact and tough. Whilst smaller particles with higher fractal dimensions have therefore higher compactness and toughness [10,11]. This methodology has been previously used to characterize precipitate particles to understand precipitate populations under different shear stress environments [23], the resistance to shear break-up during centrifugation [10,11] or the influence of the flocs on the cake formation and filtration performance [24–27]. Hence, fractal dimension is an interesting tool to predict the particle behaviour during solid-liquid separation, both centrifugation-based and filtration-based.

In this study we investigated the effect of gradual and stepwise PEG addition on the particle size distribution, fractal dimension and its effect on process parameters such as yield and purity. We used fractal dimension analysis to study the 3D structure of the precipitates, compactness and strength, and how these properties are influenced by the PEG dosage time. Furthermore, we studied the correlation between these properties and the ease of separation by TFF and depth filtration.

2. Materials and methods

2.1. CHO cell culture supernatants

Experiments were performed with clarified Chinese hamster ovary (CHO) cell culture supernatants of Trastuzumab, Adalimumab and additional antibodies labelled mAb1, mAb2 and mAb3. mAb2 and mAb3 are the same antibody but from different batches, previously used in Sommer et al. [2,7]. These antibodies were used for evaluation of the effect of batch-to-batch variations on particle size distribution. Prior to the experiments, Trastuzumab was treated with 150 mM $CaCl_2$ and 1 % CA at pH 4.5 and the pH was adjusted to 7.5 with 1 M Tris pH 8 to precipitate impurities [28]. mAb concentrations were 1 g/L (Trastuzumab), 0.36 g/L (Adalimumab), 1.4 g/L (mAb1), 1.13 g/L (mAb2) and 1.4 g/L (mAb3). The supernatants were filtered with a 0.22 µm membrane (Merck KGaA, Darmstadt, Germany) before use.

2.2. Protein precipitation

Protein precipitation was performed in a 100 mL EasyMax 102 glass reactor (Ref. num. 51161620, MettlerToledo AutoChem, Columbia, MD) by adding 40 % PEG6000 stock solution (40 w/v%) to a determined PEG concentration in 3 different modes, single addition, stepwise and gradually. In single addition, the volume of PEG6000 required to achieve a determined concentration was added in one addition, reaching 13 or 20 % PEG. Stepwise addition was performed by adding the equal amount of PEG6000 in a series of steps every 1 min with a pipette (Gilson, Middleton, WI, USA), to get to the same final PEG concentration of 20 % in 5 min or 15 min and gradual addition of PEG6000 was performed using an Azura compact pump (Flowspek AG, Hegenheimerstrasse, Basel) during 3, 5 and 15 min. For further chromatographic analysis specific to the precipitate, precipitates were washed twice with 20 % PEG6000 and centrifuged at 5000 *g* for 5 min. The supernatant was withdrawn and the pellet was resuspended with 1 x PBS pH 3.5 [6].

2.3. FBRM experiments

Particle size distribution was measured using the Particle Track G400 probe equipped with Focused Beam Reflectance Measurement (FBRM) technology (Mettler Toledo AutoChem, Columbia, MD) [3,9]. The 100 mL EasyMax 102 glass reactor with an inner radius of 52 mm, 90 mm height and 2.5 mm wall (Ref. num. 51161620, MettlerToledo AutoChem, Columbia, MD) was filled with 70 mL antibody supernatant. The reactor mixing was set to 150 rpm. The recording settings were 2 m/s chord length selection of Primary (fines), on a chord length from 0 to 1000 µm. After 5 min of equilibration, the desired amount of a stock solution of 40 % PEG solution was added at different times, in gradual, stepwise or single addition manner and particle size distribution was recorded during 30 min. Results were analysed using the iC FBRM software (MettlerToledo AutoChem, Columbia, MD).

2.4. Protein A chromatography

Antibody concentration was determined using an Affinity column POROS A 20 µm Column (2.1 × 30 mm, 0.1 mL; Thermo Scientific, MA, USA), as previously described [29]. The equilibration buffer was 50 mM potassium phosphate buffer with 150 mM NaCl at pH 7.0 and the elution buffer was a 100 mM glycine buffer, pH 2.4.

2.5. Size exclusion chromatography

Sample purity was determined using a TSKgel® G3000SWXL HPLC Column (5 µm, 7.8 × 300 mm, Tosoh, Tokyo, Japan) with a TSKgelSWXL Guard Column (7 µm, 6.0 × 40 mm; Tosoh, Tokyo, Japan). We used a Dionex Ultimate 3000 HPLC system with a diode array detector (Thermo Fisher Scientific, MA, USA). The absorbance was measured at 280 nm. The antibody purity was calculated as the ratio of the monomer peak area to the sum of all peak areas, based on the 280 nm signal. The running buffer was a 50 mM potassium phosphate buffer with 150 mM NaCl at pH 7.0 (Merck KGaA, Darmstadt, Germany), filtered through 0.22 µm filters (Merck KGaA, Darmstadt, Germany) and degassed. 20 µL of sample were injected into the column. Data was evaluated with Chromeleon™software (ThermoFisher Scientific, MA, USA).

2.6. Fractal dimension analysis

Fractal dimension analysis was determined using a Leica DMI6000B wide-field fluorescence microscope with an objective HCX PL APO 100×/1.40 Oil, as previously described [23]. Matlab2020 and the Image Processing Toolbox of MatLab were used for object detection and binarization. Box counting on different scales was used to calculate the fractal dimension, the surface, total volume, and density for each object.

2.7. Depth filtration

The precipitated antibody solution was filtered using a non-sterile PVDF syringe Millex GV filter of 0.22 µm, 4.5 cm^2(Merck KGaA, Darmstadt, Germany) at a flow rate of 1333 LMH. Pressure was recorded with a PendoTech pressure sensor (PendoTech, Princeton, NJ, USA) connected to a PressureMAT Sensor Monitor (PendoTech, Princeton, NJ, USA).

2.8. Tangential flow filtration

Tangential flow filtration (TFF) was performed with a 0.2 µm polyethersulfone (PES) MicroKros® hollow fiber filter module (Repligen, MA, USA). In a first step, the precipitate was concentrated at a constant tangential flow rate of 460 LMH and the filtrate flux of 20 LMH. In a second step, the precipitate was washed with 20 % PEG6000 solution, using the same conditions as those used in the first step. The transmembrane pressure (TMP) was recorded with a PendoTech pressure sensor (PendoTech, Princeton, NJ, USA) connected to a PressureMAT Sensor Monitor (PendoTech, Princeton, NJ, USA). Data was evaluated using the PressureMAT software (PendoTech, Princeton, NJ, USA).

3. Results and discussion

3.1. Influence of the addition time on particle size distribution

We used PEG6000, a well-known industrial precipitating agent for plasma and monoclonal antibodies, to characterize the overall precipitation behaviour of the antibodies. We added PEG to 5 different antibody cell free culture harvests either with a single addition, by gradual or stepwise addition (Fig. 1). Other experimental conditions such as energy input and temperature were kept identical between the different addition schemes to minimize the impact of addition, since such factors can have significant impact on precipitation performance [30–33]. In addition, as PEG is polydisperse and the distribution of molecular weights could change from lot to lot, we used the same stock from the same lot number of chemicals. Effects besides the addition time due to changing shear rate, temperature or PEG composition have been done in the past and we focused on the addition time in this study. The influence of the dosage time of PEG on the particle size distribution was therefore investigated. In single addition, the volume of PEG6000 required to achieve a determined concentration was added in one addition, reaching 13 or 20 % PEG. In gradual mode, PEG6000 was added without interruption until a PEG concentration of 20 % was achieved. Gradual addition was done either over a period of 5 or 15 min. Stepwise addition was performed by adding the equal amount of PEG6000 in a series of steps every 1 min, to get to the same final PEG concentration of 20 % in either 5 min or 15 min, corresponding to 5 or 15 additions respectively. These precipitation experiments were monitored with FBRM measuring the mean particle size and the particle size distribution. Since there were no variations on PSD when precipitation was performed in stepwise and gradual mode, the experiment was only performed in gradual mode with

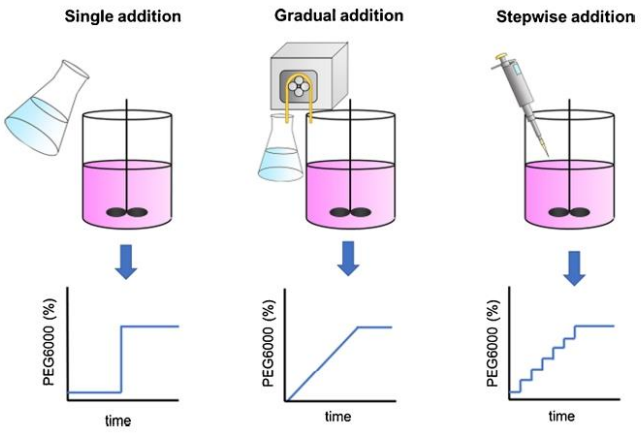

Fig. 1. Experimental setup of the single addition, gradual and stepwise PEG6000 addition.

Trastuzumab. In addition, to analyse if previous treatment of the antibody has an effect on the PSD, prior to the experiments, Trastuzumab was purified using multiple precipitation steps [28,34]. In the first step the supernatant was treated with 150 mM $CaCl_2$ to precipitate HMWI such as dsDNA and aggregates. Afterwards, 1 % CA at pH 4.5 was added to precipitate HCPs and prior the PEG addition to precipitate the antibodies in a purified and concentrated form, the pH was adjusted to 7.5 with 1 M Tris pH 8. The PSD obtained from the 5 antibodies precipitated at different conditions (single, gradual and stepwise), dosage times (3 min, 5 min and 15 min) and a final concentration of 20 % or 13 %, are shown in Table 1.

Similar behaviour was found for all the antibodies. The fast addition of PEG resulted in higher median PSD whereas, longer additions showed the opposite result. Interestingly, the single addition and long (15 min) addition times yielded the same median particle size. Additionally, no significant differences were found in particle size when PEG was added gradually or stepwise (Table 1). Single addition of PEG at higher concentrations resulted in a significant increase of median chord length, by a factor around 1.8 compared to lower concentrations. However, this effect was not observed on longer dosage times. A possible reason to explain this increase of median chord length could be caused by the coprecipitation during PEG precipitation (discussed in the next section). The direct addition of precipitant in excess would create immediately supersaturation conditions and impurities such as HMWI or HCPs which are heedlessly coprecipitated with the main product [6]. Thus, this effect would be more pronounced for single addition of PEG and at higher concentrations than with a gradual addition. However, mAb1 and mAb2 precipitated in a single addition of 13 % PEG presented similar purity compared to the single addition of 20 % PEG. Besides mAb1 and mAb2 precipitated in a single addition of 13 % PEG presented higher yield, 61 % and 78 % respectively, compared to 50 % obtained with the 20 % PEG single addition and gradual addition. These results show that higher PEG concentrations have no positive effect on yield and probably purity. Nevertheless, according to theory longer addition times either gradual or stepwise should consequently lead to larger particle size in comparison to shorter and faster addition, but that is not observed for the 15 min time period in our experiments. Since protein precipitation reaches the kinetic equilibrium, relatively fast, in less than 15 min [7,35], we assumed that mixing during PEG addition was completed. Additionally, particle size distribution change was recorded for 30 min to ensure full particle growth. We see consequently slightly higher medium chord lengths during 3 or 5 min addition of PEG compared to single time additions, but we see smaller cord lengths for 15 min addition. In these experiments, we used a mixing vessel during precipitation, which also means that we introduce shear force gradually during the experiment, and 15 min mixing combined with relatively soft precipitates might lead to continuous breaking of formed precipitates during the experiment. Such behaviour has been shown for similar systems [21,36,37].

To better understand the forming particle sizes and their distribution, we utilized the cord length distribution provided by the FBRM measurement (Fig. 2). The medium chord length was larger for single time addition of 20 % PEG in comparison to 3, 5 or 15 min addition times, here presented for the gradual addition of PEG. Such a broad size distribution is undesirable for further processing, as all subsequent unit operations have to be engineered to handle both small and large particles. Longer addition times, or most likely, the combination of longer addition time and longer mixing times, lead to smaller particles sizes and a smaller particle size distribution. Furthermore, the effect of antibody concentration in the supernatant was evaluated. It can be seen from the results that changes of the particle size distribution due to higher protein concentration were negligible at this range (Table 1). This effect,

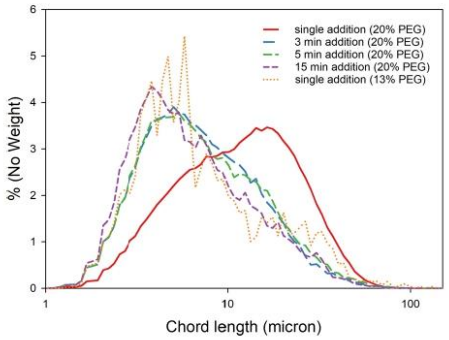

Fig. 2. Normalized particle size distribution obtained for mAb1 at different PEG6000 addition times (single addition, 3 min, 5 min and 15 min gradual addition).

Table 1
Median and mean chord length (μm) with different PEG addition times, (single addition, 3 min, 5 min and 15 min in gradual and stepwise mode) and PEG concentration (20 % PEG and 13 % PEG) for five monoclonal antibodies (Trastuzumab (1 g/L), Adalimumab (0.36 g/L), mAb1 (1.4 g/L), mAb2 (1.13 g/L) and mAb3 (1.4 g/L).

	Trastuzumab		Adalimumab		mAb1		mAb2		mAb3	
Addition time	Median chord length (μm)	Mean particle size (μm)	Median chord length (μm)	Mean particle size (μm)	Median chord length (μm)	Mean particle size (μm)	Median chord length (μm)	Mean particle size (μm)	Median chord length (μm)	Mean particle size (μm)
Single addition (20 %)	10.79	14.23 ± 1.15	n.d.	n.d.	11.13	14.86 ± 1.24	12.04	14.08 ± 1.27	11.52	12.03 ± 1.22
Single addition (13 %)	n.d.	n.d.	5.18 §	6.89 ± 2.41 §	5.89	11.12 ± 1.33	6.55	6.36 ± 1.34	n.d.	n.d.
Gradual 3 min (20 %)	8.34	11.33 ± 1.25	7.31 §	9.32 ± 1.97 §	6.49	9.09 ± 1.32	n.d.	n.d.	6.41	12.49 ± 1.21
Gradual 5 min (20 %)	7.08	10.70 ± 1.27	6.48 §	8.67 ± 2.22 §	6.49	9.37 ± 1.29	6.48	9.85 ± 1.29	6.68	9.02 ± 1.33
Stepwise 5 min (20 %)	7.09	10.90 ± 1.25	n.d.	n.d.	n.d.	n.d.	n.d.	n.d.	n.d.	n.d.
Gradual 15 min (20 %)	6.70	11.97 ± 1.21	5.62 §	7.60 ± 2.19 §	5.60	8.36 ± 1.34	5.65	9.08 ± 1.34	5.77	9.02 ± 1.27
Stepwise 15 min (20 %)	6.37	11.30 ± 1.90	n.d.	n.d.	n.d.	n.d.	n.d.	n.d.	n.d.	n.d.

n.d., not determined.
§ Experiments performed with 13 % PEG6000.

however, is expected to become considerable at higher protein concentrations [11].

3.2. Influence of the addition time on purity

To determine the influence of the dosage time of PEG on yield and purity and respectively the inclusion of HMWI and HCP in the precipitate itself, samples from different precipitation methods and times were analysed. Precipitates were washed twice with 20 % PEG6000 and the pellet was resuspended with 1 x PBS pH 3.5. Concentration of impurities, were assessed by integration of total area in size exclusion chromatography and the monomer antibody concentration. Yield was determined by comparing the monomer antibody peak of the cell culture supernatant and the precipitation samples using an analytical protein A chromatography. Then, the purification factor was calculated as the ratio of the concentration of impurities and antibodies after PEG precipitation, over the respective supernatant before PEG precipitation. The purification factors obtained after different time of dosage are shown in Fig. 3.

The three antibodies showed a similar tendency in respect to the achieved purification factor. There was no significant effect of the addition time on the purification factor. Different purity factors have been obtained with different antibodies, but this is expected due to the nature of the antibody and the composition of the respective supernatant. For instance, the relative initial purity of mAb1, mAb2 and mAb3 were respectively, 13.64 %, 12.04 % and 28.29 % and differences in the HCP composition are to be expected as well.

In prior studies [2,7] the combination of $CaCl_2$ and CA before PEG precipitation showed an improvement on the purity values comparable to protein A purification. The effect of the $CaCl_2$/CA pre-treatment of the antibodies on purity was also assessed. The different mode of addition, single, gradual and stepwise were tested with Trastuzumab pre-treated with 150 mM $CaCl_2$ and 1 % CA at pH 4.5 and the pH adjusted to 7.5 with 1 M Tris pH 8 [28]. When the pre-treated culture supernatant, with a relative purity of 11.04 %, was further purified with PEG precipitation the mode of addition had a substantial influence on the obtained purity, 96–99 % purity was achieved with sequential and gradual addition in comparison to 88 % obtained in batch addition (Fig. 4).

Compared to single addition the stepwise or gradual resulted in an up to 4-fold higher purity factor. This effect could not be observed when the culture supernatant was directedly precipitated with PEG and not pre-treated. Increasing the duration of the addition and number of steps

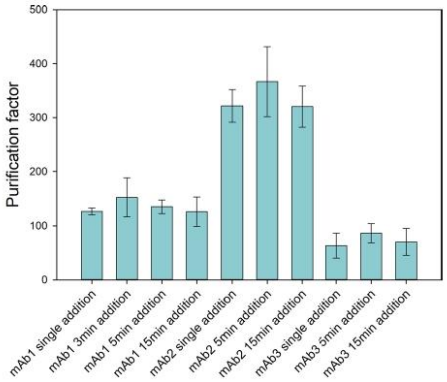

Fig. 3. Purification factors achieved using single and gradual addition for mAb1, mAb2 and mAb3. Precipitates were recovered by centrifugation, washed with 20 % PEG6000 and resolubilized with 1xPBS pH 3.5. Experiments were performed in triplicates and data is given as mean ± standard deviation.

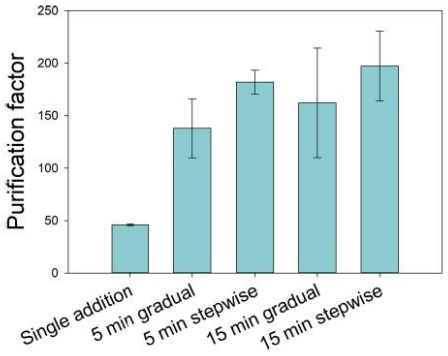

Fig. 4. Purification factors achieved using single, stepwise and gradual PEG addition for Trastuzumab. Precipitates were recovered by centrifugation, washed with 20 % PEG6000 and resolubilized with 1xPBS pH 3.5. Experiments were performed in triplicates and data is given as mean ± standard deviation.

did not further increase purification factor. The gradual or stepwise addition of PEG avoids a localized overshoot of precipitant concentration due to mixing inhomogeneities. Other impurities are co-precipitated by the overshoot and do not readily re-dissolve or they are effectively occluded in the precipitate. These results reinforce that gradual and stepwise precipitation can be a favourable approach for increasing process robustness, reducing the coprecipitation and can reduce issues related to batch variations.

3.3. Influence of the addition time on fractal dimension

Fractal dimension (Df) analysis was used to characterize the precipitate particles and to understand the influence of PEG addition time and mode of addition on particle compactness, density and 3D structure. The analysis was performed with mAb1 precipitated in a single addition, 5 and 15 min gradual addition. We did not test sequential addition, as no benefits were seen for the purification factor in previous experiments. For all the precipitate samples, the fractal dimension, particle diameter, particle volume and density were determined by microscopy and subsequent particle 3D-structure reconstruction (Table 2).

In order to get an insight into the homogeneity of the fractal characteristics of particles were investigated and determined if mono- or multifractality were present. Mono-fractal precipitates show the same fractality on all size scales, while multifractal objects have different fractalities depending on the size scale. This either translates to a uniform structure in small and large scale features present (monofractality) or relates to a microstructure that significantly differs from the macrostructure in the case of multifractality. Multifractality could point to the formation of features of different sizes by different mechanisms, while mono-fractality is the expected behaviour for a single mechanism for the formation. All samples presented mono-fractality that indicates that precipitate properties are uniform on all size scales (Fig. 5). Despite the mono-fractality of each individual precipitate, there was considerable

Table 2
Median fractal dimension and density obtained with mAb1 at different PEG addition times (single addition and 5 min and 15 min gradual addition).

	Single addition (n = 10)	5-min addition (n = 10)	15-min addition (n = 10)
Fractal dimension (median)	2.41 ± 0.12	2.22 ± 0.20	2.41 ± 0.06
Density (median)	0.16 ± 0.07	0.27 ± 0.07	0.18 ± 0.03

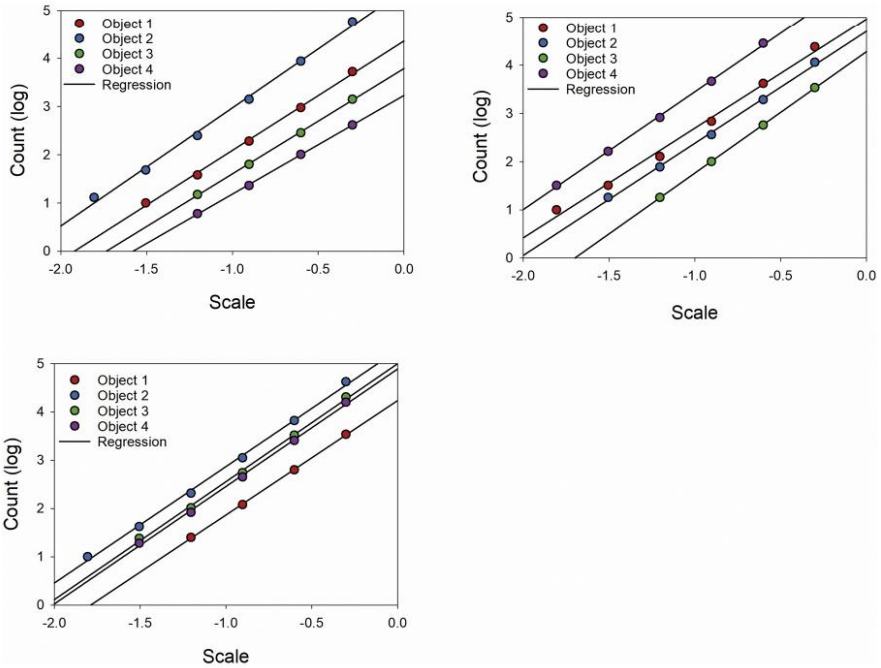

Fig. 5. Fractal dimension plots of mAb1 precipitated with different PEG addition times (single addition, 5 min and 15 min gradual addition) presented as size scale vs box count number of representative precipitate objects in the sample. The slope represents the fractal dimension, while the linear nature of the curve shows monofractality.

variance in the slope and fractality within each sample, most pronounced for single (2.41 ± 0.12) and 5 min addition (2.22 ± 0.20). For 15 min, slopes were very similar and more homogeneous (2.41 ± 0.06). Simulation studies have shown that reaction limited precipitates and diffusion limited precipitates show differing fractal dimensions of 1.7 for reaction limited and 2.4 for diffusion limited precipitation. Our results firmly point to diffusion limited precipitation in all cases, irrespectively of single addition or continuous addition over 5 or 15 min [38]. The narrower size distribution achieved during 15 min addition is of further importance, because a narrower fractal dimension distribution refers to more uniform densities of particles present in the mixture [23]. The slope of the linear curve shown in Fig. 5 is the fractal dimension and this value is correlated to the compactness and toughness of the aggregates, where higher fractal dimensions point to a more compact precipitate. The highest fractal dimension was obtained by precipitates formed in a single addition and by 15-min with a similar value and 5-min addition with the lowest fractal dimension. This should indicate that single addition and 15-min precipitates are more compact and less porous than the 5-min precipitates, which is not what we initially expected. The classical expectation would be that single addition should lead to less dense particles, and longer additions should lead to more compact precipitates, as rapid addition would lead to instant nucleation, fast growth and subsequent agglomeration of precipitates. In contract, continuous addition should lead to nucleation only in the beginning, and afterwards to a gradual growth of already existing precipitates. In addition, single addition should lead to significantly broader particle size distributions. In our case, this behaviour is not visible clearly, as 5 min addition has the highest variation and less dense particles. While the fractal dimension is somewhat similar between the samples, especially the average fractal dimension, the average size and size distribution is significantly different. As seen in the chord length distribution in Table 1

As fractal dimension on its own is somewhat similar, we tried to analyse if a combination of multiple factors like fractal dimension, the particle size in number of voxels in the 3D precipitate structure reconstruction, and the density calculated from the same structure as volume occupied by the precipitate vs volume of an encompassing sphere yield distinct populations from one experiment to the next (Fig. 6). There is a clear cut between populations generated at different dosage times for particle sizes obtained by this method, which is in line with the FBRM measurements before, with the single addition showing the largest particles. To further understand these populations, density was plotted against the particle size in number of voxels (Fig. 6). When looking at the density of resulting particles against fractal dimension, the particle population for 15 min addition time has a more constant density and fractal dimension, whereas the distribution of density is very broad in the other samples. With the limited number of particles in each of the analysis no definitive assessment can be made, but it seems that 15 min addition time results in both the most constant size distribution as assessed by FBRM and microscopy analysis as well as the most constant fractal dimension and density. This analysis highlights the importance of methodologies capable of generating size distributions, density distributions and fractal dimension distributions to assess precipitation behaivor, as measurements that only generate an average characteristic for the whole population will miss how broad the distribution in that sample actually is.

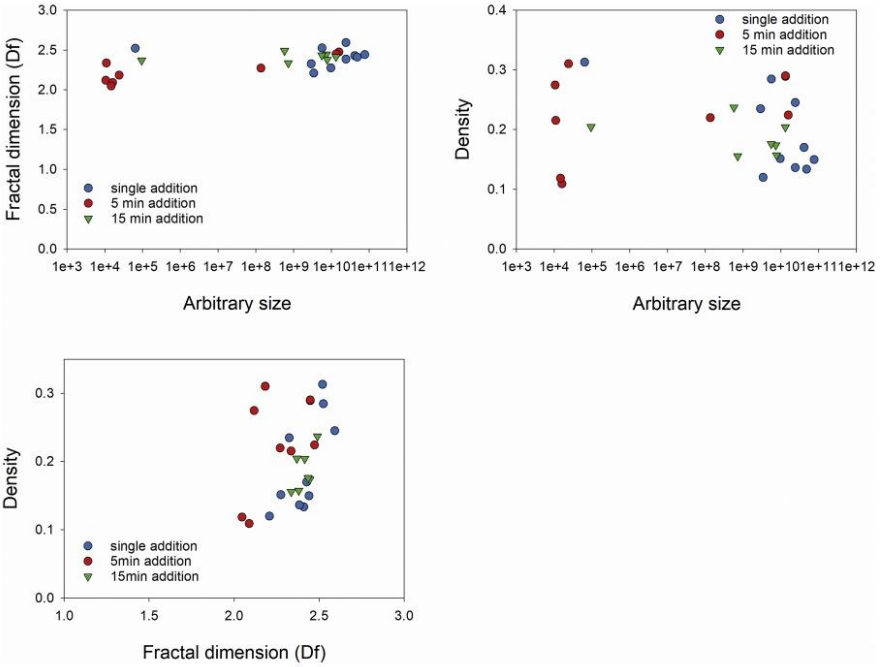

Fig. 6. Correlations between particle size, particle density and fractal dimension at different PEG addition times (single addition, 5 min and 15 min gradual addition). Particle size is determined by voxel count of the reconstructed 3D structure of particles and particle density by the volume occupied by the precipitate vs the encompassing sphere of the particle.

3.4. Influence of the addition time on depth filtration

To evaluate the impact of PEG dosage and the 3D structure of the precipitates on liquid-solid separation, precipitated solutions were filtered through a depth filter at constant flow. Here, since speed was kept constant, filtration performance was studied based on the pressure built up in the filter. The pressure-buildup during filtration indicates the maximum possible load on a specific filter size and therefore determines the necessary scalable filtration area for a given process. Recorded pressure mass flow per unit area membrane curves are shown in Fig. 7.

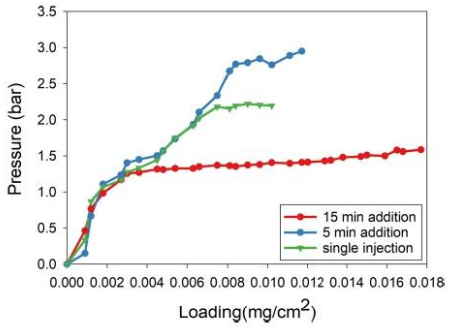

Fig. 7. Impact of addition time of PEG for precipitation (single addition, 5 min and 15 min gradual addition) on the performance of depth filtration for mAb1 showing pre-filter pressures during filtration.

The pressure increase is significantly steeper for single injection and 5-min addition. This is expected because a corresponding broader PSD was observed in the experiments, compared to 15-min addition with the narrowest PSD (Fig. 2). With a wide particles size distribution the voids in the cake will be filled with fine particles and therefore the pressure drop is higher compared to cakes with narrow PSD. Furthermore, the specific cake resistance and compressibility, are also affected by precipitate size, density and porosity [24,25], and showed a big impact on filterability. Cakes formed with more homogeneous precipitates will show lower backpressure, even with small particles. Unfortunately, we could not correlate the filtration performance to the fractal dimension results (Table 2) meaning that in our case the particle size distribution was the only determining factor for pressure build-up during filtration. Density and porosity of the resulting precipitate was either too similar as indicated by a similar fractal dimension, or the effect was negligible in our experiments. As pointed out, theory would dictate that for solid-liquid separation it is desirable to have large particles rather than fine particles to facilitate the filterability, but our results differ from that premise and in contrast we see a high impact from the broadness of the PSD and not the average size of particles. In order to improve filterability, the PSD can be influenced by the mode of addition of precipitant and narrow PSDs should be prioritized. From a process perspective, depth filtration is capable of removing precipitates efficiently, but recovering precipitated product from the depth filtration can be difficult, and we therefore recommend it mainly for the case of impurity precipitation where no recovery of precipitate from the filter is necessary.

3.5. Influence of addition time on tangential flow filtration

For product recovery, tangential flow filtration is preferred in comparison to depth filtration, as the recovery of the precipitate is much easier and dissolution of the precipitate can be done after flushing it from the filter capsule. So we evaluated the impact of PEG dosage and the 3D structure of the precipitates on TFF and compared the results to our results for depth filtration. The precipitated solutions were filtered using a TFF in a constant flux mode recording the TMP during the process to monitor membrane fouling during operation (Fig. 8). TMP remained almost constant for the 5 and 15 min addition time samples, throughout the experiments at around 0.4 bar. However, TMP for single PEG addition increased gradually indicating a gradual fouling of the membrane. As for depth filtration, membrane fouling was affected by PSD but also for precipitate density and compactness, and interestingly the behaivor between depth filtration and TFF was significantly different [26,27]. Zhao et al. [26] observed that precipitates that are largest and strongest will lead to a cake formation much more porous and less compressible. Thus, showing an improvement on the flux decline compared to smaller and less strong precipitates populations. However, our obtained results do not corraborate with this idea as the smallest precipitates in our experiments are the ones from the 15 min addition time, which shows the best filtration performance in both depth filtration and tangential flow filtration. Although precipitates formed in a single addition exhibit larger average particles size, the variability of the particle poplulation in size, density and strength seemed to have a bigger influence on the filtration performance than the average particle size. Interestingly, although the depth filtration experiment showed significant differences between 5 and 15 min addition time, no difference was observed in TFF performance.

We were able to show significant differences in filterability for single addition of precipitant as well as gradual addition over 5 min and 15 min, highlighting the importance of process development for precipitation that does include the solid-liquid separation step. Results only based on particle size and inferring the filterability from the average particle size would have led to bad design decisions. We were also able to provide data on density and size distributions as well as fractal dimension distributions, shedding light on possible causes for these differences, and such parameters could be expanded in the future to serve as engineering key parameters to determine filterability. However, average size and average fractal dimension did not show any clear correlation in our data, with the most importing parameter shown to be the broadness of the particle size distribution. Our findings will also impact the design of continuous precipitation processes, as we could clearly show that a gradual or stepwise addition of the precipitant yields significant benefits for filtration and can be easily implemented independent of the establishment of engineering design rules based on particle size distribution or fractality of particles.

4. Conclusions

The mode of addition of precipitant influences the purity of the precipitate and has an impact on the filterability during subsequent solid removal by depth filtration or tangential flow filtration. By gradual and stepwise addition, we were able to demonstrate the influence on the final precipitate size and particle size distribution, significantly improving further processing and making the setup of subsequent unit operations significantly easier. We achieved significantly higher purification factors with gradual and stepwise precipitation compared to single addition by limiting the co-precipitation of other compounds. Additionally, we were able to influence characteristics of the resulting precipitate like toughness, density and fractal dimension to boost the performance of subsequent unit operations. We showed that specific precipitate characteristics can relate to the filterability for precipitate harvest by TFF or depth filtration significantly, highlighting the importance of precipitate structure for the solid-liquid separation step.

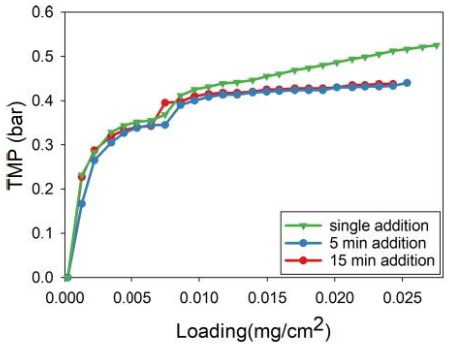

Fig. 8. Impact of time addition of PEG (single addition, 5 min and 15 min gradual addition) on transmembrane pressure (TMP) during tangential flow filtration (TFF) for mAb1.

This is especially true for particle size distribution. Fractal dimension analysis and focused beam reflectance measurements are perfect tools for investigating precipitation processes and future models can build upon such data to predict filterability of the resulting precipitate for depth filtration which was shown in our study. For the tested TFF, more studies need to implement such measurements to deduct a clearer picture and a mechanistic morel, and they should be employed in the process development of precipitate unit operation regularly. Use of such tools could cut down development cost and time drastically if used for predicting process performance of subsequent solid-liquid separations.

Funding

Grant agreement No 812909 CODOBIO, within the Marie Skłodowska-Curie International Training Networks framework.

Author contributions

Maria del Carme Pons Royo: Conducted the experiments and wrote the manuscript. Jean Luc Beulay: managed and coordinated the research plan. Eric Valery: acquired the financial support for the project. Alois Jungbauer: reviewed and edited the manuscript. Peter Satzer: reviewed and edited the manuscript.

Declaration of Competing Interest

The authors declare that there is no conflict of interests.

Acknowledgments

This work has received funding from the European Union's Horizon 2020 research and innovation program under the Marie Skłodowska-Curie grant agreement No 812909 CODOBIO, within the Marie Skłodowska-Curie International Training Networks framework.

References

[1] M. Martinez, M. Spitali, E.L. Norrant, D.G. Bracewell, Precipitation as an enabling technology for the intensification of biopharmaceutical manufacture, Trends Biotechnol. 37 (3) (2019) 237–241.
[2] R. Sommer, A. Tscheliessnig, P. Satzer, H. Schulz, B. Helk, A. Jungbauer, Capture and intermediate purification of recombinant antibodies with combined precipitation methods, Biochem. Eng. J. 93 (2015) 200–211.
[3] A. Tscheliessnig, P. Satzer, N. Hammerschmidt, H. Schulz, B. Helk, A. Jungbauer, Ethanol precipitation for purification of recombinant antibodies, J. Biotechnol. 188 (2014) 17–28.

[4] D. Burgstaller, A. Jungbauer, P. Satzer, Continuous integrated antibody precipitation with two-stage tangential flow microfiltration enables constant mass flow, Biotechnol. Bioeng. 116 (5) (2019) 1053–1065.
[5] N. Hammerschmidt, B. Hintersteiner, N. Lingg, A. Jungbauer, Continuous precipitation of IgG from CHO cell culture supernatant in a tubular reactor, Biotechnol. J. 10 (8) (2015) 1196–1205.
[6] N. Hammerschmidt, S. Hobiger, A. Jungbauer, Continuous polyethylene glycol precipitation of recombinant antibodies: sequential precipitation and resolubilization, Process. Biochem. 51 (2) (2016) 325–332.
[7] R. Sommer, P. Satzer, A. Tscheliessnig, H. Schulz, B. Helk, A. Jungbauer, Combined polyethylene glycol and CaCl2 precipitation for the capture and purification of recombinant antibodies, Process. Biochem. 49 (11) (2014) 2001–2009.
[8] Z. Li, Q. Gu, J.L. Coffman, T. Przybycien, A.L. Zydney, Continuous precipitation for monoclonal antibody capture using countercurrent washing by microfiltration, Biotechnol. Prog. 35 (6) (2019) e2886.
[9] G. Dutra, D. Komuczki, A. Jungbauer, P. Satzer, Continuous capture of recombinant antibodies by ZnCl 2 precipitation without polyethylene glycol, Eng. Life Sci. 20 (7) (2020) 265–274.
[10] E. Byrne, J. Fitzpatrick, L. Pampel, N. Titchener-Hooker, Influence of shear on particle size and fractal dimension of whey protein precipitates: implications for scale-up and centrifugal clarification efficiency, Chem. Eng. Sci. 57 (2002) 3767–3779.
[11] M. Martinez, G. Mannall, M. Spitali, E.L. Norrant, D.G. Bracewell, Reactor design for continuous monoclonal antibody precipitation based upon micro-mixing, J. Chem. Technol. Biotechnol. (2020).
[12] S. Crelier, A. Muhr, R. Dufresne, Aqueous two-phase systems as an alternative to chromatography? Characterization of a PEG-citrate system for antibody purification, N. Biotechnol. 44 (2018) S139–S140.
[13] N. Kateja, H. Agarwal, A. Saraswat, M. Bhat, A.S. Rathore, Continuous precipitation of process related impurities from clarified cell culture supernatant using a novel coiled flow inversion reactor (CFIR), Biotechnol. J. 11 (10) (2016) 1320–1331.
[14] H.F. Liu, J. Ma, C. Winter, R. Bayer, Recovery and purification process development for monoclonal antibody production, MAbs 2 (5) (2010) 480–499.
[15] M. Hoare, P. Dunnill, D.J. Bell, Reactor design for protein precipitation and its effect on centrifugal separation, Ann. N. Y. Acad. Sci. 413 (1983) 254–269.
[16] M. Boychyn, W. Doyle, M. Bulmer, J. More, M. Hoare, Laboratory scaledown of protein purification processes involving fractional precipitation and centrifugal recovery, Biotechnol. Bioeng. 69 (1) (2000) 1–10.
[17] J. Dizon-Maspat, J. Bourret, A. D'Agostini, F. Li, Single pass tangential flow filtration to debottleneck downstream processing for therapeutic antibody production, Biotechnol. Bioeng. 109 (4) (2012) 962–970.
[18] C.J. Yehl, A.L. Zydney, High performance countercurrent membrane purification for protein separations, J. Membr. Sci. 633 (2021) 119396.
[19] C.J. Yehl, M.G. Jabra, A.L. Zydney, Hollow fiber countercurrent dialysis for continuous buffer exchange of high-value biotherapeutics, Biotechnol. Prog. 35 (2) (2019) e2763.
[20] K. Mohanty, R. Ghosh, Novel tangential-flow countercurrent cascade ultrafiltration configuration for continuous purification of humanized monoclonal antibody, J. Membr. Sci. 307 (1) (2008) 117–125.
[21] P.M. Doran, Bioprocess Engineering Principles, 2nd ed., 2012.
[22] D. Bell, M. Hoare, P. Dunnill, The Formation of Protein Precipitates and Their Centrifugal Recovery, 2006, pp. 1–72.
[23] P. Satzer, D. Burgstaller, W. Krepper, A. Jungbauer, Fractal dimension of antibody-PEG precipitate: light microscopy for the reconstruction of 3D precipitate structures, Eng. Life Sci. 20 (3-4) (2019) 67–78.
[24] J.-D. Lee, S.-H. Lee, M.-H. Jo, P.-K. Park, C.-H. Lee, J.-W. Kwak, Effect of coagulation conditions on membrane filtration characteristics in coagulation–Microfiltration process for water treatment, Environ. Sci. Technol. 34 (17) (2000) 3780–3788.
[25] S.A. Lee, A.G. Fane, R. Amal, T.D. Waite, The effect of floc size and structure on specific cake resistance and compressibility in dead-end microfiltration, Sep. Sci. Technol. 38 (4) (2003) 869–887.
[26] B. Zhao, D. Wang, T. Li, C.W.K. Chow, C. Huang, Influence of floc structure on coagulation–microfiltration performance: effect of Al speciation characteristics of PACls, Sep. Purif. Technol. 72 (1) (2010) 22–27.
[27] J. Guan, R. Amal, T.D. Waite, Effect of aggregate size and structure on specific resistance of biosolids filter cakes, Water Sci. Technol. 44 (10) (2001) 215–220.
[28] A. Jungbauer, R. Sommer, Purification of Proteins, 2014.
[29] P. Satzer, A. Jungbauer, High-capacity protein A affinity chromatography for the fast quantification of antibodies: two-wavelength detection expands linear range, J. Sep. Sci. 41 (8) (2018) 1791–1797.
[30] Y. Ding, J. Zhao, L. Wei, W. Li, Y. Chi, Effects of mixing conditions on floc properties in magnesium hydroxide continuous coagulation process, Appl. Sci. 9 (5) (2019) 973.
[31] M. Hoare, P. Dunnill, D.J. Bell, Reactor design for protein precipitation and its effect on centrifugal separation, Ann. N. Y. Acad. Sci. 413 (1) (1983) 254–269.
[32] D.J. Bell, P. Dunnill, The influence of precipitation reactor configuration on the centrifugal recovery of isoelectric soya protein precipitate, Biotechnol. Bioeng. 24 (11) (1982) 2319–2336.
[33] F. Macritchie, Effects of temperature on dissolution and precipitation of proteins and polyamino acids, J. Colloid Interface Sci. 45 (2) (1973) 235–241.
[34] R. Sommer, Continuous Precipitation of Therapeutic Proteins, with an Emphasis on Monoclonal Antibodies, 2013.
[35] S.-L. Sim, T. He, A. Tscheliessnig, M. Mueller, R.B.H. Tan, A. Jungbauer, Branched polyethylene glycol for protein precipitation, Biotechnol. Bioeng. 109 (3) (2012) 736–746.
[36] E. Byrne, J.J. Fitzpatrick, L.W. Pampel, N.J. Titchener-Hooker, Influence of shear on particle size and fractal dimension of whey protein precipitates: implications for scale-up and centrifugal clarification efficiency, Chem. Eng. Sci. 57 (2002) 3767–3779.
[37] D. Burgstaller, W. Krepper, J. Haas, M. Maszelin, J. Mohoric, K. Pajnic, A. Jungbauer, P. Satzer, Continuous cell flocculation for recombinant antibody harvesting, J. Chem. Technol. Biotechnol. 93 (7) (2018) 1881–1890.
[38] C.W. Neil, J.R. Ray, B. Lee, Y.-S. Jun, Fractal aggregation and disaggregation of newly formed iron(iii) (hydr)oxide nanoparticles in the presence of natural organic matter and arsenic, Environ. Sci. Nano 3 (3) (2016) 647–656.

Paper II

Maria del Carme Pons Royo, Ignacio Montes-Serrano, Eric Valery, Alois Jungbauer, Peter Satzer,

Milliscale reactors for integration of continuous precipitation and filtration

Journal of Chemical Technology and Biotechnology

https://doi.org/10.1002/jctb.7187

Research Article

Received: 25 May 2022 Revised: 5 July 2022 Accepted article published: 9 July 2022 Published online in Wiley Online Library:

(wileyonlinelibrary.com) DOI 10.1002/jctb.7187

Milliscale reactors for integration of continuous precipitation and filtration

Maria del Carme Pons Royo,[a,b] Ignacio Montes-Serrano,[b] Eric Valery,[a] Alois Jungbauer[c,b*] and Peter Satzer[c,b]

Abstract

BACKGROUND: The development of integrated continuous biomanufacturing processes faces a significant challenge when the parameters for the design of the process cannot be accurately estimated from those of batch experiments. Process design is even more challenging if the outcome of one unit operation highly influences the performance of the subsequent one, such as in harvesting of a precipitate by filtration. In the case of protein precipitation, results from the batch and continuous experiements deviate and their scale-down is limited. Microfluidics suffer from poor mixing characteristics. Thus, milliscale devices were developed to maintain mixing performance but at the expense of a slightly larger scale.

RESULTS: Milliscale devices were developed for the precipitation of antibodies in continuous tubular reactors to compare different dosage times in small scale. The reactors have multiple addition points for precipitant for the continuous, controlled and precise addition of the precipitating agent without valves. The designed devices have a narrow residence time distribution to achieve fast mixing and a small volume that reduces the time and cost for experiments tenfold. Milliscale devices were used to evaluate the most appropriate dosage time for protein precipitation, thus improving purity by a factor of 3 compared to single addition. The resulting filterability of precipitates in tangential flow filtration and depth filtration was improved.

CONCLUSION: Results demonstrated that multiple additions were more beneficial than single addition because they help to reduce pressure and increase filter capacity. Such devices can be used to determine and adjust the precipitation methodology to optimize floc formation and improve solid–liquid separation while reducing development time and cost.

Keywords: scale-down; precipitation; mAbs; IgG; continuous

INTRODUCTION

There is significant interest in the biopharmaceutical industry for developing end-to-end continuous manufacturing platforms for monoclonal antibodies.[1,2] Protein precipitation has been proven to be an efficient alternative to chromatography A columns.[3] It can be easily adapted and operated in a fully continuous mode with consistent and reproducible results.[4,5] Furthermore, the latest studies have demonstrated that precipitation can achieve a similar yield and purity to protein A chromatography.[4,6-9] Despite all these advantages and its availability at the industrial scale, its implementation in antibody purification is still not widespread. A main challenge when developing an integrated continuous biomanufacturing process is the lack of methodologies to accurately estimate the engineering parameters for continuous batchwise processes. Such a challenge escalates when the outcome of one unit operation highly influences the performance of the subsequent one. This is the case with harvesting a precipitate by filtration. When a lot of material is required, long-term experiments become expensive. In the case of protein precipitation, the results from batch and continuous processes deviate and scale-down is limited. Microfluidics suffer from poor mixing characteristics. Thus, so milliscale devices were developed to maintain mixing performance but at the expense of a slightly larger scale.

Although several continuous reactors have been proposed for continuous precipitation, the process is still being performed in stirred tank reactors (STRs).[5,10] An example is blood plasma fractionation, where a continuous process has been stablished,[11] but the industrial process is still performed in batch mode. The use of stirred tank reactors carries certain disadvantages, such as inefficient mixing that can result in inhomogeneous distribution and concentration gradients of the precipitating agent.[5] In addition to inhomogeneities of concentrations, all mixing vessels have an inhomogeneous power input and shear forces throughout the

* *Correspondence to: A Jungbauer, Department of Biotechnology, University of Natural Resources and Life Sciences, 1190 Vienna, Austria. E-mail: alois.jungbauer@boku.ac.at*

a *Department of Innovation, Novasep, Pompey, France*

b *Austrian Centre of Industrial Biotechnology (ACIB), Vienna, Austria*

c *Department of Biotechnology, University of Natural Resources and Life Sciences, Vienna, Austria*

reactor. This changes the precipitate structure and will lead to further inconsistencies between small- and large-scale mixing vessels. Furthermore, studies focused on protein precipitation are often based on batch addition of the precipitating agent. Sequential precipitation can be advantageous over single addition in terms of purity, yield, and filterability.[6,12-14] An interesting reactor design for protein precipitation uses tubular reactors. Since precipitation is carried out while the mixture of protein solution and precipitant agents are flowing through the tube, several precipitation strategies can be tested that would not be possible in stirred tank reactors and that would avoid any problems due to mixing inhomogeneities. Further benefits of tubular reactors include the simple and flexible design that can be modified depending on the required maturation time or on the desired aging. Precipitation occurs almost instantaneously when the phase transition occurs by addition of a precipitant. Static mixers can be inserted in the tubular reactor to narrow the residence time distribution and to achieve fast mixing. Power input in stirred tank reactors has often been associated with precipitation performance but it has been misinterpreted. The power input in STRs reduces the mixing time and, therefore, it has been wrongly associated with precipitation. Floc size distribution is influenced by power input but not precipitation kinetics, which happens in a matter of seconds. Freedom in designing mixing and shear stress behavior is especially important during the design of a precipitation process and its scale-up.

For several years, Camp number (N_{ca}) was used as a main parameter for scaling-up flocculation processes. However, this approach has been widely criticized because flocculation is a complex process in which several variables and factors interfere;[15-17] thus, a multidimensional approach is necessary. Recent studies proposed other criteria for scale-up flocculation processes, such as constant power input, flocculent dosage, or flocculation time between reactors.[18] Efforts have been made to scale-down to mL downstream process (DSP) units keeping analogous process criteria. The complex geometries and systems used at the industrial scale make miniaturization down to the microscale complicated, especially for mixing phenomena that are hydrodynamically vastly different in the microscale.[19] However, there are some examples of DSP microdevices developed to study solid–liquid separations,[20] crystallization,[21-23] membranes or adsorption; even the EU project CODOBIO[24] is an example of the efforts being made to develop microfluidic devices for chromatography systems and extraction.

To design and develop millifluidic devices, computational fluid dynamics (CFD) is a valuable methodology to predict fluid flows, mass transfer, mixing behavior, residence time distribution, and other hydrodynamic phenomena. It can help to predict homogenous mixing in the small scale because laminar flow mixing becomes a difficult task and, at the microscale, mixing is slow and achieved essentially by diffusion.[25] Due to the velocity of the flows and the length of the channels in the devices, there is frequently not sufficient diffusion for proper mixing. It is often necessary to test different designs to find a proper geometry that introduces enough turbulence for proper mixing with the anticipated flow velocities and viscosities. Several patterns and passive mixing geometries have been studied to enhance mixing performance.[26] CFD allows for estimating essential parameters, such as pressure drop, power input, mixing efficiency, and other hydrodynamic parameters, to determine the mixing between inlet streams in milli- and microdevices[27] and further scaling parameters.

In this study, a milliscale device has been developed for the precipitation of antibodies in continuous tubular reactors to compare different dosage times in a small scale. The designed milliscale device has a small volume and narrow residence time distribution that reduces the time and cost of the experiments. In addition, different approaches for scaling-down flocculation process are discussed.

MATERIALS AND METHODS

CHO cell culture supernatants

Cell culture supernatants from Chinese hamster ovary (CHO) of antibodies labelled mAb1 (1 g/L) and mAb2 (1.4 g/L) were filtered with a 0.22 µm membrane (Merck KGaA, Darmstadt, Germany) prior to use. Respectively, their HCP concentrations were 10.25 g/L and 3.5 g/L and their dsDNA concentrations were 4.56 ng/mL and 17.74 ng/mL.

Protein A chromatography

Antibody quantification was performed using an affinity column POROS A 20 µm Column (2.1 × 30 mm, 0.1 mL; Thermo Scientific, MA, USA), with 50 mM phosphate buffer, pH 7.0 as equilibration buffer, and a 100 mM glycine buffer, pH 2.5, as elution buffer. This method was already described in the literature.[28]

Size exclusion chromatography

The purity of each sample was determined using a size exclusion TSKgel® G3000SWXL HPLC Column (5 µm, 7.8 × 300 mm) with a TSKgelSWXL Guard Column (7 µm, 6.0 × 40 mm; Tosoh, Tokyo, Japan) connected to a Dionex Ultimate 3000 HPLC system with a diode array detector (Thermo Fisher Scientific, MA, USA). The running buffer was a 50 mM sodium phosphate buffer with 150 mM NaCl at pH 7.0 (Merck KGaA, Darmstadt, Germany).[4,9]

Depth filtration

The precipitated antibody solution was filtered using a non-sterile PVDF syringe Millex GV filter of 0.22 µm, 4.5 cm^2 (Merck KGaA, Darmstadt, Germany), at a flow rate of 1333 $L{\cdot}m^{-2}{\cdot}h^{-1}$. Pressure was recorded with a PendoTech pressure sensor (PendoTech, Princeton, NJ, USA) connected to a PressureMAT Sensor Monitor (PendoTech, Princeton, NJ, USA), as in the work by Pons Royo *et al.*[29]

Tangential flow filtration

Filterability experiments were performed using a 0.2 µm polyethersulfone (PES) tangential flow filtration (TFF) MicroKros® hollow fiber filter module (Repligen, MA, USA). Supernatant was filtrated at a constant tangential flow of 460 $L{\cdot}m^{-2}{\cdot}h^{-1}$ and the filtrate flux of 20 $L{\cdot}m^{-2}{\cdot}h^{-1}$. Transmembrane pressure (TMP) was recorded using a PendoTech pressure sensor (PendoTech, Princeton, NJ, USA) connected to a PressureMAT Sensor Monitor (PendoTech, Princeton, NJ, USA). Data was evaluated using the PressureMAT software (PendoTech, Princeton, NJ, USA), as in the work by Pons Royo *et al.*[29]

Design of precipitation reactors

Millifabrication

Milliscale devices were designed using CorelDRAW 2020 (Corel Co., Canada) and crafted by laser cutting (Laser Trotec Speedy 100, Trotec GmbH, Austria). The microchannels were 1 mm wide and 3 mm deep. The main mixing channels and addition microchannels were cut in 3 mm and inlets and outlet were cut in 4 mm poly(methyl methacrylate) (PMMA) sheets (Acrylstudio GmbHW, Austria). The

Journal of Chemical Technology and Biotechnology published by John Wiley & Sons Ltd on behalf of Society of Chemical Industry (SCI).

PMMA sheets were heated up to 165 °C for at least 45 min and cooled down at room temperature. Prior to the bonding process, PMMA sheets were cleaned by rinsing them with 70% ethanol.

Continuous precipitation setup

Continuous PEG6000 precipitation was performed using the designed milliscale devices with one inlet connected to an Azura compact pump (Flowspek AG, Hegenheimerstrasse, Basel) for the antibody solution and a second pressure pump to the 40% (w/w) PEG6000 solution. Protein precipitation in a stirred tank reactor was performed in a 100 mL EasyMax 102 glass reactor (Ref. num. 51 161 620, Mettler Toledo AutoChem, Columbia, MD). The collected precipitated solution was continuously mixed for 15 min to ensure complete precipitation. Then, the precipitated solutions were washed with 20% (w/w) PEG6000 and resolubilized with 1xPBS solution (pH 3.5).

Computational fluid dynamics (CFD) simulations

Geometries were designed using Autodesk Inventor 2019 (Autodesk, San Rafael, CA, USA). The CFD simulations for comparative analysis of the different geometries were conducted using the software STAR-CCM+ V.12.02.011 provided by Siemens. Due to the binary mixture of water and 40% (w/w) PEG6000 solution, an Eulerian n-phase model was used to study the fluid dynamics inside the mixing geometries. The mesh of the channel geometry was made using the trimmed meshing technique. This technique divides the geometry into cubic elements and improves the computational time. The number of elements was kept at around 20 000 to allow for an adequate reproduction while maintaining a low computational time. To test the possible dependence of the results on the structure of the mesh, other techniques (such as tetrahedral meshing) were performed. The end results did not deviate from each other, but the trimmed technique provided lower residuals while maintaining short computational times. The mixing designs were analyzed considering the working fluids as a mix between water and 40% (w/w) PEG6000 solution with a density ρ of 1.000 kg·m^{-3} and 1.068 kg·m^{-3}, and a viscosity μ of 0.001 Pa·s and 0.049978 Pa·s, respectively. For the serpentine models 1 and 2, corresponding to the Y-shape and T-shape serpentines, each working solution was introduced though the opposite inlet. For the serpentine model 3, the working solutions were introduced through the canals using the same inlet. The outlet was kept as a split outlet. The mass fraction of the species and pressure were both set to zero. For the walls on the inside of the channels, no slip condition was specified. Further information was iterated from the neighboring cells. The mass flow rates in all cases were 0.0083 kg s^{-1} for the water flow and 0.0089 kg ·s^{-1} for the 40% (w/w) PEG6000 flow to obtain a final solution of 20% (w/w) PEG6000. Both fluids are considered incompressible and don't show any mass transfer between phases. Due to the small size of the channels, the regime is taken as laminar flow. Thus, the conservation equations of mass and momentum are obtained from the Navier–Stokes model without any adjustment of turbulence:

$$\frac{\partial \rho}{\partial t}+\nabla\cdot\left(\rho\vec{v}\right)=0 \tag{1}$$

$$\frac{\partial\left(\rho\vec{v}\right)}{\partial t}+\nabla\cdot\left(\rho\vec{v}\vec{v}\right)=-\nabla p+\nabla\left(\mu\nabla\vec{v}\right)+\rho\vec{g}+\vec{F_\sigma} \tag{2}$$

where ρ is the fluid density, $\vec{v}$ is the fluid velocity, p is the pressure, μ is the dynamic viscosity, g refers to gravity in m s^{-2}, and $\vec{F_\sigma}$ refers to surface tension forces in N. A semi-implicit pressure-linked equation (SIMPLE) algorithm and third-order upwind discretization (MUSCL) were used to solve the above equations.

The implementation of the different phases was implemented with the following equations:

$$\frac{1}{\rho_i}\left[\frac{\partial}{\partial t}\left(\alpha_i\rho_i\right)+\nabla\cdot\left(\alpha_i\rho_i\vec{v}_i\right)\right]=0 \tag{3}$$

where alpha is the mass fraction of each phase. This has the following consideration:

$$\Sigma_{i=1}^{n}\alpha_i=1 \tag{4}$$

This enables us to adequately capture and model the motion of the different fluid phases contained in the system.

Mixing performance was calculated as follows:[30]

$$\tau^2=\frac{1}{n}\sum_{i=1}^{n}\left(\alpha_i-\alpha_\infty\right)^2 \tag{5}$$

$$M_i=1-\sqrt{\frac{\tau^2}{\tau_{max}}} \tag{6}$$

Energy dissipation was used to determine the volumetric power input:

$$\frac{P}{V}=\frac{\int\mu\phi_v dV}{V} \tag{7}$$

where ϕ_v is the energy dissipation due to motion in s^{-2}. This is calculated with the following equation:[31]

$$\phi_v=\left(2\left[\left(\frac{\partial v_x}{\partial x}\right)^2+\left(\frac{\partial v_y}{\partial y}\right)^2+\left(\frac{\partial v_z}{\partial z}\right)^2\right]+\left[\frac{\partial v_x}{\partial y}+\frac{\partial v_y}{\partial x}\right]^2+\left[\frac{\partial v_z}{\partial x}+\frac{\partial v_x}{\partial z}\right]^2+\left[\frac{\partial v_z}{\partial y}+\frac{\partial v_y}{\partial z}\right]^2\right) \tag{8}$$

Shear rate (γ) and shear stress (η) was calculated as:

$$\gamma=\sqrt{\left(2\left[\left(\frac{\partial v_x}{\partial x}\right)^2+\left(\frac{\partial v_y}{\partial y}\right)^2+\left(\frac{\partial v_z}{\partial z}\right)^2\right]+\left[\frac{\partial v_x}{\partial y}+\frac{\partial v_y}{\partial x}\right]^2+\left[\frac{\partial v_z}{\partial x}+\frac{\partial v_x}{\partial z}\right]^2+\left[\frac{\partial v_z}{\partial y}+\frac{\partial v_y}{\partial z}\right]^2\right)} \tag{9}$$

Journal of Chemical Technology and Biotechnology published by John Wiley & Sons Ltd on behalf of Society of Chemical Industry (SCI).

Table 1. Geometrical parameters of the designed channel geometries

Channel geometry	Length (mm)	Width (mm)	Height (mm)	Wavelength (λ)	Amplitude (mm)
Simple T mixer	8.5	0.9	3.0	—	—
2D serpentine	8.5	0.9	6.0	1.5	3.0
3D serpentine	8.5	0.9	9.0	2.1	3.0

$$\eta = \mu\gamma \tag{10}$$

Camp number (N_{Ca}) was calculated as:

$$G = \frac{dv}{dz} = \sqrt{\frac{P}{\mu V}} \tag{11}$$

$$N_{Ca} = Gt \tag{12}$$

where G is the average shear rate and t is the time of exposure to shear.

RESULTS

Several methodologies can be used to determine the suitable precipitation conditions, including addition time and mode of precipitating agents in batchwise processes. However, there is no technology to evaluate such conditions in continuous mode. Furthermore, in both approaches, experiments require large amounts of buffer protein solutions and long experimental and manipulation times. To enhance precipitation studies, millifluidic devices were designed for continuous precipitation at different dosage times and evaluated the filterability of the precipitates. First, several geometries for static mixers were designed and evaluated by CFD. After selecting the most appropriate geometry, the device was crafted by laser cutting and experimentally tested.

Geometry computational study

3 different serpentine models were proposed with different grades of complexity to determine the most suitable mixing design for viscous liquids (Table 1). A comparative analysis of the different serpentine channel geometries was performed using CFD model (Fig. 1). The optimal design was examined based on the mixing index and pressure drop. Additionally, the Camp number and shear stress were calculated (Table 2).

CFD simulations were performed using the same flow conditions in the three cases: 0.5 mL/min of 40% (w/w) PEG6000 solution mixed with 0.5 mL/min MilliQ reaching 20% (w/w) PEG6000. Results showed that the first geometry did not induce any perturbation on the flow. The simple design for the diffusion of the streams resulted in insufficient diffusion and no mixing because of the characteristics of each flow. To improve the first design, a second geometry with 2D turns was proposed to enhance further mixing. However, the second design did not induce sufficient perturbation or interactions between PEG and water for them to be mixed, resulting in the formation of two phase layers. For the third model, a geometry with 3D turns was proposed. Previous studies have shown that 3D turns enhance mixing by generating chaotic flows and create secondary flows, thus braiding the fluids.[26] As observed, the induction of more chaotic flows allows the third geometry to perform adequate mixing within a few turns, obtaining the best mixing performance compared with the other two models, where the mixing quality was insufficient. Dividing and interlacing the streams was more efficient than just relying on diffusion (where mixing occurs slowly and requires longer channels).[26]

The mixing performance was evaluated using the mixing index, which ranges from 0 (corresponding to the worst mixing) to 1 (the best performance); results are shown in Table 2. The best mixing performance was obtained with the 3D serpentine (yield of 0.66), while the worst was obtained with the simple T mixer (0.25). In addition, mixing with the 2D serpentine was very poor, showing that 2D does not create enough of the chaotic flows required for mixing (which the 3D achieves). The power input required to induce proper mixing is one the factors to consider for reducing costs, especially because this cost should be kept as low as possible. Power input can also be correlated to the pressure drop; here, the pressure drop required for each mixing geometry was calculated. The highest value was obtained with the 3D serpentine, which performs up to 12 times better than the other designs. The secondary flows generated by this complex geometry will enhance mixing but it will also increase the pressure drop and, thus, the power required.[30] Even with the high pressure drop, the serpentine model 3 was selected for the design of the milliscale devices.

Visual validation of CFD simulations

Water and 40% (w/w) PEG6000 solution were colored with food coloring to verify the calculated mixing performance of the CFD models with the prototypes (Fig. 2). Both solutions were injected into each inlet using a pressure pump at the same rate as those in the CFD simulations (Fig. 2). Results agreed well with the

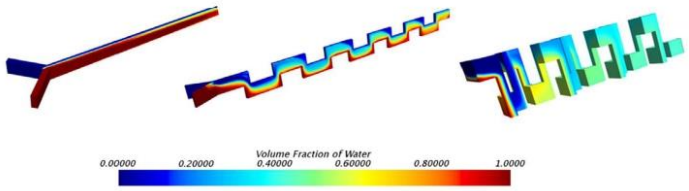

Figure 1. Design of different channel geometries in CFD. Mixing performance in (a) Simple T mixer, (b) 2D serpentine model, and (c) 3D serpentine model.

Journal of Chemical Technology and Biotechnology published by John Wiley & Sons Ltd on behalf of Society of Chemical Industry (SCI).

Table 2. Mixing index and pressure drop obtained with the different channel geometries

Channel geometry	Mixing index	Pressure drop (Pa)	Camp number	Shear stress (s^{-1})
Simple T mixer	0.15	160	169	10
2D serpentine	0.25	380	406	27
3D serpentine	0.66	1952	2044	55

simulated mixing efficiencies. In the case of the simple Y mixer and the 2D serpentine, they both resulted in the formation of a double layer of the colored solutions, thus proving the poor mixing of these geometries. However, immediate mixing was clearly observed with the 3D serpentine. Based on this good agreement, it can be concluded that the CFD simulations were valid and can be used to study the effect of geometries on mixing and to find the optimum design.

Design of the devices

Devices were designed with CorelDRAW and manufactured from Polymethylmethacrylate (PMMA) by laser cutting. To prevent further leakage between the PMMA sheets, heat binding at 165 °C was used to adhere them to each other. The multiple precipitation devices (Fig. 3) consisted of a main mixing channel (1) with an inlet for the addition of the solution to be purified (2) and a single outlet (3). This main channel was coupled to a second channel for the precipitating agent (4) with a valves-free dispenser with several outlets grouped in 5 addition zones along the surface of the main channel (corresponding to approximately 1/5 of the total volume). For single addition experiments, the device consisted of a single addition channel for the precipitating agent coupled to the mixing channel. To ensure proper mixing, the main channel was designed with the selected geometry (Fig. 3). Devices were designed to obtain 1, 2, 3, and 5 min addition times at a flow of 1 mL/min. The flow of the precipitating agent can be modified to achieve a desired concentration depending on the experimental needs. To facilitate precipitation studies, milliscale devices were designed to be directly connected to an automated system, like an Äkta system or a peristatic pump, without the need for further materials. The nature of the pumping did not influence the performance of the devices. A standardized female luer lock was integrated on each inlet and outlet. The luer lock was created by drilling with an M6 broach to obtain the same shape as a female luer lock.[32] Hence, devices can be directly connected to the required system by simply rotating the tube connector. To further reduce manufacturing costs and to simplify the complexity of the design, the devices were designed with a valves-free dispenser comprised of several outlets (0.1 mm in diameter) along the mixing channel that allow for the gradual and controlled addition of the precipitating agent, thus avoiding oversaturation (Fig. 3(c)). Besides the dispenser, milliscale devices were designed to be operated with the minimum number of pumps, only 2: one for the supernatant and a second for the precipitating agent. In addition, issues related to sample evaporation during experiments can be avoided because of the low gas permeability that PMMA presents.[33] Such a design allowed for a fast screening to obtain the required data for further scale-up of the precipitation process, including the addition time and resulting filterability.

Determination of the time of precipitant addition

Previous studies have demonstrated that multiple additions of the precipitant substantially improved the final purity.[29] The designed milliscale devices were used to evaluate the influence

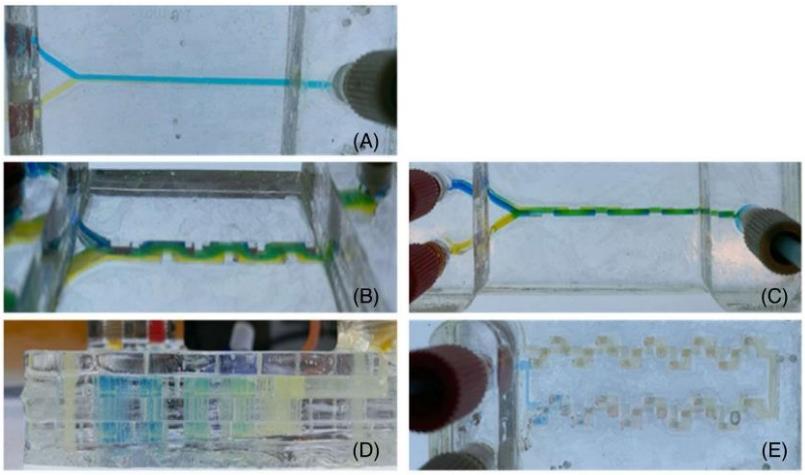

Figure 2. Experimental validation of the 3 different mixing models. (a) Top view of the simple Y mixer; (b) Side view and (c) Top view of the 2D serpentine; and (d) Side view and (e) Top view of the 3D serpentine.

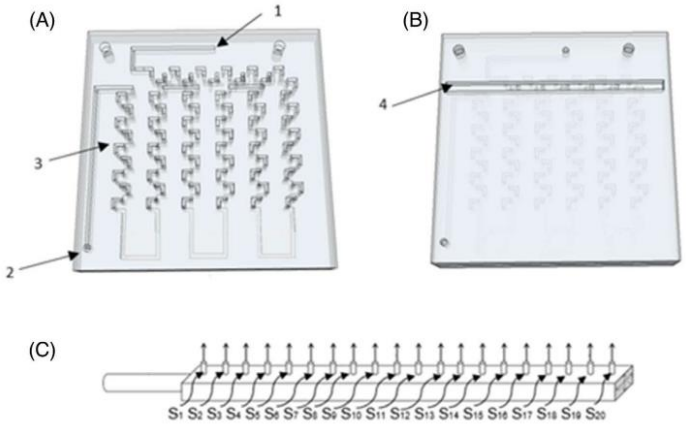

Figure 3. Design of the multiple precipitation devices. (a) Mixing channel for the addition of solution to be purified; (b) main channel for the precipitating agent; (c) example of addition channels distributed along the surface of the mixing channel connecting the mixing channel with the main channel for the precipitating agent.

of the time addition of PEG on the final purity. The milliscale device for single addition consisted of a single addition point coupled to the mixing channel. For continuous addition, the milliscale devices consisted of several addition points coupled to the mixing channel (Fig. 4). The 40% (w/w) PEG6000 solution was added in volume ratios reaching 20% (w/w) PEG6000 at the outlet of the mixing channel during 1, 2, 3, and 5 min. The collected samples were analyzed for purity and yield. The purity of each sample was assessed as the ratio of the monomer peak area corresponding to the antibody to the total area in size exclusion chromatography. Recovery yield was determined by comparing the monomer antibody peak of the initial cell culture supernatant and the precipitation samples using an analytical protein A chromatography. Concentration of impurities and recovery yield were assessed by purification factor (Fig. 5).[29]

The effect of the $CaCl_2$/CA pre-treatment of the antibodies on purity was also evaluated. Prior to the experiments, mAb1 was purified with multiple precipitation steps of $CaCl_2$/CA[34] to study the influence previous treatments on the purification factor. First, mAb1 was treated with 150 mM $CaCl_2$ to precipitate dsDNA and HMWI. To precipitate HCPs, 1% (v/v) CA was added at pH 4.5 and then the pH was adjusted to 7.5 with 1 M Tris (pH 8) prior to PEG experiments. The different times of addition were tested with pre-treated mAb1 supernatant and mAb2 without pre-treatment. In both cases, the time of addition had an influence on the purification factor; this resulted in a 3-fold higher purity factor for mAb1 and 5-fold for mAb2 when PEG was added during 3 and 5 min. The continuous addition of PEG along the tubular reactor prevents the co-precipitation of impurities and mixing inhomogeneity, as occurs with single addition. These results show that the designed milliscale devices can be used to determine the most appropriate dosage time to reduce the co-precipitation of impurities during precipitation.

Scale-down flocculation for precipitate filterability

In addition to improving the final purity of the precipitates, multiple additions of precipitant significantly improved the filterability of the precipitates. Flocculation is a complex process; to be able to use the milliscale devices to determine the dosage time for better filterability, the influence of typical scale-down parameters (such as shear stress and power input) were investigated to mimic the flocculation conditions of a stirred tank, but in the milliscale devices. Two approaches were evaluated to scale down the flocculation conditions by changing the channel size of the milliscale

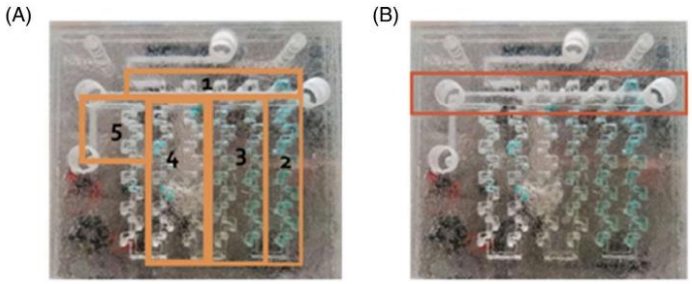

Figure 4. Multilayer milliscale devices with multiple additions at different layers showing (a) main channel to introduce the precipitant agent continuously injected at different points along the mixing channel and (b) addition channels grouped in addition zones along the surface of the mixing channel.

Journal of Chemical Technology and Biotechnology published by John Wiley & Sons Ltd on behalf of Society of Chemical Industry (SCI).

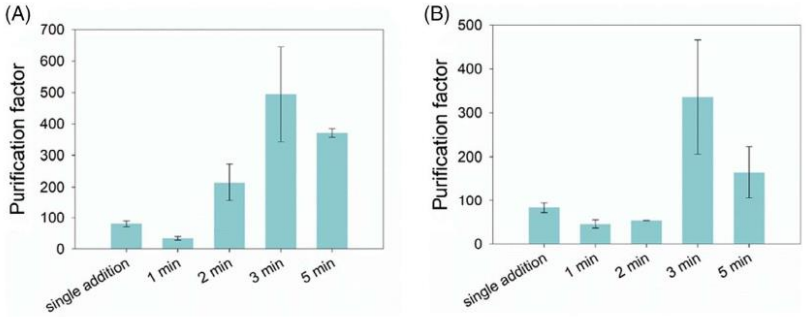

Figure 5. Purification factors achieved using milliscale devices for (a) mAb1 and (b) mAb2 in a single addition, 1, 2, 3, or 5 min addition of the precipitating agent. Precipitates were recovered by centrifugation, washed with 20% PEG6000, and resolubilized with 1 × PBS pH 3.5. Data are given as mean ± standard deviation in the case of triplicate analysis.

devices: first, to obtain a shear stress similar to that in a stirred tank, and second, to obtain a similar power input. Calculations were performed using the CFD models (Table 3).

CFD calculations were performed using the same flow conditions and residence times for all the cases. Results showed that channel sizes ranging from 0.9 to 1.5 mm had similar shear stress values to those obtained with the stirred tank reactor. A similar power input was obtained with channel sizes ranging from 1.7 to 3 mm.

To evaluate both scale-down approaches, mAb2 solution was precipitated by adding 40% (w/w) PEG stock solution to reach a final concentration of 20% (w/w) PEG6000. Precipitation experiments were performed using different tubular reactors with different channel sizes (1.2, 1.5, 2, 2.5, 3 mm). The precipitated solutions were filtrated using a depth filter and the pressure was measured throughout the experiment (Fig. 6). Results were compared to the filtration behavior of a solution precipitated in a stirred tank reactor. To avoid variations on the Camp number, the devices were designed with the same residence time (5 min).

Two filterability trends were found depending on the scale-down condition applied. When the culture supernatant was precipitated using channels satisfying N_{ca} = const., the filterability behavior of the solution differed from that of the stirred tank reactor. However, when the culture supernatant was precipitated using channels satisfying P/V = const, a similar filterability was obtained. That behavior was clearly observed on the milliscale device with a 1.7 mm channel size that had the same shear stress as the reactor with a 2.5 mm channel size, but the power input increased by a factor of 2. This shows that the particle population was influenced mainly by the power input, instead of by the shear stress or Camp number. These results corroborate previous studies that demonstrate that flocculation scale-down could not be achieved by constant Camp number or shear stress.[18] Since flock breakage and collision are mainly taking place in the impeller region and considering the energy dissipation over a tank is typically approximated to the power input by the impeller, power input is clearly a more accurate parameter for scaling down. Higher energy dissipation rates (165–4.5 W/m^3) lead to particle populations that are much more homogeneous and stronger than those obtained when flocculation occurs in a stirred tank reactor (2.25 W/m^3). Hence, by satisfying the flocculation conditions P/V = const., the filterability behavior of a tank reactor was mimicked in the milliscale devices. For further filtration experiments, milliscale devices were adapted to 3 mm channel size.

Table 3. Calculated parameters for different channel sizes of the tubular reactors. The same experimental time (5 min) was used for the calculation of the Camp number. Experiments with the stirred tank reactor were previously performed by Pons Royo *et al.*[29]

Channel size	Shear stress	Camp number	Power input
0.9 mm	55	2044	165.0
1.2 mm	21	612	16.5
1.5 mm	17	219	9.0
1.7 mm	13	47	6.4
2 mm	11	41	4.5
2.5 mm	10	36	3.7
3 mm	10	36	2.5
Stirred tank reactor	32	980	2.3

Influence of multiple additions on depth filtration

The impact of the multiple additions of PEG on liquid-solid separation was evaluated using the milliscale devices. Filterability was studied based on the built-up pressure in the filter by keeping

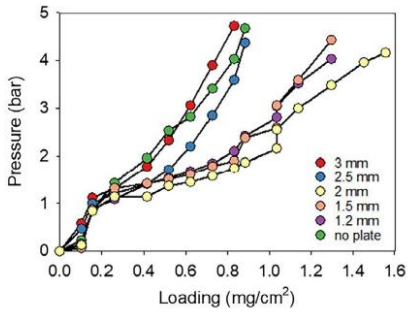

Figure 6. Impact of the channel size of the reactor on the performance of depth filtration for mAb2.

Journal of Chemical Technology and Biotechnology published by John Wiley & Sons Ltd on behalf of Society of Chemical Industry (SCI).

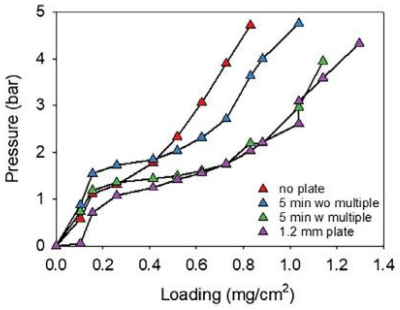

Figure 7. Impact of addition time of PEG for precipitation on the performance of depth filtration for mAb2 showing pre-filter pressures during filtration. Protein precipitation was performed in a stirred tank reactor with single addition, 1.2 mm channel size device, and 5 min devices with and without multiple additions of PEG6000.

a constant flow. To scale-up a given process, it is essential to determine the maximum possible load on a specific filter, which is indicated by the built-up pressure. Antibody solution was precipitated using milliscale devices with and without multiple additions of PEG6000 (Fig. 3). Precipitated solutions were filtered using a depth filter at a constant flow of 10 mL/min. Recorded pressure mass flow per unit area membrane curves were recorded (Fig. 7). Results were compared to the filtration behavior of a solution precipitated in a stirred tank reactor with a single addition and a 1.2 mm channel size device without multiple additions.

Result showed a similar filterability when precipitation was carried out in a stirred tank reactor and a tubular reactor without multiple addition. In contrast, when protein precipitation occurred in the devices with multiple additions, a shift on filterability was observed approaching the trend observed when protein precipitation was performed in a device with 1.2 mm channel size. These results were already shown in previous studies.[29] Floc properties (such as particle size, density, and porosity) were affected by multiple additions of PEG. These multiple additions also affected the specific cake resistance and compressibility, showing a big impact on filterability. Based on these results, flocculation performance can be improved by installing multiple addition points instead of increasing the stirring speed or power input, and this will be less expensive.

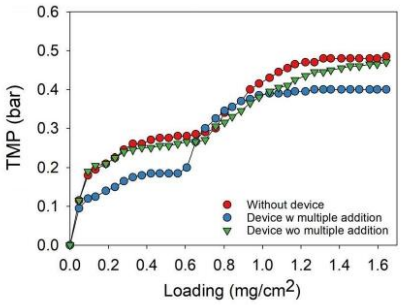

Figure 8. Impact of addition time of PEG for precipitation on the performance of depth filtration for mAb2 showing pre-filter pressures during filtration. Protein precipitation experiments were performed in a stirred tank reactor and 5 min devices – 3 mm with and without multiple additions.

Table 4. Comparison of the required material for each methodology for a single experiment in comparison to experiments performed by Pons Royo *et al.*[29]

	Milliscale devices (mL)	Stirred tank reactor (mL)
Antibody solution	5	50
40% PEG6000	5	50

Influence of multiple additions on tangential flow filtration

For the recovery of precipitated antibodies, solid–liquid separation can be performed with tangential flow filtration (TFF), which simplifies the recovery process and the subsequent purification steps compared to depth filtration. Therefore, the impact of the multiple additions of PEG was evaluated using the milliscale devices on liquid-solid separation by using a TFF. Solutions precipitated in a stirred tank reactor and 5 min additions of PEG with and without multiple additions were filtrated using a TFF system at a constant flow. TMP was recorded throughout the experiment (Fig. 8).

Results show significant differences in the filterability of protein precipitates for samples precipitated using multiple additions and without. When precipitation was performed in a stirred tank reactor with a single addition of PEG, TMP increased gradually, meaning that the filter was gradually fouling. Similar behavior was observed when a protein solution was precipitated without multiple addition points in a milliscale device. However, when solutions were precipitated gradually with the multiple addition points, a lower TMP was observed. As for depth filtration, multiple additions of PEG affected the properties of the resulting flocs and membrane fouling. This behavior was already shown in previous studies.[29] Findings show that the milliscale devices can be used to determine the most appropriate dosage time and the resulting filterability, both of which will impact the design of the process. In addition, the use of milliscale devices showed a clear reduction in the material and experimental time required for each experiment by a factor of 10 (Table 4).

The freedom in designing the milliscale devices allows for evaluating different precipitation strategies at very small volumes, which would not be possible in stirred tank reactors or other small-scale approaches. Additionally, the simple design of the device will enhance the automation of precipitation studies, thus allowing for the screening of larger experimental conditions to reduce time and costs, and to further operator effects.[35]

CONCLUSIONS

In this study, a proof of concept for milliscale devices as a screening tool to facilitate precipitation studies was presented. Milliscale devices can be used to compare different dosage times and their resulting filterability to find the most favorable precipitation conditions. Such experimental conditions cannot be acquired by small scale batch experiments of μ-fluidics. To ensure fast and proper mixing for viscous liquids, a 3D serpentine mixer was used; however, this was at the expense of a higher pressure drop. In addition, the installation of multiple addition points improves flocculation performance and the filterability of the precipitate.

Journal of Chemical Technology and Biotechnology published by John Wiley & Sons Ltd on behalf of Society of Chemical Industry (SCI).

Since these devices are suited for automated and parallel high-throughput process development, the experimental time and sample volume were reduced by a factor of 10, as well. CFD was a relevant tool to evaluate key design parameters, such as mixing performance, for determined fluid conditions and further scalability approaches. Further advantages of using such a software during prototyping include the additional time and cost reductions. Additionally, power input proved to be the key variable to consider for scaling flocculation processes, instead of Camp number. Such milliscale devices are an interesting tool to facilitate further development and optimization of precipitation processes. These screening tools allow for testing new precipitation strategies that would not be possible in batch or other small-scale alternatives, thus reducing experimental time and costs.

NOMENCLATURE

$\vec{F_\sigma}$	Surface tension forces (N)
M_i	Mixing index
$\vec{v}$	Velocity (m/s)
CA	Caprylic acid
CFD	Computational fluid dynamics
CHO	Chinese hamster ovary
DSP	Downstream process
G	Average shear rate (s^{-1})
HCP	Host cell proteins
HMWI	High molecular weight impurities
MUSCL	Third-order upwind discretization
N	Newton
N_{Ca}	Camp number
P	Power (W)
PEG	Polyethylene glycol
PMMA	Poly(methyl methacrylate)
SIMPLE	Semi-implicit pressure-linked equation
TFF	Tangential flow filtration (to $L{\cdot}m^{-2}{\cdot}h^{-1}$)
TMP	Transmembrane pressure (bar)
V	Volume (m^3)
g	Gravity ($m{\cdot}s^{-2}$)
n	Number of phases
p	Pressure (Pa)
t	Time (s)
α	Mass fraction
γ	Shear rate (s^{-1})
η	Shear stress (Pa)
μ	Dynamic viscosity (Pa·s)
ρ	Fluid density ($kg{\cdot}m-^3$)
τ	Mixing performance
τ_{max}	Maximum mixing performance
φ_v	Energy dissipation (m^2/s^3)

ACKNOWLEDGEMENTS

This work has received funding from the European Union's Horizon 2020 research and innovation program under the Marie Skłodowska-Curie grant agreement No. 812909 CODOBIO, within the Marie Skłodowska-Curie International Training Networks framework.

CONFLICT OF INTEREST

The authors declare that there is no conflict of interests.

AUTHOR CONTRIBUTIONS

Carme Pons Royo: Designed the device, conducted the experiments, and wrote the manuscript. Ignacio Montes-Serrano: Performed the CFD simulations. Eric Valery: designed the mixing device. Alois Jungbauer: drafted the research project, reviewed and edited the manuscript. Peter Satzer: supervised the project, reviewed and edited the manuscript.

REFERENCES

1 Kateja N, Tiwari A, Thakur G and Rathore AS, Complete or periodic continuity in continuous manufacturing platforms for production of monoclonal antibodies? *Biotechnol J* **16**:2000524 (2021).
2 Mahal H, Branton H and Farid SS, End-to-end continuous bioprocessing: impact on facility design, cost of goods, and cost of development for monoclonal antibodies. *Biotechnol Bioeng* **118**:3468–3485 (2021).
3 Gerstweiler L, Bi J and Middelberg APJ, Continuous downstream bioprocessing for intensified manufacture of biopharmaceuticals and antibodies. *Chem Eng Sci* **231**:116272 (2021).
4 Burgstaller D, Jungbauer A and Satzer P, Continuous integrated antibody precipitation with two-stage tangential flow microfiltration enables constant mass flow. *Biotechnol Bioeng* **116**:1053–1065 (2019).
5 Jungbauer A, Continuous downstream processing of biopharmaceuticals. *Trends Biotechnol* **31**:479–492 (2013).
6 Sommer R, Tscheliessnig A, Satzer P, Schulz H, Helk B and Jungbauer A, Capture and intermediate purification of recombinant antibodies with combined precipitation methods. *Biochem Eng J* **93**:200–211 (2015).
7 Sommer R, Satzer P, Tscheliessnig A, Schulz H, Helk B and Jungbauer A, Combined polyethylene glycol and CaCl2 precipitation for the capture and purification of recombinant antibodies. *Process Biochem* **49**:2001–2009 (2014).
8 Großhans S, Wang G, Fischer C and Hubbuch J, An integrated precipitation and ion-exchange chromatography process for antibody manufacturing: process development strategy and continuous chromatography exploration. *J Chromatogr A* **1533**:66–76 (2018).
9 Dutra G, Komuczki D, Jungbauer A and Satzer P, Continuous capture of recombinant antibodies by ZnCl 2 precipitation without polyethylene glycol. *Eng Life Sci* **20**:265–274 (2020).
10 Martinez M, Spitali M, Norrant EL and Bracewell DG, Precipitation as an enabling Technology for the Intensification of biopharmaceutical manufacture. *Trends Biotechnol* **37**:237–241 (2019).
11 Watt JG, Automatically controlled continuous recovery of plasma protein fractions for clinical use. A preliminary report. *Vox Sang* **18**:42–61 (1970).
12 Tscheliessnig A, Satzer P, Hammerschmidt N, Schulz H, Helk B and Jungbauer A, Ethanol precipitation for purification of recombinant antibodies. *J Biotechnol* **188**:17–28 (2014).
13 Kateja N, Agarwal H, Saraswat A, Bhat M and Rathore AS, Continuous precipitation of process related impurities from clarified cell culture supernatant using a novel coiled flow inversion reactor (CFIR). *Biotechnol J* **11**:1320–1331 (2016).
14 Hammerschmidt N, Hobiger S and Jungbauer A, Continuous polyethylene glycol precipitation of recombinant antibodies: sequential precipitation and resolubilization. *Process Biochem* **51**:325–332 (2016).
15 Zauner R and Jones AG, Mixing effects on product particle characteristics from semi-batch crystal precipitation. *Chem Eng Res Des* **78**:894–902 (2000).
16 Zauner R and Jones AG, Scale-up of continuous and Semibatch precipitation processes. *Ind Eng Chem Res* **39**:2392–2403 (2000).
17 Espuny Garcia Del Real G, Davies J and Bracewell DG, Scale-down characterization of post-centrifuge flocculation processes for high-throughput process development. *Biotechnol Bioeng* **111**:2486–2498 (2014).
18 Šulc R and Ditl P, Scale-up rules for flocculation. *Int J Miner Process* **167**:79–85 (2017).
19 Novotný J and Foret F, Fluid manipulation on the micro-scale: basics of fluid behavior in microfluidics. *J Sep Sci* **40**:383–394 (2017).
20 Rayat ACME, Chatel A, Hoare M and Lye GJ, Ultra scale-down approaches to enhance the creation of bioprocesses at scale:

Journal of Chemical Technology and Biotechnology published by John Wiley & Sons Ltd on behalf of Society of Chemical Industry (SCI).

impacts of process shear stress and early recovery stages. *Curr Opin Chem Eng* **14**:150–157 (2016).
21 Shi H-h, Xiao Y, Ferguson S, Huang X, Wang N and Hao H-X, Progress of crystallization in microfluidic devices. *Lab Chip* **17**:2167–2185 (2017).
22 Tetala KKR and Vijayalakshmi MA, A review on recent developments for biomolecule separation at analytical scale using microfluidic devices. *Anal Chim Acta* **906**:7–21 (2016).
23 Huft J, Haynes CA and Hansen CL, Microfluidic integration of parallel solid-phase liquid chromatography. *Anal Chem* **85**:2999–3005 (2013).
24 CODOBIO–Continuous Downstream Processing of Biologics.
25 Afzal A and Kim K-Y, *Mixing at Microscale, in Analysis and Design Optimization of Micromixers*. Springer Singapore, Singapore, pp. 1–10 (2021).
26 Ward K and Fan ZH, Mixing in microfluidic devices and enhancement methods. *J Micromech Microeng* **25**:94001 (2015).
27 Suh YK and Kang S, A review on mixing in microfluidics. *Micromachines (Basel)* **1**:82–111 (2010).
28 Satzer P and Jungbauer A, High-capacity protein a affinity chromatography for the fast quantification of antibodies: two-wavelength detection expands linear range. *J Sep Sci* **41**:1791–1797 (2018).
29 Pons Royo MC, Beulay J-L, Valery E, Jungbauer A and Satzer P, Mode and dosage time in polyethylene glycol precipitation process influences protein precipitate size and filterability. *Process Biochem* **114**:77–85 (2022).
30 Solehati N, Bae J and Sasmito AP, Optimization of Wavy-Channel micromixer geometry using Taguchi method. *Micromachines (Basel)* **9**:70 (2018).
31 Wutz J, Steiner R, Assfalg K and Wucherpfennig T, Establishment of a CFD-based k(L) a model in microtiter plates to support CHO cell culture scale-up during clone selection. *Biotechnol Prog* **34**:1120–1128 (2018).
32 Pons Royo MC, Beulay J-L, Valery E, Jungbauer A and Satzer P, Design of millidevices to expedite apparent solubility measurements. *React Chem Eng* (2022).
33 Ren K, Zhou J and Wu H, Materials for microfluidic chip fabrication. *Acc Chem Res* **46**:2396–2406 (2013).
34 Sommer R, Continuous precipitation of therapeutic proteins, with an emphasis on monoclonal antibodies (2013).
35 Christler A, Felföldi E, Mosor M, Sauer D, Walch N, Dürauer A *et al.*, Semi-automation of process analytics reduces operator effect. *Bioprocess Biosyst Eng* **43**:753–764 (2020).

Paper III

Maria del Carme Pons Royo, Jean-Luc Beulay, Eric Valery, Alois Jungbauer, Peter Satzer,

Design of millidevices to expedite apparent solubility measurements

Reaction Chemistry & Engineering

Volume 114, 2022

https://doi.org/10.1039/D2RE00022A

Reaction Chemistry & Engineering

ROYAL SOCIETY OF CHEMISTRY

PAPER

View Article Online
View Journal

Cite this: DOI: 10.1039/d2re00022a

Design of millidevices to expedite apparent solubility measurements

Maria del Carme Pons Royo, [abc] Jean-Luc Beulay,[a] Eric Valery,[a] Alois Jungbauer [*bc] and Peter Satzer[b]

Received 21st January 2022,
Accepted 23rd April 2022

DOI: 10.1039/d2re00022a

rsc.li/reaction-engineering

Protein solubility is a critical attribute in the development and production of monoclonal antibodies. Available solubility data refer to pure solutes which do not consider solvents and impurities which have a significant effect on solubility. Thus, solubility curves need to be determined experimentally. Previously established methods to determine the apparent solubility of proteins are based on manual assays which are time-consuming and labor-intensive. We present the design of simple and adaptable millidevices for fast solubility curve determination. Such a device in the form of a tubular reactor was manufactured from polymethylmethacrylate by laser cutting. The reactors had multiple injection points for the precipitant that allowed a controlled and precise addition of the precipitating agent at different concentrations. Hence, antibodies could be directly harvested at different concentrations of precipitating agents. The simple and flexible design allowed the number of pumps required to be reduced to only one for each solution and the distribution of the precipitating agent at different concentrations without valves. To demonstrate the wide applicability of the prototype in determining solubility curves, we used 2 industrially relevant precipitating agents, PEG6000 and $ZnCl_2$, to measure the apparent solubilities of 4 antibodies and $CaCl_2$ to measure the apparent solubility curves for dsDNA. In all cases, the data obtained were consistent between the device and manual assays with good reproducibility. This millidevice can be used for fast characterization of protein solutions such as solubility, degradation or stability of the antibodies under different conditions.

Introduction

Protein solubility is a key parameter during development and production of therapeutic proteins. It is especially important during identification of drug candidates or formulation at high protein concentrations.[1–3] Detailed data on solubility are necessary to avoid issues with solubility such as aggregation, which impact negatively on protein stability, immunogenicity and efficacy. Furthermore, protein solubility plays an important role in the development of precipitation processes, which have received renewed interest as an alternative to protein A chromatography for the purification of antibodies.[4–13] Solubility curves are defined as the thermodynamic equilibrium between the solid and the liquid phase. This equilibrium can be affected by several parameters, including external factors like solution composition, pH and ionic strength[1,14] as well as intrinsic factors and properties of the protein itself, such as size, charge distribution, overall charge, *etc.*[15] For the process design of protein precipitation, it is essential to determine the solubility curve of each component in the harvest, including impurities. To predict the process performance and to evaluate the separation behavior, it would be necessary to collect the solubility data on each component from the cell culture supernatant under certain buffer conditions and concentrations.[14] However, published solubility data refer to pure solutes and solvents while impurities can have a significant effect on solution properties. Previous studies[16,17] determined that curves obtained from purified antibodies and total protein impurities present different features and can result in different apparent solubilities. Therefore, the solubility in solution is typically referred to as "apparent solubility".[4] Typically, antibodies present higher solubility and steeper curves than impurities, with lower solubility and flatter curves. These differences in solubility can be exploited to precipitate mAbs avoiding coprecipitation of impurities. For that reason, apparent solubility curves need to be determined experimentally.[18] As described by Juckes,[19] the apparent solubility of purified antibodies and impurities can

[a] *Department of Innovation, Novasep, 81 Boulevard de la Moselle, 54340 Pompey, France*
[b] *Department of Biotechnology, University of Natural Resources and Life Sciences Vienna, 1190 Vienna, Austria. E-mail: alois.jungbauer@boku.ac.at*
[c] *Austrian Centre of Industrial Biotechnology (ACIB), Muthgasse 18, 1190 Vienna, Austria*

be derived from a linear regression following a semi-logarithmic behavior, where the apparent maximum solubility will be extrapolated from the intercept in the absence of a precipitating agent such as PEG.[20] From these studies, a model for non-ionic precipitation was established. Hence, a common method to determine the relative apparent solubility of each component is using non-ionic polymers as precipitating agents like PEG (polyethylene glycol) to decrease protein solubility.[1,21] This methodology has been extensively used to determine the apparent solubility curves of various proteins.[22–31]

Nevertheless, all these methodologies for determining the relative apparent solubility require a vast stock of reagents at different pH values, ionic strength, viscosity, *etc.* as well as several manipulation steps such as filtration, centrifugation or additional mixing systems, which complicate the utilization of handling systems.[22,29,32–34] The emergence of microfluidic technology provides a new method to investigate protein solubilization under several solution conditions. Analysis with microdevices can be performed with high precision, high speed, and high throughput, while reducing the required experimental time and the amount of protein required.[35] Furthermore, it is important to highlight that microdevices can lead to more automated labs and miniaturized analyses.[36] Characterization of protein solutions using microdevices has been already described,[37,38] to select flocculating agents[39] or investigate protein phase behavior.[40] Unfortunately, these devices are not widely used in laboratories.[36] Most of these microdevices require a clean-room environment for their fabrication,[41] which is not available in most laboratories. Besides the lack of appropriate facilities, the cost and expertise to develop and fabricate such microdevices are another drawback. For example, the integration of microvalves or micropumps to achieve better flow control will increase the complexity and the cost of the device.[42,43] Additionally, valves or pumps cannot be easily integrated in several materials such as glass or silicon, because of their rigidity. Thus, these materials must be combined with more flexible materials such as PDMS, which will allow the integration of valves or connection to pumps.[41,44] Another difficulty is the implementation of appropriate kinetics into microfluidic devices. As all flows are laminar in such devices, achieving proper mixing between highly viscous solutions like a PEG solution and low viscous solutions like the harvest from a monoclonal fermentation is not always easy.[45] All in all, going to such small scales allows for a reduction in protein solution consumption, but comes with a large cost in terms of necessary equipment and expertise, not present in many labs.

In this work, we have developed a millifluidic device to determine apparent solubility profiles to circumvent the issues typical for already presented microfluidic devices. We demonstrated the feasibility of apparent solubility curve determination using these new millidevices in various industrially relevant buffers for protein and DNA purification. We compared our methodology with a typical manual assay to evaluate the accuracy and precision of our millidevices. In addition, we demonstrated a proof of concept to develop more automated devices for accelerating downstream processing.

Materials and methods

CHO cell culture supernatants

Experiments were performed with 4 different clarified Chinese hamster ovary (CHO) cell culture supernatants of antibodies labeled mAbA, mAbB, mAbC and mAbD. The concentration of the antibodies was, respectively, 1.4 g L^{-1}, 1.2 g L^{-1}, 1.15 g L^{-1} and 1.3 g L^{-1}. Respectively, the HCP concentration was 3.5 g L^{-1}, 8.3 g L^{-1}, 8.6 g L^{-1} and 10.25 g L^{-1}, and for dsDNA, 17.74 ng mL^{-1}, 10.37 ng mL^{-1}, 5.21 ng mL^{-1}, and 4.56 ng mL^{-1}. The supernatants were filtered with a 0.22 μm membrane (Merck KGaA, Darmstadt, Germany) before use.

Protein A chromatography

Protein A chromatography for protein concentration was performed using an affinity column POROS A 20 μm Column (2.1 × 30 mm, 0.1 mL; Thermo Scientific, MA, USA), as previously described.[46] The column was equilibrated with 50 mM phosphate buffer with 150 mM NaCl, pH 7.0, and eluted with 100 mM glycine buffer, pH 2.4.

dsDNA assay

Quantification of double-stranded DNA was performed using a Quant-iT PicoGreen dsDNA reagent (Invitrogen, Waltham, MA, United States). Samples were diluted in serial 1:2 dilutions in a 96-well plate using 1× TE buffer (10 mM Tris-HCl, 1 mM ethylenediaminetetraacetic acid, pH 7.5). 100 μL of sample dilution was transferred to a black microtiter plate and mixed with 100 μL of diluted PicoGreen reagent. The intensity was measured at 480 nm excitation and with an emission filter of 520 nm. The concentration was calculated using a standard lambda DNA solution (Invitrogen, Waltham, MA, United States).

Prototype fabrication

Millidevices were designed using CorelDRAW 2020 (Corel Co., Canada) and a laser cutter (Laser Trotec Speedy 100, Trotec GmbH, Austria). The microchannels were 1 mm wide and 3 mm deep. The main mixing channels and injection microchannels were cut in 3 mm, and the inlets and outlets in 4 mm poly(methyl methacrylate) (PMMA) sheets (Acrylstudio GmbHW, Austria). The PMMA sheets were heated to 165 °C for at least 45 min and cooled down at room temperature. Prior to the bonding process, PMMA sheets were cleaned by rinsing with 70% ethanol.

Apparent solubility curve determination – manually

Manual apparent solubility curve determination was performed in 1.5 mL vials (Eppendorf, Germany), by adding

each stock solution, 30 mM $ZnCl_2$, 40% PEG6000 and 300 mM $CaCl_2$, in a determined ratio into 1 mL cell culture supernatant to obtain the desired final concentrations, 2.7 mM to 8.6 mM $ZnCl_2$, 3.6% to 11.4% PEG600 and 27.3 mM to 85.7 mM $CaCl_2$. After 15 min of incubation at room temperature on an end-over-end shaker, the samples were centrifuged at 4.000*g* for 10 min. The supernatant was withdrawn and analysed with protein A affinity chromatography for mAb concentration or with the PicoGreen assay for dsDNA concentration.

Apparent solubility curve determination – devices

Continuous apparent solubility curve determination was performed with the millidevice directly connected to an ÄKTA pure 25 system (Cytiva, Uppsala, Sweden). The flow rate was set at 4 mL min^{-1} for the mAb supernatant and 1 mL min^{-1} for the precipitating solution to obtain the desired final concentrations, 2.7 mM to 8.6 mM $ZnCl_2$, 3.6% to 11.4% PEG600 and 27.3 mM to 85.7 mM $CaCl_2$. The collected precipitated solution was continuously mixed for 15 minutes to ensure complete precipitation. After that, the samples were centrifuged at 4.000*g* for 10 min. The supernatant was withdrawn and analysed with protein A affinity chromatography for mAb concentration or with the PicoGreen assay for dsDNA concentration.

Results and discussion

Design of precipitation reactors

Although several methodologies have been developed to determine apparent solubility, manual methods are time-consuming and labor-intensive due to the large amounts of buffer solutions and concentrations that need to be managed: sample, precipitant, buffer, *etc.* To facilitate this procedure, we designed millifluidic devices that can be used in an automated system such as an Äkta system to determine the protein solubility. The millidevices were designed using CorelDRAW and manufactured from polymethylmethacrylate (PMMA) by laser cutting. PMMA sheets were stacked and adhered to each other by heat binding at 165 °C to ensure that they are fully sealed and there is no leakage. The millidevice was composed of a main inlet path for the protein solution (1) and a second path for the selected precipitating agent (2), both connected through a valve-free dispenser with different injection points (3) depending on the required concentration of the precipitating agent to be added (Fig. 1). To ensure proper mixing even for viscous liquids, the millidevice was designed with a complex serpentine pattern as a passive mixer, 1 mm wide and 3 mm deep (4) (Fig. 1), and with several outlets for each tested condition (5). Our millidevices were designed to be microvalve-free to reduce the manufacturing costs and the complexity of the design and to simplify the experimental setup by reducing the number of pumps required to only 2, one for the supernatant and one for the precipitating agent (Fig. 1). The dispenser was composed of several outlets grouped in different injection zones, which regulate the addition of precipitating agents. In this case, the device was composed of 4 zones with 1, 2, 3 and 4 holes of 0.1 mm in diameter. The total precipitant flow running in the main channel was divided in different fractions, which will result in different concentrations of the precipitating agent. For example, at 1 ml min^{-1} flow of 40% PEG6000 stock solution, 1 hole corresponds to 3.6 ± 0.4% PEG6000 in 1 mL antibody solution, 2 holes to 6.6 ± 0.5%, 3 holes to 9.2 ± 0.5% and 4 holes to 11.4% ± 0.5%. The same mechanism was used to distribute equally the main antibody solution in 4 different mixing channels, but in that case, the number of holes was kept constant (Fig. 1c) to obtain the same flow in the mixing channels, 1 mL min^{-1}. The mixing channels were also coupled to the dispenser for precipitating agents, in which a

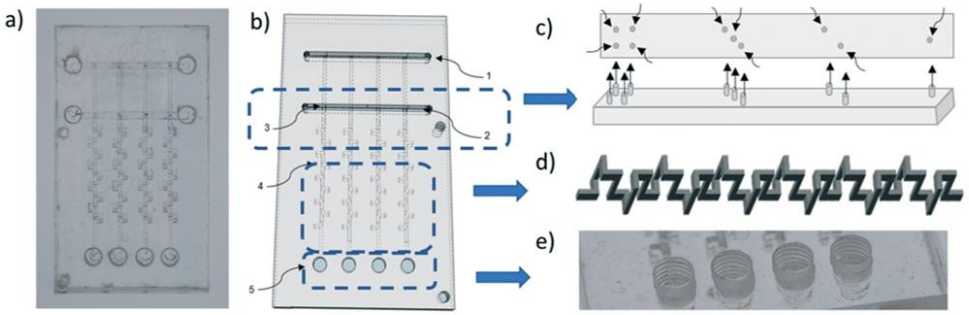

Fig. 1 a) Final result of the device for apparent solubility curve determination and b) 3D design of the developed device for apparent solubility curve determination: 1) cell culture supernatant addition channel, 2) precipitating agent addition channel, 3) injection points, 4) mixing/maturation area and 5) outlet for each studied condition. c) Schematic representation of the injection channel. The injection channels are grouped in different injection zones to introduce the precipitating agent continuously and at different concentrations. d) Geometrical design of the mixing channel for liquids with distinct viscosities. e) Female luer lock fitting integrated in the inlets and outlets of the device.

determined amount of precipitating agent was added onto the number of holes connected to the selected mixing channel with the antibody solution. Therefore, antibodies can be harvested at different precipitating agent concentrations in the outlet of each mixing channel. Furthermore, the device integrated a standardized female luer lock system (Fig. 1) in each inlet and outlet, which allows the device to be directly connected to commonly used lab equipment such as peristaltic pumps or more complex equipment such as an Äkta system, without the need for flexible materials such as polydimethylsiloxane (PDMS) (Fig. 2).

The female luer lock fitting was achieved by drilling with an M6 broach the PMMA to obtain the same mold as a female luer lock. Therefore, the male luer lock from the laboratory equipment can be simply connected by rotating the tube connector. In addition, as PMMA is barely permeable to gasses, sample evaporation can be neglected.[41] The automation of the precipitation methodology allowed the screening of a larger number of conditions and solutions, identifying rapidly and accurately the necessary solubility information for molecule selection or the design of a precipitation process at an early stage. Additionally, the flexibility of the design and the mixing system allows the developed prototypes to be customized and modified for any precipitation protocol or precipitation strategy.

Apparent solubility curves

Antibody precipitation with PEG6000. To demonstrate the feasibility and accuracy of the prototype to determine a wide range of solubility curves, we determined the solubility behavior of 4 antibodies and their impurities. The effectiveness and accuracy of the millidevice were qualitatively evaluated by comparing the solubility curves determined manually and with the devices. Firstly, the millidevice was tested using PEG6000, a known and commonly used precipitating agent to measure the apparent solubility of proteins. The device was connected directly to the pumps of an Äkta system with the flow rate set to 4 mL min^{-1} for the supernatant and 1 mL min^{-1} for the 40% PEG6000 solution. Thus, the precipitating agent was distributed creating solubility curves over a range of 3.6% to 11.4% PEG6000. The samples were taken from the devices and filtered prior to mAb quantification. Afterwards, solubility measurements were repeated manually and compared to the results obtained with the devices to determine their effectiveness and accuracy. The antibody concentration in the liquid phase was plotted against the precipitating agent concentration (Fig. 3). The increase in PEG concentration led to a decrease in antibody concentration in the supernatant as expected. For PEG concentrations below 4% PEG 6000, all mAbs remained in solution (>90%). When the PEG concentration increased above 11%, only 10% of the total antibodies remained in solution, except for mAbA, where 40% remained in solution. In contrast, mAbC required the lowest PEG concentration to achieve complete precipitation, compared to the rest. The different behaviours and concentrations of the mAbs used in this study show that the device is capable of accurately measuring the apparent solubility also in complex solutions. The apparent solubility curves for all 4 antibodies do not follow a strong sigmoidal curve like typically expected.[29,47,48] This is normal and typical for apparent solubilities recorded using crude harvest. With the presence of impurities, the apparent solubility of mAbs can be drastically different from the solubility recorded for pure protein.[49] The use of millidevices resulted in comparable shapes of the precipitation curves to those from experiments performed manually, with differences between methods below 10%, except for mAbA which presents a deviation of 15%. We can assume that the variation was caused by shear stress that caused different sizes and size distributions of the precipitated particles.[50]

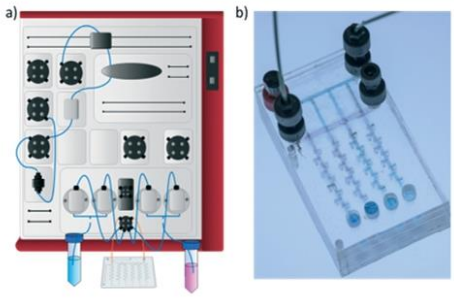

Fig. 2 a) Graphical representation of the device performance under laboratory conditions. The device is directly connected to the dual pumps of an Äkta chromatography system. b) Picture of the device connected under laboratory conditions.

Antibody precipitation with $ZnCl_2$. The millidevice was also tested using $ZnCl_2$, another known antibody precipitating agent recently presented with and without the combination with PEG6000.[5,51,52] While PEG6000 shows the mixing behavior in the system of a highly viscous stock solution (PEG), with $ZnCl_2$ we can evaluate the mixing behavior for stock solutions with lower viscosity. The apparent solubility curve was determined over a range of 2.7 mM to 8.6 mM $ZnCl_2$ with mixing a flow rate of 4 mL min^{-1} for the supernatant and 1 mL min^{-1} for 30 mM $ZnCl_2$ solution. The samples were taken from the devices and filtered, prior to mAb quantification. Afterwards, the antibody concentration in the liquid phase was plotted against the precipitating agent concentration (Fig. 4). Antibodies in solution decreased with the increase of $ZnCl_2$ concentration (Fig. 4). Similar behavior was observed to that in previous experiments (Fig. 4). For $ZnCl_2$ concentrations below 2 mM, antibodies remained in solution (>90%), except for mAbC which required lower precipitant concentrations to achieve

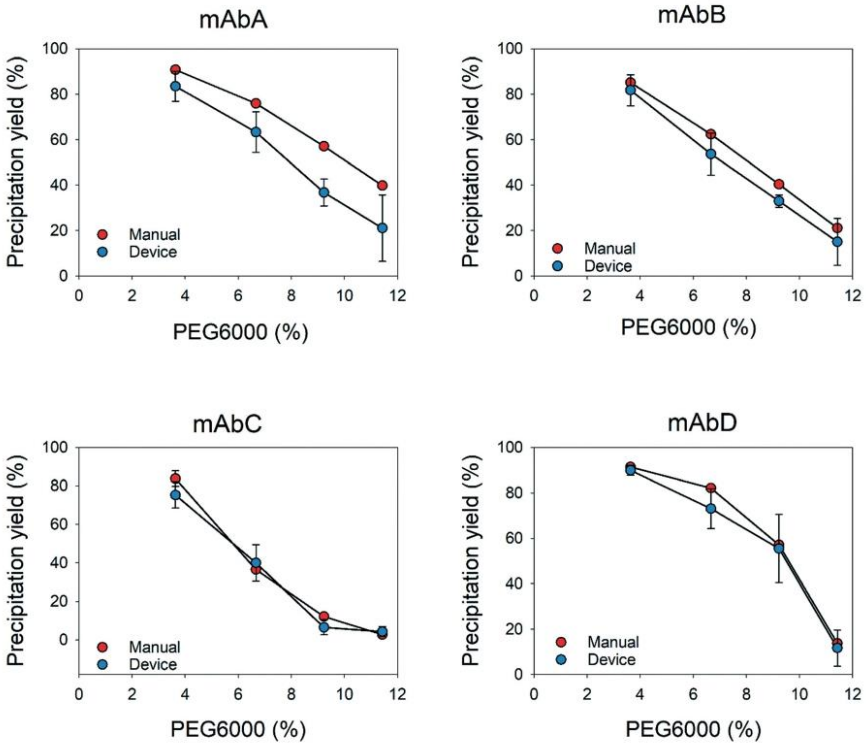

Fig. 3 Comparison of apparent solubility curves obtained with 40% PEG6000 over a range of 3.65–11.43% for mAbA, mAbB, mAbC and mAbD manually and using the millidevices. Experiments were performed in triplicate and data are given as mean ± standard deviation.

almost complete protein precipitation. With 8.5 mM $ZnCl_2$, almost all antibodies were precipitated except for mAbA, which is also the case for PEG6000. Afterwards, apparent solubility measurements were repeated manually and compared to the results obtained with the devices to determine their effectiveness and accuracy. Again, the different behaviors and concentrations of the mAbs used in this study show that the device is capable of accurately measuring the apparent solubility using other precipitating agents, with differences between methods below 10%, except for mAbA which presents a deviation of 12%. These results again show that the variation could be produced by the shear stress inducing different particle sizes and size distributions.[50,53]

Double-strand DNA precipitation with $CaCl_2$. Impurities present in the cell culture supernatants such as HCP and dsDNA can be easily precipitated by pH precipitation[54] and precipitating agents like $CaCl_2$ [8,55] or CA.[9,56] To demonstrate the application of the millidevice to measure the apparent solubility of different dsDNA concentrations, the experiment was performed with $CaCl_2$ with the 4 different mAb supernatants. The apparent solubility curves were determined over a range of 27.3 mM to 85.7 mM $CaCl_2$ with mixing a flow rate of 4 mL min^{-1} for the supernatant and 1 mL min^{-1} for 300 mM $CaCl_2$ solution. The samples were taken from the devices and filtered, prior to dsDNA quantification. Afterwards, the dsDNA concentration in the liquid phase was plotted against the precipitating agent concentration (Fig. 5). The addition of $CaCl_2$ resulted in the precipitation of dsDNA (Fig. 5). Due to the differences in the initial concentration of dsDNA of each supernatant, each apparent solubility curve showed a particular shape, different also from the required $CaCl_2$ concentration to obtain acceptable dsDNA concentrations, comparable to currently used purification methods. Impurities such as dsDNA in solution decreased with the increase of $CaCl_2$ concentration. For mAbA, mAbB and mAbD, lower $CaCl_2$ concentration was necessary to achieve almost complete dsDNA precipitation, almost no dsDNA was found at 85.7 mM $CaCl_2$ (>0.3 ng mL^{-1}), while for mAbC higher concentration, 0.5 ng mL^{-1}, was found.

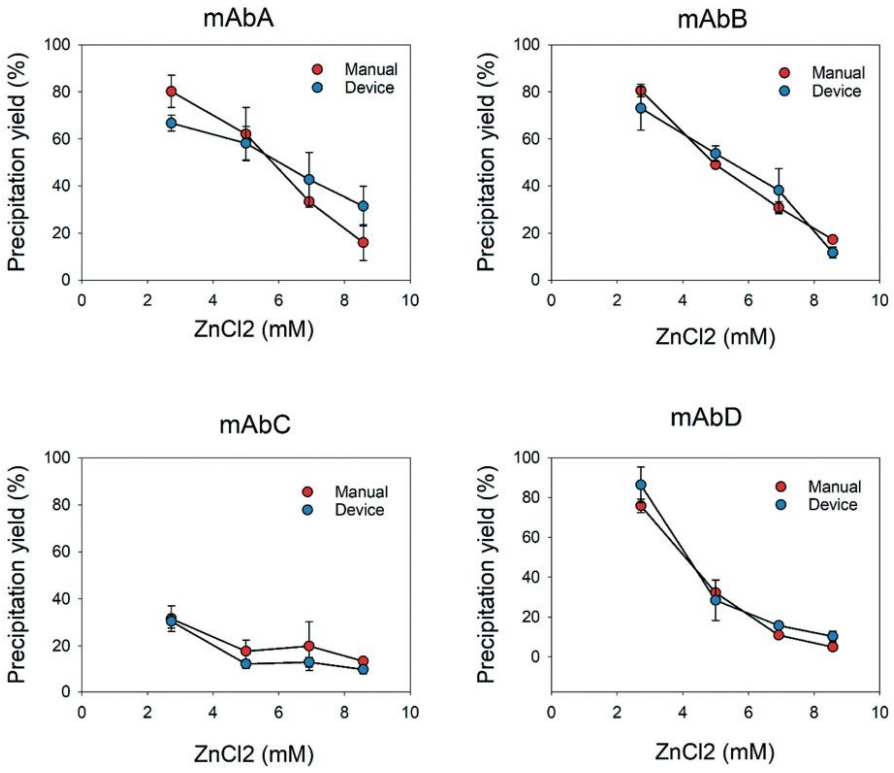

Fig. 4 Comparison of apparent solubility curves obtained with 30 mM $ZnCl_2$ over a range of 2.7 mM to 8.6 mM for mAbA, mAbB, mAbC and mAbD manually and using the millidevices. Experiments were performed in triplicate and data are given as mean ± standard deviation.

The different behaviors and concentrations of the impurities used in this study show that the device is capable of accurately measure the apparent solubility for impurities such as dsDNA and using another precipitating agent. Afterwards, apparent solubility measurements were repeated manually. We compared both methods to determine the effectiveness and accuracy of the prototypes. The use of millidevices resulted in comparable shapes of the precipitation curves to those from experiments performed manually. Since results of dsDNA of mAbA did not show similar deviations as with PEG6000 and $ZnCl_2$, that may confirm that previous variation on the solubility curves were caused by shear stress.

In addition, the results showed that the flow distribution was very accurate and precise, similar to the results obtained manually for the different supernatants and precipitating agents. The use of millidevices resulted in comparable shapes of the precipitation curves to those from experiments performed manually. There was a clear reduction in the experimental time and sample manipulation handling by a factor of 5 (Table 1), since intermediate steps, such as centrifugation to remove precipitates or transferring the supernatants to 96-well plates for the analysis, can be skipped. The above-mentioned issues can be overcome by using a more sophisticated prototyping tool such as a 3D printer, where more soft and complex geometries can be obtained. Hence, it will provide proper mixing with lower shear stress and volume reduction, which will lead to a higher reduction of material consumption compared to the manual method.[57] In comparison with similar devices previously reported, several precipitant concentrations can be tested simultaneously with a single solution in a couple of minutes, without extra sample handling steps, as observed in previous devices, where samples need to be manipulated and transferred to other devices,[22,57–59] or methods to determine the apparent solubility of proteins.[14,17,60]

Additionally, the flexibility of the design and the mixing system allows the developed prototypes to be customized and modified for any precipitation protocol or precipitation strategy. An example of an alternative process could be

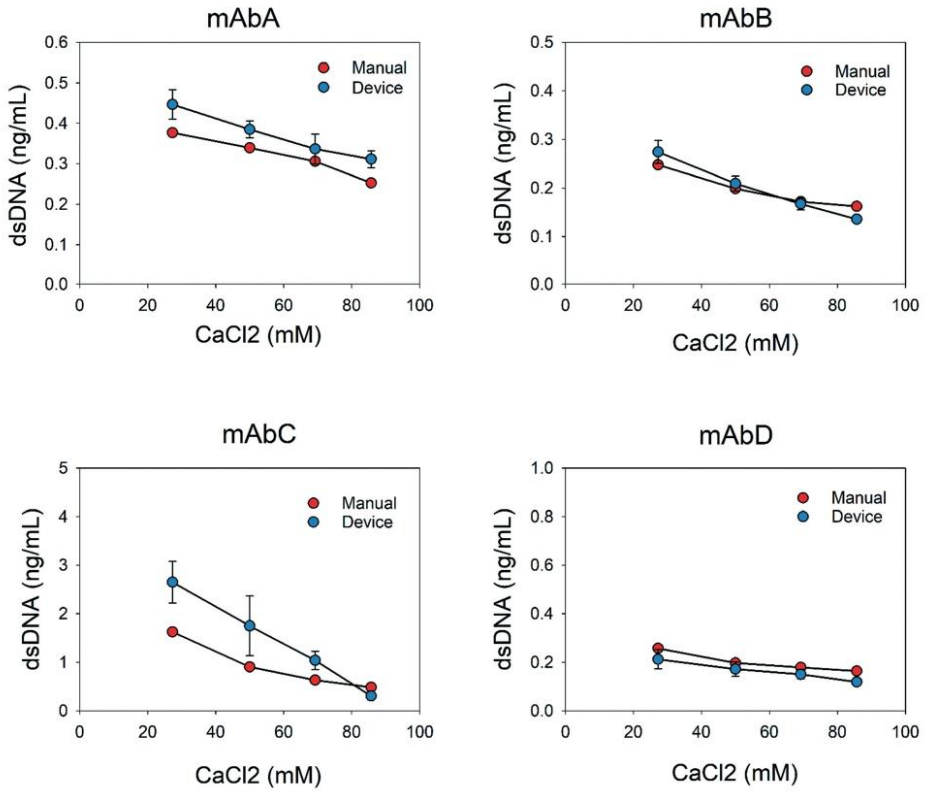

Fig. 5 Comparison of apparent solubility curves obtained with 300 mM $CaCl_2$ over a range of 27.3 mM to 85.7 mM for mAbA, mAbB, mAbC and mAbD manually and using the millidevices. Experiments were performed in triplicate and data are given as mean ± standard deviation.

protein resolubilization, which is often neglected during precipitation studies. Commonly, samples are diluted in different buffers and concentrations to determine the optimal dilution ratio. Millidevices can be used to screen resolubilization buffers at different concentrations and dilutions. Other interesting uses could be for formulation development for protein stability and to assess protein aggregation under certain conditions. Furthermore, our millidevices provide enhanced mixing which accelerates mAb resolubilization and reduces experimental times, as compared to previous resolubilization studies.[17] In addition, the automation of the experiments will allow the screening of larger experimental conditions in shorter time and will reduce operator effects.[61]

Table 1 Comparison of the required material for each methodology for a single solubility curve performed in triplicate

	Millidevices	Manual
Antibody solution	2.5 mL	12 mL
40% PEG6000	0.2 mL	1 mL
30 mM $ZnCl_2$	0.2 mL	1 mL

Conclusions

In this study, we showed a proof of concept of millidevices for determining apparent solubility curves for antibodies and impurities. The developed prototype showed consistent performance and very good reproducibility compared to conventional techniques such as manual apparent solubility determination. Further advantages of using these millidevices are the reduction of reagents, sample consumption and experimental time by reducing the experimental steps, such as centrifugation. A much higher number of experimental conditions can be screened with the automation of the PEG precipitation methodology while removing further human-prone errors such as operator effects. In addition, the easy, flexible and manufacturable in-house screening tools can be modified depending on the experimental needs, for example, determination of

degradation or stability of antibodies at different concentrations during formulation. Millidevices are an interesting tool to develop and optimize processes, which should start being implemented for screening and down-scaling processes.

Author contributions

Carme Pons Royo: designed the devices, conducted the experiments and wrote the manuscript. Jean Luc Beulay: managed and coordinated the research plan. Eric Valery: designed of the mixing device. Alois Jungbauer: drafted the research project and reviewed and edited the manuscript. Peter Satzer: supervised the project and reviewed and edited the manuscript.

Conflicts of interest

The authors declare that there are no conflicts of interest.

Acknowledgements

This work has received funding from the European Union's Horizon 2020 research and innovation program under the Marie Skłodowska-Curie grant agreement no. 812909 CODOBIO, within the Marie Skłodowska-Curie International Training Networks framework.

References

1 S. R. Trevino, J. M. Scholtz and C. N. Pace, *J. Pharm. Sci.*, 2008, **97**, 4155–4166.
2 V. M. Toprani, S. B. Joshi, L. A. Kueltzo, R. M. Schwartz, C. R. Middaugh and D. B. Volkin, *J. Pharm. Sci.*, 2016, **105**, 2319–2327.
3 D. G. Lim, J. C. Lee, D. J. Kim, S. J. Kim, H. W. Yu and S. H. Jeong, *J. Pharm. Invest.*, 2020, **50**, 493–503.
4 D. Burgstaller, A. Jungbauer and P. Satzer, *Biotechnol. Bioeng.*, 2019, **116**, 1053–1065.
5 G. Dutra, D. Komuczki, A. Jungbauer and P. Satzer, *Eng. Life Sci.*, 2020, **20**, 265–274.
6 N. Hammerschmidt, B. Hintersteiner, N. Lingg and A. Jungbauer, *Biotechnol. J.*, 2015, **10**, 1196–1205.
7 N. Hammerschmidt, S. Hobiger and A. Jungbauer, *Process Biochem.*, 2016, **51**, 325–332.
8 R. Sommer, P. Satzer, A. Tscheliessnig, H. Schulz, B. Helk and A. Jungbauer, *Process Biochem.*, 2014, **49**, 2001–2009.
9 R. Sommer, A. Tscheliessnig, P. Satzer, H. Schulz, B. Helk and A. Jungbauer, *Biochem. Eng. J.*, 2015, **93**, 200–211.
10 M. Bhat, A. Mullerpatan, J. Chen, M. Holstein, S. Ghose, Z. J. Li and S. Cramer, *J. Biotechnol.*, 2021, **338**, 1–4.
11 V. Warikoo and R. Godawat, *Biotechnol. J.*, 2015, **10**, 1101–1102.
12 M. Zelger, S. Pan, A. Jungbauer and R. Hahn, *Process Biochem.*, 2016, **51**, 1610–1621.
13 N. Kateja, D. Kumar, S. Sethi and A. S. Rathore, *J. Chromatogr. A*, 2018, **1579**, 60–72.
14 R. M. Kramer, V. R. Shende, N. Motl, C. N. Pace and J. M. Scholtz, *Biophys. J.*, 2012, **102**, 1907–1915.
15 S.-J. Wu, G. Gilliland and Y. Feng, *Solubility and Early Assessment of Stability for Protein Therapeutics*, 2014, pp. 65–91, DOI: **10.1002/9781118354698.ch3**.
16 R. Sommer, *Continuous Precipitation of Therapeutic Proteins, with an Emphasis on Monoclonal Antibodies*, 2013.
17 S. Großhans, S. Suhm and J. Hubbuch, *Bioprocess Biosyst. Eng.*, 2019, **42**, 1039–1051.
18 P. M. Doran, *Bioprocess engineering principles*, 2nd edn, 2012.
19 I. R. Juckes, *Biochim. Biophys. Acta*, 1971, **229**, 535–546.
20 L. Li, A. Kantor and N. Warne, *Protein Sci.*, 2013, **22**, 1118–1123.
21 S. L. Sim, T. He, A. Tscheliessnig, M. Mueller, R. B. Tan and A. Jungbauer, *J. Biotechnol.*, 2012, **157**, 315–319.
22 M. Oeller, P. Sormanni and M. Vendruscolo, *Sci. Rep.*, 2021, **11**, 21932.
23 D. H. Atha and K. C. Ingham, *J. Biol. Chem.*, 1981, **256**, 12108–12117.
24 R. N. Haire, W. A. Tisel, J. G. White and A. Rosenberg, *Biopolymers*, 1984, **23**, 2761–2779.
25 F. Haskó, R. Vaszileva and L. Halász, *Biotechnol. Bioeng.*, 1982, **24**, 1931–1939.
26 H. Mahadevan and C. K. Hall, *Fluid Phase Equilib.*, 1992, **78**, 297–321.
27 C. Middaugh, W. Tisel, R. Haire and A. Rosenberg, *J. Biol. Chem.*, 1979, **254**, 367–370.
28 T. J. Gibson, K. McCarty, I. J. McFadyen, E. Cash, P. Dalmonte, K. D. Hinds, A. A. Dinerman, J. C. Alvarez and D. B. Volkin, *J. Pharm. Sci.*, 2011, **100**, 1009–1021.
29 Q. Chai, J. Shih, C. Weldon, S. Phan and B. E. Jones, *mAbs*, 2019, **11**, 747–756.
30 V. M. Toprani, S. B. Joshi, L. A. Kueltzo, R. M. Schwartz, C. R. Middaugh and D. B. Volkin, *J. Pharm. Sci.*, 2016, **105**, 2319–2327.
31 L. Li, A. Kantor and N. Warne, *Protein Sci.*, 2013, **22**, 1118–1123.
32 H. Zhao, O. Graf, N. Milovic, X. Luan, M. Bluemel, M. Smolny and K. Forrer, *J. Pharm. Sci.*, 2010, **99**, 2279–2294.
33 T. J. Gibson, K. McCarty, I. J. McFadyen, E. Cash, P. Dalmonte, K. D. Hinds, A. A. Dinerman, J. C. Alvarez and D. B. Volkin, *J. Pharm. Sci.*, 2011, **100**, 1009–1021.
34 L. J. Lohmann and J. Strube, *Processes*, 2021, **9**, 488.
35 R. Bhambure, K. Kumar and A. S. Rathore, *Trends Biotechnol.*, 2011, **29**, 127–135.
36 M. N. Säo Pedro, T. C. Silva, R. Patil and M. Ottens, *Biotechnol. Bioeng.*, 2021, **118**, 3275–3286.
37 M. R. G. Kopp and P. Arosio, *J. Pharm. Sci.*, 2018, **107**, 1228–1236.
38 M. Martinez, G. Mannall, M. Spitali, E. L. Norrant and D. G. Bracewell, *J. Chem. Technol. Biotechnol.*, 2020, DOI: **10.1002/jctb.6652**.
39 A. N. P. Radhakrishnan, M. P. C. Marques, M. J. Davies, B. O'Sullivan, D. G. Bracewell and N. Szita, *Lab Chip*, 2018, **18**, 585–594.
40 C. L. Hansen, M. O. A. Sommer and S. R. Quake, *Proc. Natl. Acad. Sci. U. S. A.*, 2004, **101**, 14431.

41 K. Ren, J. Zhou and H. Wu, *Acc. Chem. Res.*, 2013, **46**, 2396–2406.
42 J. Melin and S. R. Quake, *Annu. Rev. Biophys. Biomol. Struct.*, 2007, **36**, 213–231.
43 G. T. Roman and R. T. Kennedy, *J. Chromatogr. A*, 2007, **1168**, 170–188, discussion 169.
44 X. Hou, Y. S. Zhang, G. T.-d. Santiago, M. M. Alvarez, J. Ribas, S. J. Jonas, P. S. Weiss, A. M. Andrews, J. Aizenberg and A. Khademhosseini, *Nat. Rev. Mater.*, 2017, **2**, 17016.
45 A. Afzal and K.-Y. Kim, in *Analysis and Design Optimization of Micromixers*, Springer Singapore, Singapore, 2021, pp. 1–10, DOI: **10.1007/978-981-33-4291-0_1**.
46 G. Dutra, D. Komuczki, A. Jungbauer and P. Satzer, *Eng. Life Sci.*, 2020, **20**, 265–274.
47 L. Lohmann and J. Strube, *Processes*, 2020, **8**, 58.
48 P. Sormanni, L. Amery, S. Ekizoglou, M. Vendruscolo and B. Popovic, *Sci. Rep.*, 2017, **7**, 8200.
49 Q. Gu, Z. Li, J. L. Coffman, T. M. Przybycien and A. L. Zydney, *Biotechnol. Prog.*, 2020, **36**, e3041.
50 E. Byrne, J. J. Fitzpatrick, L. W. Pampel and N. J. Titchener-Hooker, *Chem. Eng. Sci.*, 2002, **57**, 3767–3779.
51 Q. Gu, Z. Li, J. Coffman, T. Przybycien and A. Zydney, *Biotechnol. Prog.*, 2020, **36**(6), e3041.
52 Z. Li, Q. Gu, J. Coffman, T. Przybycien and A. Zydney, *Biotechnol. Prog.*, 2019, **35**(6), e2886.
53 P. Satzer, D. Burgstaller, W. Krepper and A. Jungbauer, *Eng. Life Sci.*, 2020, **20**, 67–78.
54 C. J. England, T. C. Gray, S. R. L. Malla, S. A. Oliveira, B. R. Martin, G. W. Beall and L. K. Lewis, *Anal. Biochem.*, 2021, **616**, 114099.
55 P. Satzer, A. Tscheließnigg, R. Sommer and A. Jungbauer, *Eng. Life Sci.*, 2014, **14**, 477–484.
56 Y. Wan, T. Zhang, T. Chen, Y. Wang and Y. Li, *Protein Expression Purif.*, 2019, **164**, 105460.
57 G. Peybernès, R. Grossier, F. Villard, P. Letellier, M. Lagaize, N. Candoni and S. Veesler, *Org. Process Res. Dev.*, 2018, **22**, 1856–1860.
58 V. J. Sieben, A. K. Tharanivasan, S. I. Andersen and F. Mostowfi, *Energy Fuels*, 2016, **30**, 1933–1946.
59 M. Ildefonso, N. Candoni and S. Veesler, *Org. Process Res. Dev.*, 2012, **16**, 556–560.
60 S. R. Trevino, J. M. Scholtz and C. N. Pace, *J. Pharm. Sci.*, 2008, **97**, 4155–4166.
61 A. Christler, E. Felföldi, M. Mosor, D. Sauer, N. Walch, A. Dürauer and A. Jungbauer, *Bioprocess Biosyst. Eng.*, 2020, **43**, 753–764.

Paper IV

Maria del Carme Pons Royo, Tommaso de Santis, Daniel Komuczki, Alois Jungbauer, Peter Satzer,

Continuous precipitation of antibodies by feeding of solid polyethylene glycol

Separation and Purification Technology

Continuous precipitation of antibodies by feeding of solid polyethylene glycol

Maria del Carme Pons Royo[1], Tommaso De Santis[1], Daniel Komuczki[2], Peter Satzer[2], Alois Jungbauer[1,2],

[1]Austrian Centre of Industrial Biotechnology (acib), Muthgasse 18, 1190 Vienna, Austria
[2]Department of Biotechnology, University of Natural Resources and Life Sciences Vienna (BOKU), 1190 Vienna, Austria

Corresponding author: Prof. Alois Jungbauer, alois.jungbauer@boku.ac.at - University of Natural Resources and Life Sciences Vienna (BOKU)

Highlights

- PEG6000 in powder form was dissolved within minutes
- Continuous protein precipitation with solid PEG6000 was performed during 4 h
- Direct addition of PEG shows comparable yield and purity as liquid PEG addition
- Manufacturing costs are reduced by 47% by the direct addition of PEG6000
- Carbon footprint is reduced by 60%

Abstract

The economic benefits of continuous PEG precipitation of antibodies compared to continuous capture by protein A affinity chromatography have been always lowered by the excess amount of material needed for the process. PEG is added as a concentrated stock solution and therefore liquid handling is increased during this step. To fully exploit the benefits of PEG precipitation, the precipitant must be added in solid form. We used an in-line feeding device with a screw conveyor delivery system directly from solids for the continuous addition of PEG6000 in a powder form. The powder feeding device was connected to a tubular reactor where the precipitation occurs. Protein precipitation was continuously performed for 4h. A yield of 76 and 79% with a purity of 98% was achieved. The total cost of goods and the environmental footprint were compared with typical chromatography-based purification methods; batch and continuous periodic countercurrent protein A affinity chromatography with four columns. Solid PEG precipitation showed a remarkable reduction in water consumption and equipment size, reducing production costs by 45% compared to liquid PEG and 53% cheaper than Protein A periodic counter-current chromatography. Process mass intensity was reduced by 55% and carbon emissions by 60%. The reduction of water by the direct addition of PEG also impacted the environmental footprint and process costs. This is an attractive approach for a continuous capture step yielding an uninterrupted mass flow of the product and will pave the way for PEG precipitation as a capture step.

Keywords: Monoclonal antibodies, continuous precipitation, solid PEG, IgG, SuperPro Designer, protein A affinity chromatography

Abbreviations: CAPEX, capital expenditures; COGm, Cost of Goods Manufactured; COGs, Cost of Goods; GMP, Good Manufacturing Practice; HVAC, Heating Ventilation and Air Conditioning; mAbs, monoclonal antibodies; PEG, Poly(ethylene glycol); PMI, Process Mass Intensity; PMMA, Poly(methyl methacrylate); PCC, Periodic countercurrent chromatography; WAter Related Impact of Energy, WARIEN; WFI, Water for Injection.

1. Introduction

Polyethylene glycol (PEG) precipitation is an interesting method for direct capture of recombinant antibodies from clarified culture supernatant. Precipitation can be easily adapted to work in a continuous mode using tubular reactors and scaled up [1-9]. The method is also insensitive to variations in shear forces [10] and in feed concentrations as previously shown, the same reactor configurations could be used for a feed ranging from 0.5-8 g/l antibody in the supernatant [11]. Despite the robustness of the process, the economic benefits of continuous PEG precipitation of antibodies compared to continuous capture by protein A affinity chromatography have been always lowered by the excess amount of material needed. PEG is added as a concentrated stock solution and therefore liquid handling is increased during this step. To fully exploit the benefits of PEG precipitation, the precipitant must be added in solid form and becomes fully competitive to chromatographic capture.

Economic analysis showed that precipitation-based processes reduce costs at all stages compared to protein A based systems [12, 13]. In these Costs of Goods (CoGs) studies, the main cost contribution of materials in precipitation was the use of large amounts of concentration stock solutions of precipitating agents and washing and redissolution buffers [14, 15]. Protein precipitation is carried out by adding a stock solution of a precipitating agent to the supernatant to reach precipitation conditions. The addition of the stock solution increases the volume which must be processed to harvest and redissolve the precipitate and further purification, and thus, it increases equipment size and buffer consumption and consequently, manufacturing costs [11, 16-19]. Hence, the elevated buffer consumption is still an impediment to fully consider protein precipitation as an option to substitute chromatography systems. Another drawback of working with precipitating agents such as PEG6000 is that stock solutions need to be close to the maximal solubility. The preparation of such stock solutions requires long mixing times and high viscosity is obtained. Since viscosity has a significant impact on the performance of the unit operations, the bioprocess design and economics need to be adapted accordingly [20]. Therefore, working at such PEG concentrations can be challenging and unfavourable. Besides production costs, another important factor to consider in a process is the environmental footprint. This can be evaluated by process mass intensity (PMI), a parameter that related the mass of consumed materials to the produced product and the Water Related Impact of Energy (WARIEN), which quantifies the energy consumption and the resulting carbon emissions per kg of product [13, 21-24]. Such metrics indicate where further improvements could be performed for potential savings in resource consumption and carbon footprint. The latest studies showed that the main contribution to the environmental footprint comes from water consumption and storage. In the case of protein precipitation, such values are relatively higher compared to conventional chromatography-based systems due to the large amounts of buffer consumption. Hence, a reduction in buffer consumption during protein precipitation would be beneficial not only from an economical point of view but also for an environmental footprint.

Undoubtedly, further challenges in bioprocesses will be assessed by novel and disruptive technologies. The emerging open sources and prototyping tools such as 3D printers or laser cutters empowered researchers to design and customize devices depending on our needs. The availability of such technologies increases

significantly the scientific capacity and opens new horizons for setting up innovative process ideas [25]. Komuczki et al. [26, 27] developed a 3D printed device for buffer preparation directly from solids. Such a device reduced the facility footprint by avoiding intermediate hold tanks and buffer preparation steps [27]. In this study, we used such a device to replace stock solutions by directly precipitating proteins with PEG6000 in solid form. This new approach minimized the buffer consumption for wash and redissolution of the antibodies, reduced the size and cost of the equipment and facilitated operation conditions as it is not necessary to work with high viscous stock solutions. Afterwards, we evaluated economical and environmentally both precipitation processes and compared to well established purification methods. The output of our analysis highlighted how our new precipitation approach is an attractive alternative for the capture step.

2. Materials and Methods

2.1 CHO Cell culture supernatants

Experiments were performed with IgG1, produced in fed-batch in Chinese hamster ovary (CHO) cell culture supernatant with a concentration of 1.2 g/L and 0.3 g/L. Antibodies were labelled mAb01 and mAb02 respectively. Antibody supernatant was previously filtered with a 0.22 µm membrane (Merck KGaA, Darmstadt, Germany) before use.

2.2 Experimental set-up

For continuous precipitation of antibodies directly from powder, we used a similar experimental set-up as performed by Komuczki et al. [27]. Experiments were performed using the Dissolvr device controlled by a minicomputer Raspberry Pi 3 (Raspberry PI Foundation, Cambridge, United Kingdom) programmed with Python (Python Software Foundation, Wilmington, United States). Solid PEG6000 was put into the storage tank in the upper part of the feeding device. The supernatant and PEG6000 were continuously fed into an in-house designed stirred tank reactor using Autodesk Inventor 2019 (Autodesk, San Rafael, CA, USA) and 3D printed by Sculpteo (Villejuif, France) with a magnetic stirrer. The outlet of the stirred tank was connected to a 5 min residence time continuous tubular reactor build-up with 3 mm poly(methyl methacrylate) (PMMA) sheets (Acrylstudio GmbHW, Austria), designed using CorelDRAW 2020 (Corel Co., Canada) and laser cut (Laser Trotec Speedy 100, Trotec GmbH, Austria), connected to an Äkta Pure 25 system (Cytiva, Uppsala, Sweden). Previously, calibration experiments were performed using an Entris® Precision balance (Sartorius, Göttingen, Germany) connected to the Raspberry Pi 3. The data were collected online using the Simple Data Logger software (Smartlux SARL, Born, Luxembourg). For continuous precipitation of antibodies directly from the stock solution, we connected both solutions to the ÄKTA Pure 25 system (Cytiva, Uppsala, Sweden) with the flow rate was set at 0.55 mL/min for the antibody supernatant and 0.45 mL/min for the 40 % PEG6000 stock solution, to a final concentration of 15 % PEG. The outlet of the ÄKTA Pure was connected to the 5 min residence time continuous tubular reactor. For further chromatographic analysis specific to the precipitate, samples were centrifuged at 4.000 x g for 10 min, the supernatant was discarded and precipitates were washed twice with 20 % PEG6000. The pellet was resuspended with 1 x PBS pH 3.5 [9].

2.3 Protein A

Affinity column POROS A 20 µm Column (2.1 × 30 mm, 0.1 mL; Thermo Scientific, MA, USA), was used to determine antibody concentration. 50 mM sodium phosphate buffer with 150 mM NaCl at pH 7.0 was used as equilibration buffer and 100 mM glycine buffer at pH 2.4 was used as elution buffer [1].

2.4 Size exclusion chromatography

Sample purity was determined using a TSKgel® G3000SWXL HPLC Column (5 µm, 7.8 × 300 mm, Tosoh, Tokyo, Japan) with a TSKgelSWXL Guard Column (7 µm, 6.0 × 40 mm; Tosoh, Tokyo, Japan), as previously performed [11]. We used a Dionex Ultimate 3000 HPLC system with a diode array detector (Thermo Fisher Scientific, MA, USA). The absorbance was measured at 280 nm. The antibody purity was calculated as the ratio of the monomer peak area to the sum of all peak areas, based on the 280 nm signal. The running buffer was a 50 mM potassium phosphate buffer with 150 mM NaCl at pH 7.0 (Merck KGaA, Darmstadt, Germany), filtered through 0.22 µm filters (Merck KGaA, Darmstadt, Germany) and degassed. 20 µl of the sample was injected into the column. Data were evaluated with ChromeleonTM software (ThermoFisher Scientific, MA, USA).

2.5 Cost data and modeling

The techno-economic evaluation of protein precipitation using solid PEG was performed using the software SuperPro Designer v.12 (Intelligen, Inc.). The process parameters were retrieved from the literature [11, 13], the experiments described herein and the built-in databases of SuperPro Designer and Biosolve Process v.8.3 (Biopharm Services, Ltd). Two processes were compared: protein precipitation via direct addition of solid PEG to the supernatant (Figure 4) versus the addition of liquid PEG also to the supernatant (Figure 5). Both the processes were modeled according to the settings of a base case scenario representing a typical medium-size antibody production facility (1000 kg yr^{-1}) that operates in continuous mode (Table 1). Since the focus of the paper is on PEG precipitation, the upstream section together with the antibody polishing steps was not included in the model. The electricity consumption of the HVAC system required in a GMP facility was calculated separately from the SuperPro model by estimating the cleanroom area and then applying an energy coefficient retrieved from a previous antibody production study [28](Table 2). The impact on costs and energy of water and steam production was also estimated separately thanks to a tool developed by Cataldo et al. (2020). Finally, the Process Mass Intensity (PMI) value was calculated (Equation (*1*)) to obtain the metrics that allow for a comparison of the overall environmental performance of the two processes [13].

$$Total\ PMI = \frac{Total\ water, raw\ materials, consmables\ used\ in\ process\ (kg)}{active\ pharmaceutical\ ingredient\ (kg)} \quad (1)$$

3. Results

3.1 Protein precipitation in batch mode

The concept of using directly PEG in powder form for protein precipitation was already investigated [16]. However, the knowledge available for such a process and its applicability was not fully exploited. First, we evaluated the influence of the form of PEG6000, whether liquid (pre-dissolved PEG) or solid, on the yield and purity of protein precipitation in batch mode (Figure 1). Protein precipitation was performed with 10

mL of supernatants of mAb01 and mAb02 by adding PEG liquid PEG6000 at 40 % solution and direct solid form (1.5g milled PEG6000) to a final concentration of 15 % PEG6000. For further chromatography analysis, we withdrew the supernatant and washed twice the precipitates with 20 % PEG6000. The pellet was resuspended with 1 x PBS pH 3.5 [6]. Recovery yields were determined using an analytical protein A chromatography column, comparing the monomer peak of the antibody in the cell culture supernatant and precipitated samples. The purity of the samples was assessed by size exclusion chromatography [1].

Results showed comparable yields for both antibodies with liquid and solid precipitation, 80 % and 87 % for mAb01 and 66 % and 59 % for mAb02, respectively. Additionally, no antibody was found in the supernatants proving that complete protein precipitation reaches the kinetic equilibrium relatively fast [29, 30]. Nevertheless, the lower yields obtained during redissolution, highlight that further optimization studies on precipitation should be focused on the redissolution of the precipitated antibodies. To further confirm that the addition of PEG in solid form did not have any influence on the protein behavior during precipitation, the purities of both methods were compared. Purity percentages of the samples were equally comparable with 100 % and 99 % for mAb01 and 89 % and 86 % for mAb02, for liquid and solid precipitation respectively. Further experiments were performed with mAb01 due to the higher recovery yield obtained. Additionally, achieving a quickly steady state is of utmost importance for a continuous process. We measured the dissolution rate of PEG to a concentration of 15 % to evaluate the viability of transferring solid PEG to a continuous process. Complete solid PEG6000 dissolution at a concentration of 15 % (w/v) was achieved in approximately 1 min, which is in contrast to the long mixing times required for stock solutions up to 50 % (w/v). Thus, direct solid precipitation can be easily adapted to work fully continuously. The possibility to reduce the PEG concentration used for the washing step was not considered since a peg concentration below 15 % will lead to product loss.

3.2 Protein precipitation in continuous mode

To perform the continuous solid addition experiment, we built up a setup consisting of a scale-flow control unit loop ensuring a constant volume of 6 mL into a mixing vessel connected to the additional device. The constant volume was ensured by visual monitoring using a scale. The mixing vessel was connected to a pump of an ÄKTA system with a flow of 2 mL / min connected to a 5 min tubular reactor and the Dissolvr was set to 0.25 g /min. To avoid the accumulation of moisture, we integrated the Dissolvr into a chamber with slight over-pressure with dry process air (Figure 2) [27]. We used a similar setup for the liquid PEG addition, but the 40 % PEG6000 stock solution was added to the supernatant using a Y-shaped connector. Samples were collected in factions of 2, 20 and 40 mL depending on the running time. Since the dosing system is depending on the hygroscopic characteristics of the powder, prior to the experiments, the device was calibrated to determine the dosing rate in grams per revolution [27].

We were able to perform continuous precipitation of antibodies with PEG in solid form during 4 h. To determine the time required to achieve the steady state and to ensure that complete precipitation was achieved, we analyzed the supernatants. Steady-state was achieved after 5 min process time. As in batch experiments, no antibody was found in the supernatants proving that complete protein precipitation reaches the kinetic equilibrium relatively fast. Furthermore, the constant linear addition of PEG over the total run demonstrates a robust and precise approach. For further analysis, we withdrew the supernatant and

washed twice the precipitates with 20 % PEG6000. The pellet was resuspended with 1 x PBS pH 3.5 [6]. Afterwards, samples were analyzed for recovery yield and purity. Results showed comparable yields and purities for both approaches, 76 % and 79 % and 98 % and 98 %, for liquid and solid respectively along the 4h run (Figure 3). Therefore, the form of PEG6000 for protein precipitation did not show any negative influence on the protein behavior during precipitation in comparison to liquid precipitation. Nevertheless, the lower yields obtained during redissolution, highlight that further optimization studies on precipitation should be focused on the redissolution of the precipitated antibodies.

3.3. Economic analysis

We evaluated and compared four different scenarios for the capture step of monoclonal antibodies with subsequent low pH virus inactivation. The first scenario corresponded to a typical batch protein A affinity chromatography capture step. The second scenario was a continuous protein A affinity chromatography capture employing periodic counter-current loading. The third scenario was a continuous precipitation by adding the PEG in a liquid form, and the fourth scenario was a continuous precipitation by direct addition of PEG in solid form (Figure *4*). The economic models simulate the purification of 1000 kg yr^{-1} of antibodies during 330 operating days. In Table 1, the main parameters used for the simulations with the relative sources are summarized. In the continuous processes, one production campaign lasted 10 days. The flowcharts in Figure 4 show the purification steps for each scenario. The continuous chromatographic capture was calculated with a scenario assuming a four-column periodic counter-current loading system while the batch scenario only has a single large column, sizes of the equipment were calculated through the mass balances. In the liquid PEG scenario, PEG is first dissolved to a final 50% stock solution in a stirred tank reactor. Because of PEG solution is close to the maximum PEG solubility in water, such solution needs to be mixed at least for 24h to ensure proper dissolution. Afterwards, the PEG stock solution is mixed into the supernatant to 15 % PEG concentration and transferred to a 10 min residence time (RT) tubular reactor where precipitation occurs. In the solid PEG scenario, the dissolution tanks of the liquid PEG process are replaced by the Dissolvr® system that mixes the solid PEG directly into the supernatant in a stirred tank to 15 % PEG concentration and then transfers the formed solution to a tubular reactor with 10 min RT. Subsequently, the product is redissolved in a tank at a low pH (1 hr RT) before passing through a second tubular reactor (10 min RT) where viral inactivation occurs thanks to the acidic conditions. The equipment is sized according to the volumetric flow of the stream to process and the RT (Supplementary materials).

The process simulations performed with SuperPro Designer show that solid PEG is the most economical method to purify antibodies among the four considered scenarios, with a COGs of 972 € kg^{-1} (Figure 5a). Overall, the Solid PEG method is 45 % cheaper compared to the liquid PEG and 53 % cheaper than Protein A PCC which is the state-of-the-art in antibody manufacturing [31]. Both the PEG processes show a similar distribution of the costs (Figure 5b) with the capital expenditures (CAPEX) representing the majority of the COGs followed by the raw materials and the labor. The reduction in the COGs between the two is due almost entirely to the lower equipment costs since two large mixing tanks (7.5 m^3 and 12.5 m^3 of capacity) are replaced by the Dissolvr® system (Figure 6,). In our base case for chromatographic capture, we assumed 175 cycles as column lifetime and a binding capacity of 60 g L^{-1} which are documented characteristics of new-generation protein A affinity chromatography media [32]. The higher cost of the

Protein A methods is explained by the very high selling price of the resin (assumed to be 10,800 € L^{-1}, bulk purchase price) which accounts for over 50 % of the COGs (consumables in Figure 5b). The smaller size of the chromatographic units in PCC mode compared to Batch mode allows to save equipment and consumable costs since less resin is needed to pack the columns. Given the large impact of the resin cost on the final COGS of antibodies, the column lifetime is a crucial parameter in the economics of protein A purification. By applying a ± 50 % change on the column lifetime, the antibody-COGs for protein A in PCC mode ranges from 3063 € kg^{-1} (-50 %) to 1609 € kg^{-1} (+50 %).

3.4 Environmental analysis

The PMI is a widely used environmental metric describing the total mass of materials consumed to manufacture a unit of product [13, 22]. Liquid PEG is the scenario with the highest PMI (953 kg kg^{-1} antibody). By the addition of PEG in solid form, PMI was reduced by 55 % similar to chromatography-based scenarios (around 400 kg kg^{-1}) (Figure 7). Water and steam are responsible for almost the entire PMI in the four scenarios, this is in line with other findings focused on the environmental analysis of biopharmaceuticals [13]. Extra WFI and steam are used to solubilize the PEG and clean the additional mixing vessels of the liquid PEG scenario hence the higher PMI and carbon emissions (Figure *7*a). Producing WFI and steam is an energy-intensive process that is described by the WAter Related Impact of ENergy (WARIEN) metrics [13]. By using the WARIEN metrics it was calculated that the carbon footprint of WFI is 56.1 gCO2 eq. kg-1 and 193.5 gCO2 eq. kg-1 for steam for solid and liquid PEG precipitation respectively, with the assumption of using the Austrian energy grid and natural gas for producing the steam. Therefore, carbon emissions were reduced by 60 % compared to liquid PEG precipitation, reaching similar values as the chromatography-based scenarios. If WFI was produced with membranes rather than via distillation the final carbon footprint of WARIEN would be 26 % lower. HVAC also contributes significantly to the emissions of the precipitations processes but it is negligible for protein A step given the small cleanroom area occupied by the chromatographic units. Overall solid PEG and the two protein A scenarios have a very similar ecological impact.

4. Conclusions

It is possible to continuously perform protein precipitation by direct addition of PEG6000 in solid form. The operation was performed for 4h demonstrating a robust and precise approach. By direct addition of the precipitant in solid form, the CoGs are substantially reduced and this also is reflected by the environmental footprint. The direct addition of solid PEG for the capture of antibodies is the most economical way compared to continuous capture by protein A affinity chromatography, continuous capture by addition of liquid PEG or batch capture by protein A affinity chromatography. Capital expenditures are the main cost drivers for continuous precipitation processes. Therefore, scaling down the equipment costs leads to a cheaper antibody purification strategy compared to conventional protein A chromatography. Moreover, It reduces the carbon footprint associated with HVAC energy consumption by smaller cleanroom and storage areas. This is an attractive approach for a continuous capture step yielding an uninterrupted mass flow of the product and will pave the way for PEG precipitation as a capture step.

Author Contributions

Maria del Carme Pons Royo: Constructed the equipment, conducted the experiments and wrote the manuscript. **Tommaso de Santis:** Performed the economic and environmental analysis. **Daniel Komuczki:** Helped with the setup and equipment. **Alois Jungbauer:** reviewed and edited the manuscript. **Peter Satzer:** reviewed and edited the manuscript and acquired the financial support for the project.

Conflict of interest

The authors declare that there is no conflict of interests

Acknowledgments

This work has received funding from the European Union's Horizon 2020 research and innovation program under the Marie Skłodowska-Curie grant agreement No 812909 CODOBIO, within the Marie Skłodowska-Curie International Training Networks framework.

References

[1] M.d.C. Pons Royo, J.-L. Beulay, E. Valery, A. Jungbauer, P. Satzer, Mode and dosage time in polyethylene glycol precipitation process influences protein precipitate size and filterability, Process Biochemistry, (2022).

[2] M.d.C. Pons Royo, I. Montes-Serrano, E. Valery, A. Jungbauer, P. Satzer, Milliscale reactors for integration of continuous precipitation and filtration, Journal of Chemical Technology & Biotechnology, n/a.

[3] M.d.C. Pons Royo, J.-L. Beulay, E. Valery, A. Jungbauer, P. Satzer, Design of millidevices to expedite apparent solubility measurements, Reaction Chemistry & Engineering, (2022).

[4] S. Großhans, G. Wang, C. Fischer, J. Hubbuch, An integrated precipitation and ion-exchange chromatography process for antibody manufacturing: Process development strategy and continuous chromatography exploration, Journal of Chromatography A, 1533 (2018) 66-76.

[5] Q. Gu, Z. Li, J.L. Coffman, T.M. Przybycien, A.L. Zydney, High throughput solubility and redissolution screening for antibody purification via combined PEG and zinc chloride precipitation, Biotechnology Progress, 36 (2020).

[6] N. Kateja, Nitika, S. Dureja, A.S. Rathore, Development of an integrated continuous PEGylation and purification Process for granulocyte colony stimulating factor, Journal of Biotechnology, 322 (2020) 79-89.

[7] L.J. Lohmann, J. Strube, Process analytical technology for precipitation process integration into biologics manufacturing towards autonomous operation—mab case study, Processes, 9 (2021).

[8] M. Minervini, A.L. Zydney, Effect of module geometry on the sustainable flux during microfiltration of precipitated IgG, Journal of Membrane Science, 660 (2022).

[9] A. Armstrong, K. Horry, T. Cui, M. Hulley, R. Turner, S.S. Farid, S. Goldrick, D.G. Bracewell, Advanced control strategies for bioprocess chromatography: Challenges and opportunities for intensified processes and next generation products, Journal of Chromatography A, 1639 (2021).

[10] P. Satzer, D. Burgstaller, W. Krepper, A. Jungbauer, Fractal dimension of antibody-PEG precipitate: Light microscopy for the reconstruction of 3D precipitate structures, Engineering in Life Sciences, 20 (2020) 67-78.

[11] D. Burgstaller, A. Jungbauer, P. Satzer, Continuous integrated antibody precipitation with two-stage tangential flow microfiltration enables constant mass flow, Biotechnology and Bioengineering, 116 (2019) 1053-1065.
[12] N. Hammerschmidt, A. Tscheliessnig, R. Sommer, B. Helk, A. Jungbauer, Economics of recombinant antibody production processes at various scales: Industry-standard compared to continuous precipitation, Biotechnology Journal, 9 (2014) 766-775.
[13] A.L. Cataldo, D. Burgstaller, G. Hribar, A. Jungbauer, P. Satzer, Economics and ecology: Modelling of continuous primary recovery and capture scenarios for recombinant antibody production, J Biotechnol, 308 (2020) 87-95.
[14] D.J. Karst, F. Steinebach, M. Soos, M. Morbidelli, Process performance and product quality in an integrated continuous antibody production process, Biotechnology and Bioengineering, 114 (2017) 298-307.
[15] H. Mahal, H. Branton, S.S. Farid, End-to-end continuous bioprocessing: Impact on facility design, cost of goods, and cost of development for monoclonal antibodies, Biotechnology and Bioengineering, 118 (2021) 3468-3485.
[16] N. Hammerschmidt, S. Hobiger, A. Jungbauer, Continuous polyethylene glycol precipitation of recombinant antibodies: Sequential precipitation and resolubilization, Process Biochemistry, 51 (2016) 325-332.
[17] G. Dutra, D. Komuczki, A. Jungbauer, P. Satzer, Continuous capture of recombinant antibodies by ZnCl 2 precipitation without polyethylene glycol, Eng Life Sci, 20 (2020) 265-274.
[18] E.N. Carredano, R. Nordberg, S. Westin, K. Busson, T.M. Karlsson, T.S. Blank, H. Sandegren, G. Jagschies, Chapter 27 - Simplification of Buffer Formulation and Improvement of Buffer Control with In-Line Conditioning (IC), in: G. Jagschies, E. Lindskog, K. Łącki, P. Galliher (Eds.) Biopharmaceutical Processing, Elsevier, 2018, pp. 513-525.
[19] A.M. Tsai, E. Carredano, K. Busson, Deploying Automated Buffer Production for cGMP Use: Points to Consider, BioProcessing Journal, (2019).
[20] P.M. Doran, Bioprocess engineering principles: Second edition, 2012.
[21] A. Cataldo, B. Sissolak, K. Metzger, K. Budzinski, O. Shirokizawa, L. Markus, A. Jungbauer, P. Satzer, Water related impact of energy: Cost and carbon footprint analysis of water for biopharmaceuticals from tap to waste, Chemical Engineering Science, 8 (2020).
[22] K. Budzinski, M. Blewis, P. Dahlin, D. D'Aquila, J. Esparza, J. Gavin, S.V. Ho, C. Hutchens, D. Kahn, S.G. Koenig, R. Kottmeier, J. Millard, M. Snyder, B. Stanard, L. Sun, Introduction of a process mass intensity metric for biologics, N Biotechnol, 49 (2019) 37-42.
[23] S.V. Ho, J.M. McLaughlin, B.W. Cue, P.J. Dunn, Environmental considerations in biologics manufacturing, Green Chemistry, 12 (2010) 755-766.
[24] S.R. Madabhushi, J. Gavin, S. Xu, C. Cutler, R. Chmielowski, W. Rayfield, N. Tugcu, H. Chen, Quantitative assessment of environmental impact of biologics manufacturing using process mass intensity analysis, Biotechnol Prog, 34 (2018) 1566-1573.
[25] J.J. Davis, S.W. Foster, J.P. Grinias, Low-cost and open-source strategies for chemical separations, Journal of Chromatography A, 1638 (2021) 461820.
[26] D. Komuczki, G. Dutra, C. Gstöttner, E. Dominguez-Vega, A. Jungbauer, P. Satzer, Media on-demand: Continuous reconstitution of a chemically defined media directly from solids, Biotechnol Bioeng, 118 (2021) 3382-3394.
[27] D. Komuczki, N. Lingg, A. Jungbauer, P. Satzer, In-situ gradient formation by direct solid addition of buffer components, Journal of Chromatography A, 1634 (2020).
[28] P. Bunnak, R. Allmendinger, S.V. Ramasamy, P. Lettieri, N.J. Titchener-Hooker, Life-cycle and cost of goods assessment of fed-batch and perfusion-based manufacturing processes for mAbs, Biotechnology Progress, 32 (2016) 1324-1335.

[29] D. Burgstaller, W. Krepper, J. Haas, M. Maszelin, J. Mohoric, K. Pajnic, A. Jungbauer, P. Satzer, Continuous cell flocculation for recombinant antibody harvesting, Journal of Chemical Technology & Biotechnology, 93 (2018) 1881-1890.
[30] R. Sommer, P. Satzer, A. Tscheliessnig, H. Schulz, B. Helk, A. Jungbauer, Combined polyethylene glycol and CaCl2 precipitation for the capture and purification of recombinant antibodies, Process Biochemistry, 49 (2014) 2001-2009.
[31] J. Gomis-Fons, H. Schwarz, L. Zhang, N. Andersson, B. Nilsson, A. Castan, A. Solbrand, J. Stevenson, V. Chotteau, Model-based design and control of a small-scale integrated continuous end-to-end mAb platform, Biotechnology Progress, 36 (2020) e2995.
[32] T.M. Pabst, J. Thai, A.K. Hunter, Evaluation of recent Protein A stationary phase innovations for capture of biotherapeutics, Journal of Chromatography A, 1554 (2018) 45-60.
[33] B. Kelley, Industrialization of mAb production technology: the bioprocessing industry at a crossroads, MAbs, 1 (2009) 443-452.
[34] A.A. Shukla, L.S. Wolfe, S.S. Mostafa, C. Norman, Evolving trends in mAb production processes, Bioengineering & Translational Medicine, 2 (2017) 58-69.

395 **Tables**

396 Table 1. Model settings defining the four scenarios for the TEA. The recipe cycle time

Main models settings					
Settings	**Solid PEG**	**Liquid PEG**	**Batch protein A**	**PCC protein A**	**Source**
Yearly throughput (kg yr^{-1})	*1000*	*1000*	*1000*	*1000*	[35]{Kelley, 2009 #5}
Operating days per year (days yr^{-1})	*330*	*330*	*330*	*330*	Assumed
Mode of operation	*Semi-continuous*	*Semi-continuous*	*Batch*	*Semi-continuous*	Assumed
Batch duration/run duration (days^{-1})	*10* [a]	*10* [a]	*1* [b]	*13* [c]	[a]Assumed [b]Calculated based on steps duration (1 cycle) [c]Calculated based on steps duration (55 cycles in PCC mode)
Recipe cycle time (days^{-1})	*14*	*14*	*14*	*14*	Assumed
# of batches/# of runs (yr^{-1})	*21*	*21*	*21*	*21*	Assumed
Antibody titre in supernatant (w w^{-1})	*0.5*	*0.5*	*0.5*	*0.5*	[36]
Antibody yield (%)	85[c]	85[c]	97[d]	97[d]	[c]Lab-scale experiments [d]Built-in database BioSolve

Figures

Figure 1. Yield and purity comparison of solid and liquid PE6000 precipitation in batch mode with mAb01 and mAb02. Precipitates were recovered by centrifugation, washed with 20% PEG6000 and dissolved with 1xPBS pH 3.5. Experiments were performed in triplicates and data are given as mean ± standard deviation.

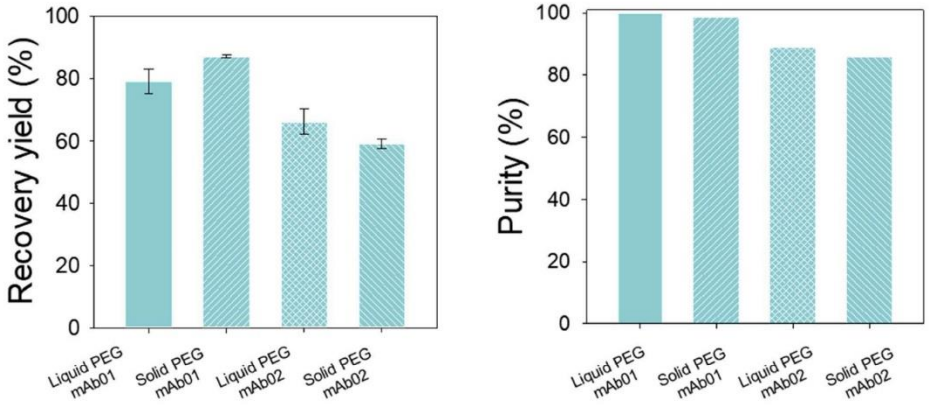

Figure 2. Experimental set-up for continuous protein precipitation using PEG6000 added in solid form. The feeding device feeds solid PEG into a mixing vessel and transported through a tubular reactor.

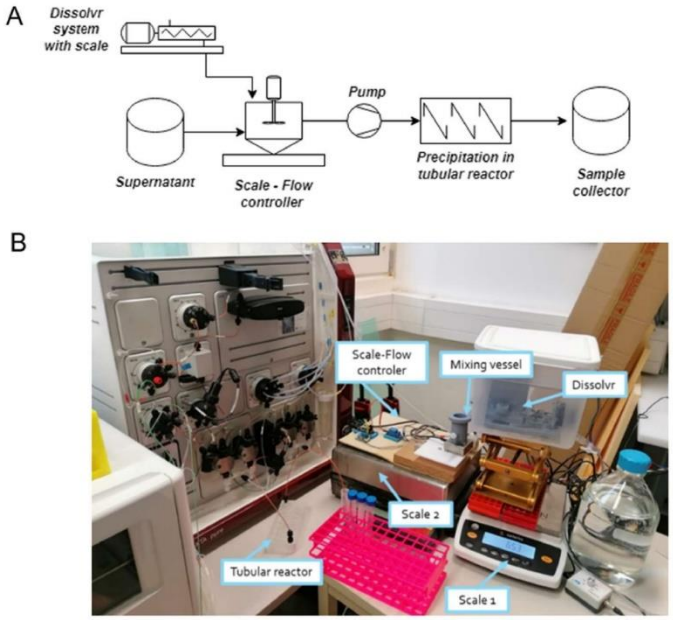

Figure 3. a) Recovery yields and b) purity of mAb01 using liquid and solid PEG precipitation. Precipitates were recovered by centrifugation, washed with 20% PEG6000 and redissolved with 1xPBS pH 3.5.

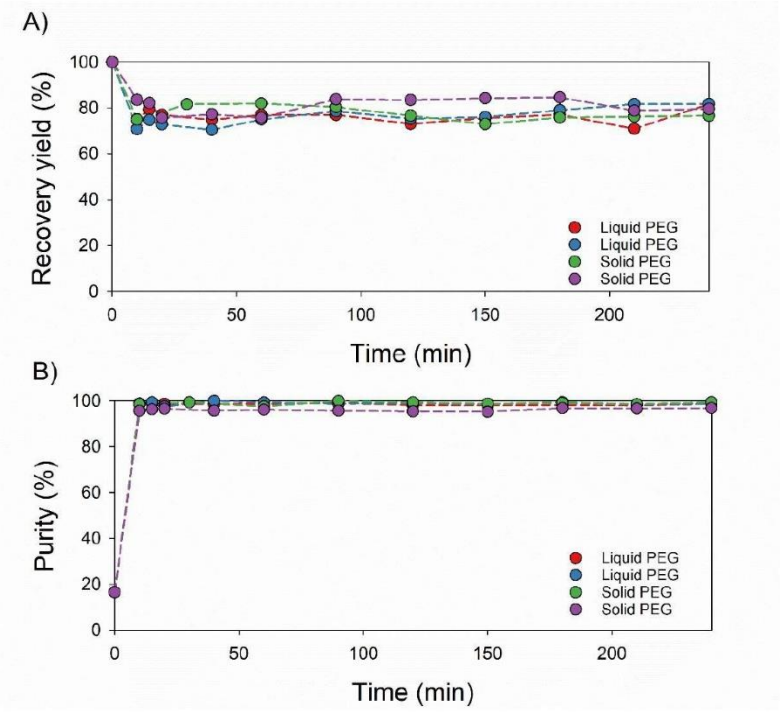

Figure 4. Processes flowcharts: **a) Batch Protein A**, after elution the antibody solution undergoes viral inactivation in a mixing tank. **b) PCC protein A**. **c) Liquid PEG**, highlighted in red the mixing tanks for the dissolution of PEG. After the precipitation step in a tubular reactor, the supernatant undergoes a two steps tangential flow filtration (TFF) followed by redissolution of antibody with phosphate buffer, dead-end filtration of the undissolved antibody and pH neutralization. **d) Solid PEG**, highlighted in red the Dissolvr® system. The following steps are identical to Liquid PEG.

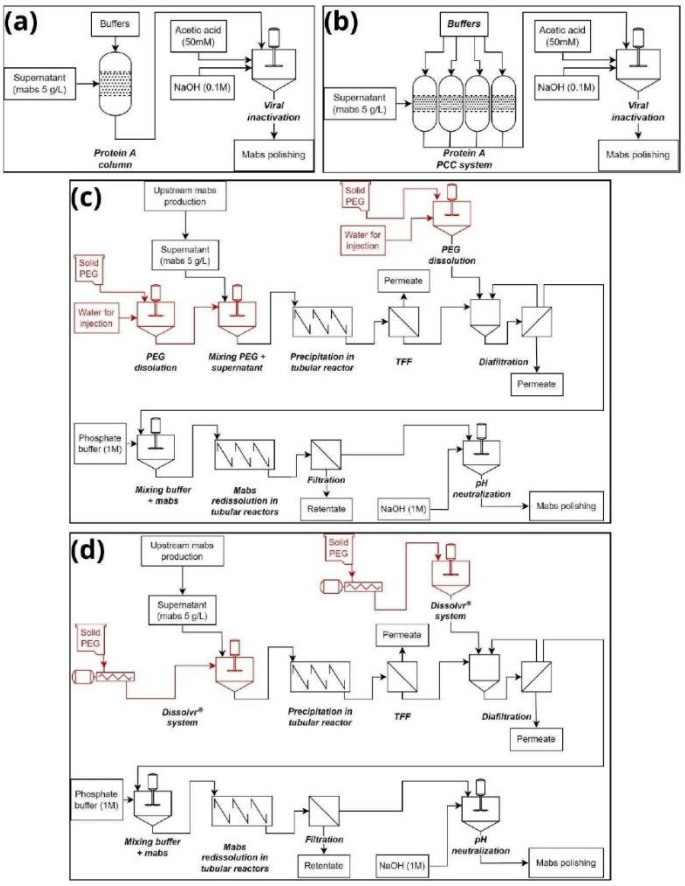

Figure 5. a) CAPEX and OPEX comparison b) COGs breakdown.

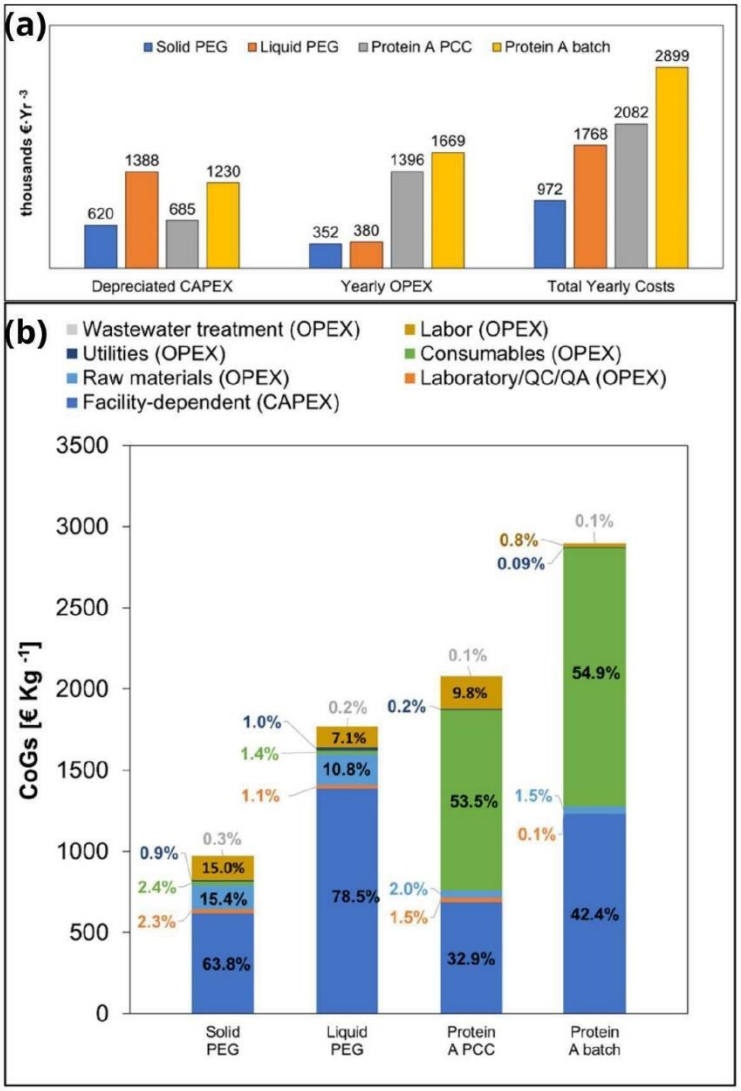

454

455

Figure 6. The difference in COGs, split into subcategories, between a) Solid and Liquid PEG b) Solid PEG and PCC protein A.

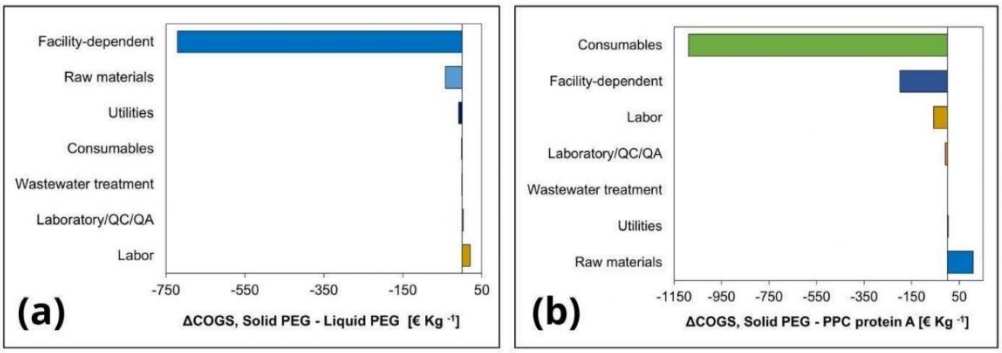

478 Figure 7. a) Carbon footprint of the four-purification methods b) PMI calculations.

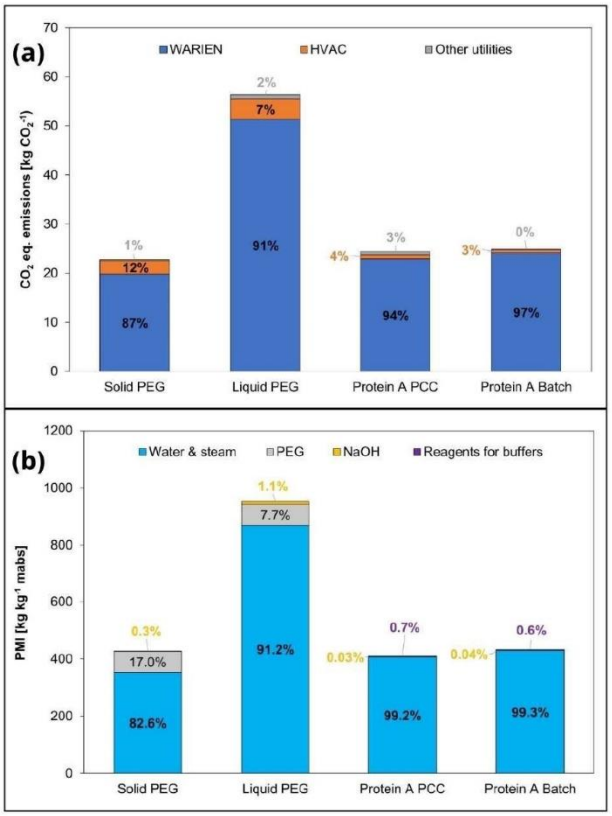

479

480

481

482

483

484

485

486

487

Supplementary material

CAPEX tables

Table 1. Total Equipment Purchasing Costs for the Solid and Liquid PEG processes.

	Solid PEG			**Liquid PEG**		
Equipment	*Quantity*	*Size*	*Total Cost (€)*	*Quantity*	*Size*	*Total cost (€)*
PEG container (hopper)	0	N/A	N/A	2	4 m^3; 2 m^3	4,000
PEG dissolution tank	2	N/A	N/A	2	7.5 m^3; 12.5 m^3	310,000
Liquid PEG + supernatant mixing tank	0	N/A	N/A	1	50 L	4,500
Dissolvr system	2	50 L (mixing tank)	13,000	0	N/A	N/A
Tubular reactor	2	Max throughput 100 L/hr	20,000	2	Max throughput 100 L/hr	20,000
Microfilter (TFF1)	1	20 m^2	55,000	1	30 m^2	70,000
Diafilter (TFF 2)	1	30 m2	77,000	1	30 m2	77,000
Redissolution tank	1	50 L	4,500	1	50 L	4,500
Dead-end filter	1	10 m^2	38,000	1	10 m^2	38,000
pH neutralization tank	1	50 L	4,500	1	50 L	4,500
Unlisted equipment (20% of total MEPC)			53,000			133,363
Main Equipment Purchase Cost (MEPC)			265,000			666,813
Auxiliary equipment PC (Clean-in-place skids)			1,200,000			1,200,000
Total Equipment Purchasing Cost (TEPC) (Incl. auxiliary eq.)			1,465,000			1,866,813

494 Table 2. Total Equipment Purchase Costs for the PCC Protein A and Protein A Batch processes.

	Protein A PCC			Protein A Batch		
Equipment	Quantity	Size	Total Cost (€)	Quantity	Size	Total Cost (€)
PBA Column	4	20 L	200,000	1	205 L	428,000
Dead-end filter	1	10 m^2	40,000	1	10m^2	40,000
pH neutralization tank	1	2 m^2	85,320	1	4 m^2	115,110
Unlisted equipment (20% of total MEPC)			81,330			145,778
MEPC			406,650			728,888
Auxiliary equipment PC (Clean-in-place skids)			300,000			300,000
TEPC			706,650			1028888

495
496
497
498
499
500
501
502
503
504
505
506
507
508
509
510
511

512

513 Table 3. Total Direct Fixed Cost for the four simulated processes.

	Solid PEG	**Liquid PEG**	**Protein A PCC**	**Protein A Batch**
Composite Lang`s factor	8.13	8.13	8.13	8.13
MEPC [€]	265,000	666,813	406,650	728,888
Total Direct Fixed Cost (TDFC) (Incl. auxiliary equipment) [€]	3,354,450	6,621,186	3,606,065	6,225,855

514

515

516

517

List of abbreviations

ATF	Alternating flow filtration
BI	Bioprocess intensification
CA	Caprylic acid
CAD	Computer-aided design
CFD	Computational fluid dynamics
CHO	Chinese hamster ovary
COP/COC	Cyclic Olefin (Co-) Polymers
CoGs	Cost of Goods
DLP	Digital light processing
DSP	Downstream process
FBRM	Focused beam reflectance measurement
FDA	Food and drug administration
FDM	Fusion deposition modeling
HCP	Host cell proteins
HMWI	High molecular weight impurities
HTS	High-throughput screening
HVAC	Heating – ventilation – air conditioning
ICB	Integrated continuous biomanufacturing
LOC	Lab on a Chip
LTCC	Low-Temperature Cofired Ceramics
mAbs	Monoclonal antibodies
MCSGP	Multi-column counter-current solvent gradient purification
mPAA	Modified polyallylamine
NCa	Camp number
PAT	Process analytical technology
PC	Polycarbonate
PCC	Periodic Counter Current Chromatography
pDADMAC	Polydiallyldimethylammonium chloride
PDMS	Polydimethylsiloxane
PEG	Polyethylene glycol
PEI	Polyethylenimine
pI	Isoelectric Point
PMI	Process mass intensity
PMMA	Poly(methyl methacrylate)

PS	Polystyrene
PSD	Particle size distribution
QbD	Quality by design
Re	Reynolds number
RTD	Residence time distribution
SMB	simulated moving bed chromatography
Tg	Glass transition temperature
USP	Upstream process
SLA	stereolithography
SPTFF	single-pass tangential flow filtration
STRs	Stirred Tank Reactor
TFF	Tangential flow filtration
TMP	Transmembrane pressure
WFI	Water for injection

List of Figures

Appendix A: Academic CV

Conferences:

1. **Bioprocessing Summit – Boston, 2021**
   Online Poster presentation: How to design continuous devices to improve tangential flow filtration and product quality in protein precipitation
2. 40th International Symposium on the Separation of Proteins, Peptides & Polynucleotides (**ISPPP) – Porto, 2021**
   Oral presentation: How to design continuous devices to improve tangential flow filtration and product quality in protein precipitation
3. **PepTalk –** The protein Science and Production Week - **San Diego, 2022**
   Online Poster presentation: How to design continuous devices to improve tangential flow filtration and product quality in protein precipitation
4. **Bioprocessing Summit Europe – Barcelona, 2022**
   Oral presentation: Milliscale devices to accelerate process development for protein precipitation and filtration
5. **Biomania – Brno, 2022**
   Oral presentation: Milliscale devices to accelerate process development for protein precipitation and filtration
6. **Recovery of Biological Products – Rome, 2022**
   Poster presentation: Milliscale devices to accelerate process development for protein precipitation and filtration
7. **Biopartitioning and purification conference – Aveiro, 2022**
   Poster presentation: Milliscale devices to accelerate process development for protein precipitation and filtration.
8. **Integrated Continuous Biomanufacturing – Sitges, 2022**
   Poster presentation: Continuous precipitation of antibodies by feeding of solid polyethylene glycol

Awards:

- Poster Award at Recovery of Biological Products XIX – Rome 2022
- Best Poster Award at Biopartitioning and purification conference – Aveiro 2022
- 2nd Shared prize at BOKU / tecnet | accent Innovation Award 2022

Patents:

- Apparatus and method for the purification of biomolecules. Patent No. WO2022083901